RESEARCH

2007-12

Demonstration of Ash Utilization in Low Volume Roads

LRRB
LOCAL ROAD RESEARCH BOARD

Take the steps... Research...Knowledge...Innovative Solutions!

Transportation Research

Technical Report Documentation Page

1. Report No.	2.	3. Recipients Accession No.
MN/RC-2007-12		

4. Title and Subtitle	5. Report Date
Demonstration of Ash Utilization In Low Volume Roads	May 2007
	6.

7. Author(s)	8. Performing Organization Report No.
Tuncer B. Edil and Craig H. Benson	

9. Performing Organization Name and Address	10. Project/Task/Work Unit No.
University of Wisconsin-Madison Department of Civil and Environmental Engineering 1415 Engineering Drive Madison, WI 53706	11. Contract (C) or Grant (G) No. (c) 86536

12. Sponsoring Organization Name and Address	13. Type of Report and Period Covered
Minnesota Department of Transportation Research Services Section 395 John Ireland Boulevard Mail Stop 330 St. Paul, Minnesota 55155	Final Report
	14. Sponsoring Agency Code

15. Supplementary Notes

http://www.lrrb.org/PDF/200712.pdf

16. Abstract (Limit: 200 words)

Two field projects are described where cementitious fly ashes (10% by dry weight) and water were mixed to stabilize recycled pavement materials and road-surface gravel to form a base during reconstruction of a city street in Waseca, MN, and construction of a flexible pavement in a segment of gravel country road, CR 53 in Chisago County, MN, respectively. Addition of fly ash improves the stiffness and strength of the base materials significantly. A resilient modulus of minimum 50 MPa appears safe to assume irrespective of the base material at the end of construction due to fly ash stabilization. However, moduli of 100 MPa or more can also be achieved. There is no evidence of frost-induced degradation in the field over a single season of winter. Chemical analysis of the draining leachate from the fly ash-stabilized layers showed that the concentrations of trace elements (with the exception of Mn) were below USEPA maximum contaminant levels and Minnesota health risk levels. Longer-term monitoring is needed to fully understand the potential for leaching of trace elements and frost action during the service life. These field cases show that fly ash stabilization provides an effective and economical means of providing a base for asphalt paving using existing roadway materials.

17. Document Analysis/Descriptors		18.Availability Statement
Fly ash, road surface gravel, recycled pavement material, stabilization,	modulus, frost action, eachate quality	No restrictions. Document available from: National Technical Information Services, Springfield, Virginia 22161

19. Security Class (this report)	20. Security Class (this page)	21. No. of Pages	22. Price
Unclassified	Unclassified	233	

DEMONSTRATION OF ASH UTILIZATION IN LOW VOLUME ROADS

Final Report

Prepared By:

Tuncer B. Edil and Craig H. Benson
Department of Civil and Environmental Engineering
University of Wisconsin-Madison
Madison, Wisconsin 53706

May 2007

Published by:

Minnesota Department of Transportation
Research Services Section
395 John Ireland Boulevard, MS 330
St. Paul, Minnesota 55155-1899

ACKNOWLEDGEMENTS

Financial support for this study was provided by the Minnesota Local Road Research Board (LRRB). The study was administered by the Minnesota Department of Transportation (Mn/Dot). The conclusions and recommendations in this report are solely those of the authors and do not reflect the opinions or policies of LRRB or Mn/DOT. Appreciation is expressed to the City of Waseca's Department of Engineering and Chisago County's Department of Public Works for supporting the field investigation, providing FWD testing, and for monitoring the lysimeters. Drs. Lin Li and Bulent Hatipoglu contributed to the analysis and project reports. Xiaodong Wang, Onur Tastan, Maria Rosa, Jeremy Baugh, Jacob Sauer, and Nathan Klett assisted with the projects in the field and laboratory.

TABLE OF CONTENTS

LIST OF TABLES

LIST OF FIGURES

EXECUTIVE SUMMARY

This report describes two field sites where cementitious fly ashes (Class C and off-specification) were used to stabilize recycled pavement materials (RPM) and road-surface gravel (RSG) to form a base during reconstruction of a city street in Waseca, MN, and construction of a flexible pavement in a segment of gravel country road, CR 53 in Chisago County, MN, respectively. The construction method is well established and requires minimal specialty equipment. Construction proceeded smoothly for both projects with experienced specialty contractors. The process is reported to be cost-effective by the project owners.

The projects consisted of mixing fly ash (10% by dry weight) and adding water into the RPM pulverized to a depth of 300 mm and into RSG to a depth of 254 mm, compacting the mixture to form a firm base, and placing a hot mix asphalt surface. California bearing ratio (CBR) and resilient modulus (M_r) tests were conducted on the RPM and RSG alone and fly-ash stabilized RPM (S-RPM) and RSG (S-RSG) mixed in the field and laboratory to evaluate how addition of fly ash improved the strength and stiffness. *In situ* testing was also conducted on the subgrade and the S-RPM and S-RSG with a soil stiffness gauge (SSG) and dynamic cone penetrometer (DCP). Falling weight deflectometer (FWD) tests were conducted after paving on two different occasions. A pan lysimeter was installed beneath the pavement in each project to monitor the rate of drainage and trace element concentrations in the leachate. Column leaching tests were also conducted on samples of S-RPM and S-RSG collected during construction. Column leach tests were conducted in the laboratory for comparison.

The most important mechanical property of a layer in the pavement structure is its modulus. It is concluded that addition of Class C (self-cementitious) fly ash (typically about 10% by dry weight) improves the stiffness and strength of the base materials, whether RPM, RSG or subgrade soil, significantly. The stabilized material has typically a mean modulus at the end of construction (roughly within 7 days of curing) that is about 1.7-3 times higher than that of the untreated material for a variety of base materials, that is the material stabilized with fly ash. It is recommended that modulus obtained from laboratory mixed specimens during mix design stage to be reduced by 1/4 to 1/3 to estimate the target resilient modulus obtainable during construction. SSG and DCP can be used as a means of monitoring construction quality. A resilient modulus of minimum 50 MPa appears safe to assume irrespective of the base material at the end of construction due to fly ash stabilization. However, moduli of 100 MPa or more can also be achieved with certain materials.

Modulus developed during construction, however, is likely to change with time due to continuing hydration reactions on one hand and due to environmental exposure such as frost action. The degree of resilient modulus reduction appear to be no more than 50% in the laboratory due to 12 cycles of freeze-thaw for a range of fly ash-stabilized materials although it was less than that for the RPM and RSG. There is no evidence of frost-induced degradation in the field based on FWD surveys over a single season of winter. However, longer term monitoring using FWD surveys is important.

Chemical analysis of the draining leachate from the fly ash-stabilized layers showed that the concentrations of many trace elements were reasonably steady toward the end of the monitoring period. Longer-term monitoring is needed to fully understand the

potential for leaching of trace elements during the service life of a pavement. However, during the monitoring period, all of the concentrations (with the exception of Mn) were below USEPA maximum contaminant levels (MCLs) and Minnesota health risk levels (HRLs) established by the Minnesota Department of Public Health. Additional study is also needed to define laboratory leach testing protocols that can more accurately simulate leaching of trace elements from fly ash-stabilized materials.

These field cases show that fly ash stabilization provides an effective and economical means of providing a base for asphalt paving using existing roadway materials.

1. INTRODUCTION

Utilization of byproducts is becoming a common method to improve the ride quality and structural capacity of roads. Use of self-cementitious fly ash in stabilizing the existing roads (gravel roads or recycled paved roads) to form a stable base for hot mixed asphalt layer is of great interest as this reconstruction approach costs significantly less compared to traditional reconstruction where road surface materials are replaced with new aggregate base (estimated to be 1/3 of the traditional total reconstruction), more rapid and convenient. This approach was implemented in two projects in Minnesota. The first project took place in the City of Waseca, MN and involved reconstruction of a city street (7^{th} Street and 7^{th} Avenue) by fly ash stabilization of recycled pavement materials. The second project involved the conversion of a gravel road (CR 53) to a paved road in Chisago County, MN. The detailed findings related to each of these projects were submitted as individual reports and are attached to this report. This report reviews the data collected at these two sites as well as other fly ash stabilization projects that the investigators monitored in Wisconsin to arrive at some general observations and conclusions. The material descriptions, the tests methods used both in the laboratory and the field, the field data collection and monitoring are described in the attached individual reports and are not repeated here.

2. MODULUS

The most important mechanical property of a layer in the pavement structure is its modulus. As pavement design moves to mechanistic-empirical pavement design methods, as proposed in NCHRP Project 1-37A (*The Mechanistic-Empirical Design Guide for New and Rehabilitated Pavement Structures*), input parameters for fly ash stabilized base materials must be developed for use in this design practice.

2.1. Modulus measured in the Laboratory

There are no standards available for resilient testing of fly ash-stabilized or chemically stabilized materials. Resilient modulus tests on the fly ash–stabilized materials have been conducted by the investigators following the methods described in AASHTO T292. Irrespective of the nature of the base material stabilized by fly ash, the final product becomes essentially “cohesive” due to chemical stabilization. Therefore, the loading sequence for cohesive soils is used. Laboratory resilient modulus tests performed on Class C fly ash-stabilized materials generally showed small dependency on bulk or deviator stresses and can be considered stress-independent for the typical range of stresses expected in the base layer of the type of asphalt paved roads considered here. Therefore, the resilient modulus at the initial stress state of 21 kPa is reported as “modulus”.

Preparation of laboratory specimens of fly ash-stabilized materials, during the mix design phase typically involve mixing of air-dry base material with the desired percentage of fly ash on dry weight basis, addition of the appropriate amount of water, allowing 1-2 hours for reactions (simulating the typical delay in the field), and compaction in special split PVC mold to the desired density or by the standard compaction effort. The specimen, thus prepared, is cured for a minimum of 7 d but also

for longer periods in a 100% relative humidity room in the mold. A 14-d curing period, intended to reflect the condition when most of the hydration is complete, is probably a better indicator of expected modulus but only 7 d of curing is also employed to compare laboratory modulus with the field measurements done after a similar period. After curing, the specimen is removed from the mold and subjected to resilient testing.

While this approach produces reasonably uniform and reproducible specimens (Tastan 2005), there are questions regarding how well it represents the field conditions, especially relative to mixing, curing, and inherent variability of base materials and construction operations. Tube sampling of fly ash-stabilized materials is difficult and often results in sample damage. Therefore, as an alternative, field mixed specimens are used. In this approach the material is sampled immediately after it is mixed during construction. After 1 hour (simulating field operations), the sample is compacted in the resilient modulus specimen mold (and/or CBR mold as appropriate) to the same density measured in that area of the field-compacted stabilized layer. Following the same curing and testing procedures as the laboratory mix specimen, its modulus is determined. Field-mix samples reflect the mixing, moisture, and density conditions that are occurring in the field as closely as possible. Field curing conditions, however, are not replicated. Field experience shows curing takes place rapidly in the field and continues with time.

The laboratory measured moduli on field-mix specimens of three types of Class C fly ash-stabilized materials are shown in Fig. 1. In this type of box plot, each box encloses 50% of the data with the median value of the variable displayed as a line. The mean value is written in the box. The top and bottom of the box mark the limits of ± 25% of the variable population. The lines extending from the top and bottom of each box mark the minimum and maximum values within the data set that fall within an acceptable range. Any value outside of this range, called an outlier, is displayed as an individual point.

The data in Fig. 1 were obtained from specimens that were made along the project route and incorporate the variability of the base material and construction process. The material in Waseca is a recycled pavement material consisting of a mixture of asphalt, base course, and subgrade materials encountered in the top 300 mm of an existing street. It consists of mostly sand and gravel-size particles, which reflects the presence of the pulverized asphalt and the original base course. The fines (the fraction passing #200 sieve) were mostly less than 10%. The material in Chisago is road-surface gravel consisting of well-graded gravelly sand with fines in the range of 11 to 14%, the sand content consistently around 60%, and the gravel content about 25%. The data from US 12 from Wisconsin are also presented in Fig. 1 to show the response of natural subgrade soils to fly ash treatment (Edil et al. 2006a). US 12 material consists of natural subgrade soils (classified as CL, SC, and SM according to the USCS or A-7-6, A-6, and A-2-6 according to AASHTO. In each case a Class C fly ash was used (10% by dry weight of Riverside fly ash in Waseca and Chisago and 12% by dry weight of Columbia fly ash in US 12). Water content of the base material also plays a role on mechanical properties. Too dry materials may not have moisture to complete the hydration process and on the other hand excess amount of water (typical of very soft subgrade soils) may result in reduction of mechanical properties. The water contents after mixing fly ash during construction of Waseca, Chisago, and US 12 materials were 7-8%, 6-7%, and 7-15%, respectively. These were the moisture contents measured during construction. All specimens were compacted to the densities achieved in the field during construction. The

resilient modulus of the specimens was measured after 7-d curing (14-d for US 12) in a 100% relative humidity room.

The data in Fig. 1 indicate that fly ash stabilized recycled pavement materials and subgrade soils have a resilient modulus in the range of 50-100 MPa whereas road-surface gravels markedly higher (130-180 MPa). It should be remembered water content of US 12 subgrade soil, having more fines and wet conditions during construction was markedly higher than that of Waseca and Chicago materials although they were cured for 14 days. On the other hand, recycled pavement materials may tend to have lower strength gain as a result of fly ash stabilization due to the presence of asphalt in some particles. In a study of recycled pavement materials stabilized by off-specification fly ashes, it was reported that laboratory mixed materials had resilient moduli ranging from 60 to 90 MPa (Wen et al. 2007). In a laboratory study on a wide range of fine-grained subgrade soils in Wisconsin (from high plasticity clays to low plasticity silts and clays), it was reported that resilient modulus depended on soil characteristics such as expressed by group index and water content (Edil et al. 2006b). Such materials can have a wide range of water contents in situ. For the soils (i.e., without fly ash) compacted at optimum water content, M_r varied between 13 to 80 MPa. Resilient moduli of the soil-fly ash mixtures prepared with 10% fly ash at 7% wet of optimum water content typically fall below the moduli of the soils compacted at optimum water content. At 18% fly ash content, however, M_r of the soil-fly ash mixtures at 7% wet of optimum water content were in the range of 50-90 MPa and up to 2.5 times higher than the modulus of the soils compacted at optimum water content. That is, addition of 18% fly ash to a soft and wet subgrade soil results in comparable or higher M_r than the same subgrade soil dried and compacted at optimum water content.

According to a Wisconsin Highway Research Program study (Eggen 2004), the resilient modulus of a wide-variety of crushed aggregate base course materials at a bulk stress of 83-100 kPa (approximate value at the base course level as recommended by NCHRP 1-28A, 2003) varied between about 48 and 110 Mpa. The resilient modulus based on field-mix fly ash-stabilized materials cured and tested in the laboratory, fall in this range for recycled pavement material and is significantly higher for road-surface gravel when stabilized with fly ash. The mean modulus for field-mix and laboratory-mix materials from a variety of projects is tabulated in Table 1. It is noted that the moisture contents of field-mix and laboratory-mix specimens are intended to be comparable and at about optimum moisture; however, they may differ from each other. Laboratory-mix specimens represent expected fly ash content, moisture, and density conditions and field-mix specimens what actually is achieved during construction. In some cases, only California bearing ratio (CBR) is available. Except for road-surface gravel in Chisago, in all case the field-mix results in lower (60-75%) modulus than the laboratory-mix. The modulus measured on tube samples was available at only one site (US 12) and given in Table 1 (designated undisturbed). The modulus of the field-mix samples (mean=71 MPa) is reasonably close to that of the undisturbed tube samples (mean =82 MPa) within the context of the variation observed in each group. Thus, the field-mix approach can be considered to be an effective method of assessing the *in situ* soil stiffness during construction.

The average laboratory resilient modulus of the unstabilized base material is also given for some projects in Table 1. Adding fly ash increased the modulus of both the recycled pavement material and the road-surface gravel by 1.7 to 3 times.

2.2. Modulus Measured in the Field

Stiffness (or modulus) of the fly ash-stabilized base was measured in the field with a soil stiffness gauge (SSG), a dynamic cone penetrometer (DCP), and a falling weight deflectometer (FWD). There are standards for SSG and DCP and were followed in the field. SSG and DCP can be performed only when the surface of the stabilized base is still uncovered. FWD is an indirect method, however, can be performed any time after the surface is paved and thus allows an assessment of time-dependent changes in the integrity of the materials. It allows monitoring of combined impacts of continuing curing, climatic conditions (moisture and temperature changes), frost action, and continuing traffic loading. Testing with the SSG and DCP was conducted directly on the stabilized surface after approximately 7 d of curing. FWD testing was conducted several times after the HMA was placed and will be continued in coming years.

The results of the SSG and DCP surveys are given in Fig. 2 for both sites. The effect of stabilization and curing is evident in Fig. 2 (SSG stiffness increases and DPI decreases with stabilization). It is possible to calculate an elastic modulus based on the measured SSG stiffness (essentially requires and assumption of Poisson's ratio). The elastic moduli back-calculated from the FWD surveys are given in Fig. 3 for the fly-ash stabilized recycled pavement material in Waseca and road-surface gravel in Chisago at two different times. The field moduli measured in November of the same year of construction (i.e., 2004 for Waseca and 2005 for Chisago) shown in Fig. 3 follow the laboratory moduli measured on field-mix specimens given in Fig. 1, i.e., Chisago moduli are markedly higher than Waseca moduli. The FWD surveys conducted in the year following construction, i.e., August 2005 and May 2006; respectively for Waseca and Chisago are markedly lower than the first survey performed in November. This is consistent with the field temperature and moisture conditions and frost penetration monitored at each site. It is early to make major conclusions. However, the lowest mean field FWD moduli are higher than the mean moduli measured in the field-mix specimens in the laboratory only after 7-d curing. It appears additional time for field curing compensates for the impacts of environmental conditions at least during the first year.

To place the moduli measured by different methods (and also different times), the data are presented in Fig. 4. Moduli obtained from field-mix specimens tested in the laboratory and SSG moduli from the field after 7-d curing and the FWD moduli corresponding to additional curing and exposure are given. Moduli obtained from the resilient modulus test on field-mix samples are lower than those obtained in the field by the SSG or the FWD. It appears that operating moduli of at least 100 MPa can be used for both materials.

2.3. Frost Effect on Modulus

A significant concern in northern climates is frost action on pavement materials. Fly ash-stabilized materials have not been used widely in such frost areas to draw conclusions regarding their long-term performance. On one hand it is argued that

materials stronger to begin with will have a greater resistance to the damaging action of frost penetration. Fly ash, being a silt-size material, implies greater propensity for frost action. However, the particles of Class C fly ash, a self-cementitious material like cement, hydrate in the presence of water and bind base material grains together. So it is not likely that the individual size characteristics of unhydrated fly ash will remain and act like silt-soil particles. Addition of fly ash is expected to lower the drainage capability of the base materials. In other words, the fly ash-stabilized base is not likely to have the same drainage capability and ability to shed water as natural base course aggregate.

There is no standard laboratory test to evaluate the effect of freeze-thaw cycles on the mechanical properties such as resilient modulus of soils or fly ash-stabilized soils. There are procedures for soil-cement or concrete products where weight loss and volume change are monitored. Such procedures are aimed at evaluating the potential of such rigid materials to spall and disintegrate. A new procedure, similar to ASTM D 6035 *Standard Test Method for Determining the Effect of Freeze-Thaw on Hydraulic Conductivity of Compacted or Undisturbed Soil Specimens Using a Flexible Wall Permeameter*, is adopted here, in which identical resilient modulus specimens are prepared and subjected to cycles of freeze-thaw and tested for resilient modulus. Weight, volume, and moisture change of these specimens at the end of each freeze-thaw cycle are also monitored. The steps in the procedure are shown in Fig. 5. The freezing temperature was chosen after determining the freezing point depression for each material in accordance with ASTM D 5918 *Standard Test Methods for Frost Heave and Thaw Weakening Susceptibility of Soils*. The freezing point depression was -12 °C for Chisago road-surface gravel stabilized with 10% Riverside 8 fly ash and -8.7 to -9.4 °C for Waseca recycled pavement materials stabilized with 10% Riverside 7 fly ash. A standard -15 °C was then applied in each freeze-thaw cycle and resilient modulus tests (and subsequent unconfined compression tests on the same specimens) were performed without freeze-thaw and at the end of 1st, 3rd, and 5th cycles of freeze-thaw on identically prepared specimens. Typically, the changes in modulus take place over 5 cycles based on observations made on fly ash-stabilized soils (Rosa 2006). The base material being granular with relatively low water content (about 7%), the compacted specimens were soaked before the freeze-thaw cycles to generate a conservative moisture condition. This resulted in about 4-5% water content gain. The volume of all specimens increased by about 2.5% at the end of 5 cycles of freeze-thaw.

In Fig. 6, resilient moduli of the base materials (without fly ash addition and without freeze-thaw but soaked) are given along with moduli obtained after fly ash stabilization (without freeze-thaw) and after the last freeze-thaw cycle (5th cycle) of the fly ash stabilized base materials (one road-surface gravel sample from Chisago and two recycled pavement materials from Waseca) are presented. A general trend of higher resilient modulus when the base materials are stabilized with fly ash even after freeze-thaw cycles compared to unstabilized soils without freeze-thaw cycles is clearly observed. Both base materials showed decrease in resilient modulus after soaking and subjecting them to freeze-thaw cycles.

Resilient modulus of the specimens that were subjected to freeze-thaw cycles were normalized by the resilient modulus of the specimen that was not subjected to any freeze-thaw cycles to determine the loss of property due to freeze-thaw. The results, shown in Fig. 6, indicate that resilient modulus drop by 17% after 5 cycles of freeze-thaw

for fly ash-stabilized road-surface gravel and 25-42% for recycled pavement material. Rosa (2006) performed freeze-thaw tests on a variety of materials including fine-grained soils alone and stabilized with fly ash. The degree of resilient modulus reduction varied with the type of material but remained to be no more than 50%. From these results can be concluded that for highway design, the safest way to represent the effect of freeze-thaw cycling on the resilient modulus of the fly ash stabilized materials is dividing the modulus of the material not subjected to freeze-thaw by 2. However, one also needs to take into account the time-dependent modulus gain due to continuing hydration reactions.

Previous research published indicated that a reduction, no variation or an increase of stiffness are observed after freeze-thaw cycles. Reduction in stiffness is attributed to the retardation of cementitious/ pozzolanic reactions by dominating freezing temperatures. When no variation or minimal variation in stiffness is observed after freeze-thaw cycles, it is attributed to a balancing of freezing and thawing temperatures in compensating each other and producing a balance in the cementitious/pozzolanic reactions. Increase in stiffness after freeze-thaw cycles has also been observed and attributed to dominating thawing temperatures that accelerate the cementitious/pozzolanic reactions.

2.4. Correlation of Modulus with Other Properties and Tests

Laboratory assessment of the resilient modulus of the fly ash stabilized materials was supplemented additional laboratory and field tests. The relationship of the resilient modulus of field-mix specimens to the CBR of similarly field-mixed specimens is shown in Fig. 8 for Chisago and Waseca but also two other sites in Wisconsin where natural soils were stabilized with Class C fly ash (US 12). There is a general tendency of increasing modulus with increasing CBR but correlation for different materials is different. Empirical correlations between modulus and CBR have been proposed for natural soils by a number of researchers. For example, Powell et al. (1984) developed an equation relating the elastic modulus obtained by wave propagation techniques and CBR. After accounting for stress and strain level characteristic of pavements, Powell et al. (1984) obtained:

$$E = 17.6\ CBR^{0.64} \tag{1}$$

where E (essentially equivalent of resilient modulus) is in MPa and CBR is in percent. Another well-known relationship that is widely used in North America was proposed by Heukelom and Foster (1960):

$$M_r = 10\ CBR \tag{2}$$

where M_r is the resilient modulus in MPa. Eq. 2 is included in the AASHTO (1993) guide for design of pavements.

Eqs. 1 and 2 are shown with the data reported for soil-fly ash mixtures in Fig. 8. Both equations, developed using natural soils, over-predicted M_r for soil-fly ash mixtures, with the over-prediction being much greater for Eq. 2. Sawangsuriya and Edil (2004) also report that Eq. 2 tends to over-predict M_r appreciably for natural soils. A better prediction was obtained by Edil et al. (2006b) with:

$$M_r = 3\ CBR \tag{3}$$

which was obtained by linear least-squares regression of the data based of a range of laboratory-mix fly ash-stabilized fine-grained soils by Edil et al. (2006b). Again M_r is

the resilient modulus in Mpa. Eq. 3 also represents Waseca and Chisago data reasonably well when considered collectively.

To assess the structural properties of the pavement materials, the DCP penetration index (DPI) values are usually correlated with the CBR of the pavement materials. Extensive research has been conducted to develop an empirical relationship between CBR and DPI for a wide range of pavement and subgrade materials. These include research by Livneh (1987), Kleyn (1975), Harisson (1987), Webster et al. (1992), and others. Based on their researches, many of the relationships between CBR and DPI can be quantitatively presented in the form of:

$$\log(\text{CBR}) = \alpha + \beta \log(\text{DPI}) \quad (4)$$

where α and β are coefficients ranging from 2.44 to 2.56 and -1.07 to -1.16, respectively, which are valid for a wide range of pavement and subgrade materials. Note also that CBR is in percent and DPI is in millimetres per blow (mm/blow). For a wide range of granular and cohesive materials, the US Army Corps of Engineers use the coefficients α and β of 2.46 and -1.12, which have been also adopted by several agencies and researchers and is in general agreement between the various sources of information. Livneh et al. (1995) also show that there exists a universal correlation between CBR and DPI for a wide range of pavement and subgrade materials, testing conditions, and technologies. In addition, the relationship between CBR and DPI is independent of water content and dry unit weight since both water content and dry unit weight equally influence CBR and DPI.

The CBR-DPI data collected at Waseca and Chisago projects are plotted in Fig. 9 along with similar data from three projects in Wisconsin where subgrade soils were stabilized by Class C fly ash (US 12, Scenic Edge, and STH 60). Also plotted is the relationship given in Eq. 4 with α and β coefficients 2.46 and -1.12, respectively. Although there is some scatter, this relationship appears to represent also the CBR-DPI relationship for a wide variety of fly ash-stabilized base materials.

The relationship of resilient modulus measured on field-mix specimens compared to SSG stiffness measured in the field at the vicinity of the location (i.e., station) where the resilient modulus specimen was made is shown in Fig. 10 for Waseca and Chicago projects as well as US 12 where subgrade soils were stabilized with fly ash. There is a general correlation but also significant scatter. The data indicate that resilient modulus is mostly larger than 50 MPa and SSG stiffness is greater than 12 for fly stabilized materials.

3. ENVIRONMENTAL SUITABILITY

As an industrial by-product, fly ash is subject to environmental regulation when being used in construction applications. The Minnesota Pollution Control Agency (MPCA) allows the use of fly ash for soil stabilization on a site-specific basis. Soil reference values (SRVs) have been used by MPCA to aid decision-making regarding the reuse of fly ash in stabilization applications.

Using fly ash for stabilization during roadway construction is expected to have minimal impacts on the environment. For example, Bloom and Gollany (2001) evaluated runoff from fly ash stabilized soils and found that concentrations of trace elements of concern are not high. Similarly, impacts to groundwater have been evaluated by Li et al.

(2006) using the WiscLEACH program, which predicts the maximum concentration of contaminants in groundwater adjacent to roadways where fly ash has been used for stabilization. Analyses with WiscLEACH showed that, in most cases where fly ash is placed above the groundwater table, impacts to groundwater are negligible. However, the level of impact depends on the type and amount of trace elements in the fly ash, the nature of the base material being stabilized (i.e., sorption capacity), the type of soils in the vadose zone, and the depth and velocity of groundwater.

To provide actual field data of the leachate from the fly-ash stabilized layer in this project, an environmental monitoring program that consists of monitoring the volume of water draining from the pavement, concentrations of trace elements in the leachate, temperatures and water contents within the pavement profile, and meteorological conditions (air temperature, humidity, and precipitation) was initiated. Monitoring of the pavement began in October 2004 in Waseca and October 2005 in Chisago and is still being conducted.

Leachate draining from the pavement was monitored using a pan lysimeter installed under the fly ash-stabilized layer in both projects. The lysimeter is 4 m wide, 4 m long and 200 mm deep and is lined with 1.5-mm-thick linear low density polyethylene geomembrane. The base of the lysimeter was overlain by a geocomposite drainage layer (geonet sandwiched between two non-woven geotextiles). Water collected in the drainage layer is directed to a sump plumbed to a 120-L polyethylene collection tank buried adjacent to the roadway. The collection tank is insulated with extruded polystyrene to prevent freezing. Leachate that accumulates in the collection tank is removed periodically with a pump. The volume of leachate removed is recorded with a flow meter, a sample for chemical analysis is collected, and the pH and Eh of the leachate are recorded. The sample is filtered, preserved, and analyzed.

3.1 Trace Elements in Lysimeter Drainage

Approximately 1.8 and 16 pore volumes of flow (PVF) have passed through the fly ash-stabilized layers during the monitoring period, in Waseca and Chisago (Waseca was monitored for two years whereas Chisago one year and is much drier than Chisago), respectively. During this period, pH of the drainage has been near neutral and oxidizing conditions have prevailed.

Concentrations of trace elements in drainage from the lysimeter in Waseca are shown in Fig. 11 as a function of PVF. Elements with peak concentrations between 3 and 102 g/L are shown in Fig. 11a, whereas those with peak concentrations less than 2.5 g/L are shown in Fig. 11b. Elements not shown in Fig. 11 include those below the detection limit (Be, Ag, Hg, Se, and Tl) and elements not typically associated with health risks (Ca and Mn). All of the concentrations are below USEPA maximum contaminant levels (MCLs) and Minnesota health risk levels (HRLs). The exception is Mn (not shown in Fig. 11), which typically had concentrations between 1 and 2 mg/L. The Minnesota HRL for Mn currently is 100 g/L, but plans exist to increase the HRL to 1.0-1.3 mg/L (www.pca.state.mn.us). USEPA does not have a MCL for Mn.

Most of the concentrations appear to be increasing, with a more rapid increase towards the end of the monitoring. Thus, higher concentrations are likely to be observed for many of the elements as the lysimeter is monitored in the future. However, concentrations of some elements appear to be decreasing (Mo and Sr) or remaining

steady (Sb and Sn). The lack of a steady-state condition or clearly diminished concentrations for most of the trace elements highlights the need for longer term monitoring of the lysimeter.

Concentrations of trace elements in drainage from the lysimeter in Chisago are shown in Fig. 12 as a function of PVF. Fig. 12 Fig. 12is divided into three parts: high concentration, moderate and persistent, and low and diminishing concentration. Elements not shown in Fig. 12 include those below the detection limit (Be, Ag, Hg, and Tl) and elements not typically associated with health risks (e.g., Ca). All of the concentrations are below USEPA maximum contaminant levels (MCLs) and Minnesota health risk levels (HRLs). The exception is Mn, which had a maximum concentration of 3,682 ug/L and exceeded the Minnesoata HRL of 100 ug/L. However, the Minnesota Department of Health no longer recommends the HRL value and plans exist to increase the HRL to 1,000 to 1,300 ug/L (www.pca.state.mn.us). USEPA does not have a primary criterion for Mn although there is a secondary criterion. Most of the concentrations appear to be stabilizing and persistent. Concentrations of some elements appear to be low and decreasing (Pb, Sb and Sn).

3.2 Trace Elements in Column Leaching Tests Effluent

A column leaching test (CLT) test was performed using material from field mix in Waseca. The elution behavior observed in the CLT effluent follows two patterns: (i) delayed response (Co, Cr, Pb, Se, Cu, and Zn), where the concentration initially increases and then falls, and (ii) persistent leaching (B, Ba, Sr, Mo, As, and V), where the concentration initially increases and then remains relatively constant. The data indicate that the trace element concentrations in the CLT effluent typically are higher than concentrations in the drainage collected in the field (Fig. 11). The poor agreement suggests that the CLT test method that was used may not be appropriate for evaluating leaching of trace elements from S-RPM, unless a conservative estimate of the trace element concentrations is acceptable. Despite the higher concentrations obtained from the CLT, most of the elements have concentrations below USEPA MCLs and Minnesota HRLs. The exceptions are for B, Pb, Se, and Sr. The peak Mn concentration was also above the current Minnesota HRL for Mn, but is less than the proposed HRL.

Two column leaching tests were performed using material from field mix in Chisago. The elution behavior observed in the CLT effluent follows two patterns: (i) first-flush response, where the concentration falls from an initially high value and then remains nearly constant and (ii) persistent leaching, where the concentration initially increases and then remains relatively constant. The trace element concentrations in the CLT effluent typically are higher than concentrations in the drainage collected in the field in the lysimeters (Fig. 12). The poor agreement suggests that the CLT test method that was used may not be appropriate for evaluating leaching of trace elements from S-RSG, unless a conservative estimate of the trace element concentrations is acceptable. Despite the higher concentrations obtained from the CLT, most of the elements have concentrations below USEPA MCLs and Minnesota HRLs. The exceptions are for B, Be, Cr, Ba,As, and Se. Additional study is also needed to define laboratory leach testing protocols that can more accurately simulate leaching of trace elements from S-RSG.

4. SUMMARY

Two field case histories have been described where Class C and off-specification cementitious fly ashes (10% by weight) were used to stabilize recycled pavement material (RPM) and road-surface gravel (RSG) during construction of a flexible pavement. The construction method is well established and requires minimal specialty equipment. Construction proceeded smoothly for both projects with experienced specialty contractors. The process is reported to be cost-effective by the project owners.

California bearing ratio (CBR) and resilient modulus (M_r) tests were conducted on the RPM and RSG alone and on the fly-ash stabilized RPM (S-RPM) and RSG (S-RSG) mixed in the field and laboratory to evaluate how addition of fly ash improved the strength and stiffness. *In situ* testing was also conducted on the subgrade and S-RSG with a soil stiffness gauge (SSG) and dynamic cone penetrometer (DCP). Falling weight deflectometer (FWD) test were conducted after paving on two different occasions. A pan lysimeter was installed beneath the pavement in each project to monitor the rate of drainage and trace element concentrations in the leachate. Column leaching tests were also conducted on samples of S-RPM and S-RSG collected during construction.

The most important mechanical property of a layer in the pavement structure is its modulus. As pavement design moves to mechanistic-empirical pavement design methods, as proposed in NCHRP Project 1-37A (*The Mechanistic-Empirical Design Guide for New and Rehabilitated Pavement Structures*,), input parameters for fly ash stabilized base materials must be developed for use in this design practice. Therefore, resilient modulus data as measured or inferred by a variety of methods are analyzed from both projects as well as a number of other fly ash stabilization projects available to the investigators. The stabilized material has typically a mean modulus at the end of construction (roughly within 7 days of curing) that is about 1.7-3 times higher than that of the untreated material for a variety of base materials. Fly ash stabilization reduces variability in measured modulus compared to the variability encountered in natural soils. Resilient modulus of fly ash stabilized materials does not exhibit the non-linear stress dependency typical of soils for the typical range of bulk and deviator stresses expected in the pavement structure and in future a single modulus can be used simplifying the design.

Measurement of the modulus of fly ash stabilized materials, however, is not easy because of the difficulty of obtaining undamaged tube samples. Field mixed specimens typically give a modulus that is only 60 to 75% of that of laboratory mixed specimens. SSG modulus obtained in situ during construction within 7 days of curing is 50% or higher than resilient modulus measured in the laboratory on field mix specimens made during construction. This reflects to a certain degree the lower strain amplitude employed in SSG compared to resilient modulus test. There is a general correlation of resilient modulus to SSG modulus. There is a general inverse correlation of DPI and SSG stiffness. Resilient modulus of fly ash stabilized materials is also correlated with their CBR and therefore with DPI in a manner similar to those correlations observed in natural soils. Therefore, such tests can be used for fly ash stabilized materials and the data provided in this report provide a basis of specifying acceptable levels in terms of these tests. A resilient modulus of minimum 50 MPa appears safe to assume irrespective of the base material at the end of construction due to fly ash stabilization. However, moduli of 100 MPa or more can also be achieved with certain materials.

Modulus developed during construction, however, is likely to change with time due to continuing hydration reactions on one hand and due to environmental exposure such as frost action. At a Wisconsin site (STH 60) where low plasticity silty and clayey subgrade soils were stabilized by fly ash, FWD moduli continued to increase over six years of monitoring. The degree of resilient modulus reduction appear to be no more than 50% in the laboratory due to many freeze-thaw cycles for a range of fly ash-stabilized materials although it was less than that for the RPM and RSG. There is no evidence of frost-induced degradation in the field based on FWD surveys over a single season of winter. However, longer term monitoring using FWD surveys is important to understand the behavior of these new materials with which there is limited field record. Currently, another 2 years of monitoring is assured through new projects of the investigators.

Chemical analysis of the draining leachate from the fly ash-stabilized layers showed that the concentrations of many trace elements were reasonably steady toward the end of the monitoring period. Longer-term monitoring is needed to fully understand the potential for leaching of trace elements during the service life of a pavement. However, during the monitoring period, all of the concentrations (with the exception of Mn) were below USEPA maximum contaminant levels (MCLs) and Minnesota health risk levels (HRLs) established by the Minnesota Dept. of Public Health. The trace element concentrations in the column leaching test (CLT) effluents typically are higher than concentrations in the drainage collected in the field in the lysimeters. The poor agreement suggests that the CLT test method that was used may not be appropriate for evaluating leaching of trace elements from fly ash-stabilized materials, unless a conservative estimate of the trace element concentrations is acceptable. Despite the higher concentrations obtained from the CLT, most of the elements have concentrations below USEPA MCLs and Minnesota HRLs. Additional study is also needed to define laboratory leach testing protocols that can more accurately simulate leaching of trace elements from fly ash-stabilized materials.

5. CONCLUSIONS AND RECOMMENDATIONS

The following conclusions and recommendations are made:

1. Addition of self-cementitious fly ash (typically about 10% by dry weight) improves the stiffness and strength of the base materials, whether recycled pavement material, road surface gravel or subgrade soil, significantly.
2. Resilient modulus of fly ash stabilized materials does not exhibit the non-linear stress dependency typical of soils for the typical range of bulk and deviator stresses expected in the pavement structure and in future a single modulus can be used simplifying the design.
3. Modulus obtained from laboratory mixed specimens during mix design stage to be reduced by 1/4 to 1/3 to estimate the target resilient modulus obtainable during construction.
4. Soil stiffness gage and dynamic cone penetrometer can be used for monitoring quality control during construction.

5. A resilient modulus of minimum 50 MPa appears safe to assume irrespective of the base material at the end of construction due to fly ash stabilization. However, moduli of 100 MPa or more can also be achieved with certain materials.
6. The degree of resilient modulus reduction appear to be no more than 50% in the laboratory due to many freeze-thaw cycles for a range of fly ash-stabilized materials although it was less than that for the recycled pavement material and road surface gravel. There is no evidence of frost-induced degradation in the field based on FWD surveys over a single season of winter.
7. Chemical analysis of the draining leachate from the fly ash-stabilized layers showed that the concentrations of many trace elements were (with the exception of Mn) were below USEPA maximum contaminant levels (MCLs) and Minnesota health risk levels (HRLs) established by the Minnesota Dept. of Public Health. Specifically, mercury was not detected in the leachate.
8. Long-term monitoring of modulus and leachate quality is recommended to delineate strength gain/frost action and leaching behavior with time.

It is noted that these conclusions are made on the basis of specific fly ashes and base materials (i.e., recycled pavement material and road surface gravel) at the given project sites. Extrapolations to other sites and materials have to be made with care and caution.

6. REFERENCES

Benson, C.H. and Bosscher, P.J., (1999) "Time-domain reflectometry in geotechnics: a review". In: W. Marr and C. Fairhurst (Editors), *Nondestructive and Automated Testing for Soil and Rock Properties*, ASTM STP 1350. ASTM International, West Conshohocken, PA, pp. 113-136.

Bin-Shafique, S., Benson, C.H., Edil, T.B. and Hwang, K., (2006) "Leachate concentrations from water leach and column leach tests on fly-ash stabilized soils". *Environmental Engineering* 23(1), pp. 51-65.

Bin-Shafique, S., Edil, T.B., Benson, C.H. and Senol, A., (2004) "Incorporating a fly-ash stabilised layer into pavement design". *Geotechnical Engineering*, Institution of Civil Engineers, United Kingdom, 157(GE4), pp. 239-249.

Bloom, P. R., and Gollany, H. (2001) "Water quality in runoff from fly ash-stabilized pads". In *Environmental Evaluation for of the use of Ash in Soils Stabilization Applications*. EPRI, Palo Alto CA, and U.S. Department of Energy, Pittsburg, PA: 2001:1005213.

Edil, T.B., Benson, C.H., Tastan, O. Li, Lin and Hatipoglu, B. (2006a) "Monitoring and field evaluation of fly ash stabilization of roadway subgrade in US 12 between Cambridge and Fort Atkinson, Wisconsin" Report #0092-04-10, Wisconsin Highway Research Program, Madison, WI

Edil, T.B., Acosta, H.A. and Benson, C.H., (2006b) "Stabilizing soft fine-grained soils with fly ash". *Journal of Materials in Civil Engineering*, ASCE, 18(2), pp. 283-294.

Edil, T.B. Benson, C.H., Bin-Shafique, M. S., Tanyu, B. F., Kim, W. H. and Senol., A. (2002) "Field evaluation of construction alternatives for roadways over soft subgrade". *Transportation Research Record*, No. 1786: National Research Council, Washington DC, pp. 36-48.

Eggen P. (2004). *Determination of influences on support strength of crushed aggregate base course due to gradational, regional and source variations*. Final Report to Wisconsin Highway Research Program, Madison, WI.

Harrison, J. R. (1987) "Correlation between California bearing ratio and dynamic cone penetrometer". Strength Measurement of Soils. *Proceeding of Institute of Civil Engineers*, Part 2, 83, Technical Note No. 463.

Heukelom, W. and Foster, C. R. (1960) "Dynamic testing of pavement".. *Journal of the Structural Division*, ASCE, 86, No. SM1.

Hunt, Roy E. (1986) *Geotechnical Engineering Techniques and Practices.* McGraw Hill Book Company, New York, N.Y..

Kleyn, E. G. (1975) 'The Use of the dynamic cone penetrometer (DCP)". *Report No. 2/74*, Transvaal Roads Department, Cape Town, South Africa.

Li, L., Benson, C. H., Edil, T.B. and Hatipoglu, B. (2006) "Fly ash stabilization of recycled asphalt pavement material in Waseca, Minnesota." *Geo Engineering Report N0. 06-18*, Department of Civil and Environmental Engineering, University of Wisconsin-Madison,WI.

Livneh, M., Ishao, I., and Livneh, N. A. (1995). "Effect of vertical confinement on dynamic cone penetrometer strength values in pavement and subgrade evaluations". *Transportation Research Record 1473*, TRB, National Research Council, Washington, D.C., pp. 1-8.

Livneh, M. (1987) "Validation of correlations between a number of penetration tests and in situ California bearing ratio tests". *Transportation Research Record 1219*, TRB, National Research Council, Washington, D.C., pp. 56-67.

Powell, W. D., Potter, J. F., Mayhew, H. C., and Nunn, M. E. (1984) "The structural design of bituminous roads". *TRRL Laboratory Report 1132*, Transportation and Road Research Laboratory, Crowthorne, Berkshire, U.K. 62 pp.

Rosa, M. (2006) *Effect of freeze-thaw cycling on soils stabilized with fly ash*. M.S. Thesis, Department of Civil and Environmental Engineering, University of Wisconsin, Madison, WI.

Sawangsuriya, A. and Edil, T.B. (2005) "Use of soil stiffness gauge and dynamic cone penetration for pavement materials evaluation". *Geotechnical Engineering*, Institute of Civil Engineers, United Kingdom, Vol. 158, No. GE4, pp. 217-230.

Tastan, E. O. (2005) *Stabilization or organic soil using fly ash.* M.S. thesis, Department of Civil and Environmental Engineering, University of Wisconsin, Madison, WI.

Tanyu, B., Kim, W., Edil, T., and Benson, C., (2003) "Comparison of laboratory resilient modulus with back-calculated elastic modulus from large-scale model experiments and FWD tests on granular materials". *Resilient Modular Testing for Pavement Components*, American Society for Testing and Materials, West Conshohocken, PA. STP 1437, pp. 191-208.

Trzebiatowski, B., Edil, T.B. and Benson, C.H., (2004) "Case study of subgrade stabilization using fly ash: State Highway 32, Port Washington, Wisconsin". In: *Beneficial Reuse of Waste Materials in Geotechnical and Transportation Applications*, GSP No. 127. ASCE, Reston, VA, pp. 123-136.

Turner, J.P., (1997) "Evaluation of western coal fly ashes for stabilization of low-volume roads". *Testing Soil Mixed with Waste or Recycled Materials*. ASTM, West Conshohocken, PA. STP 1275, pp. 157-171.

Webster, S. L., Grau, R. H., and Williams, T. P. (1992) *Description and application of dual mass dynamic cone penetrometer*. Instruction Report GL-92-3, U.S. Army Engineers Waterways Experimental Station, Vicksburg, MS, 17 pp.

Wen, H., Baugh, J. and Edil, T.B. (2007) "Use of cementitious high carbon fly ash to stabilize recycled pavement materials as a pavement base material". TRB Meeting CD, Paper No. 07-2051, National Research Council, Washington DC.

Table 1 Resilient modulus gain by fly ash stabilization and comparison of field and laboratory-mix specimens from various projects

Project	Base Material	Fly Ash Content (%)	Lab-Mix M_r (MPa)	Field-Mix M_r (MPa)	Undis-turbed M_r (MPa)	Field-Mix/Lab-Mix M_r Ratio	Base Material M_r (MPa)	M_r Gain due to Fly Ash Stabilization
Waseca	RPM	10	104	78		0.75	47	1.7
Chisago	RSG	10	112	153		0.73	51	3
US 12	SS*	12	-	73	82		38	1.9
STH 32	SS	10	13.4	21		0.63	12.4	1.7
STH60	SS	10	99 (CBR 32)	(CBR 23)		0.72	Very soft	High
Scenic Edge	SS	12	115 (CBR 37)	(CBR 28)		0.76	Very soft	High

*** subgrade soil**

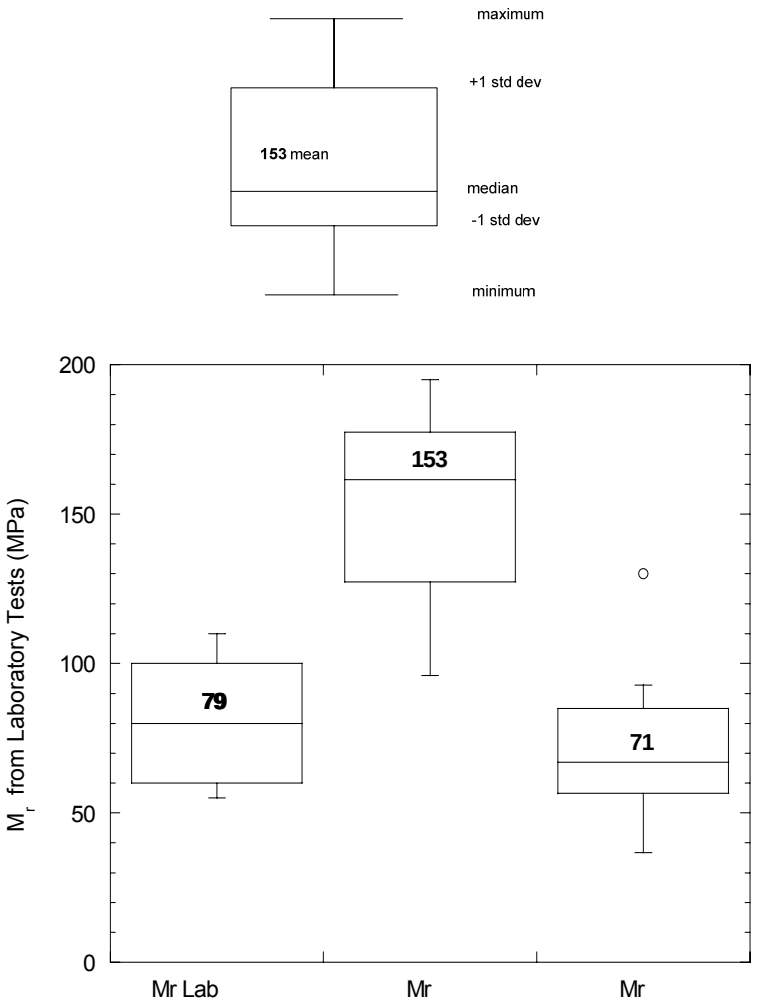

Fig. 1 Laboratory Mr of field-mix fly ash-stabilized materials (numbers on the boxes indicate mean modulus)

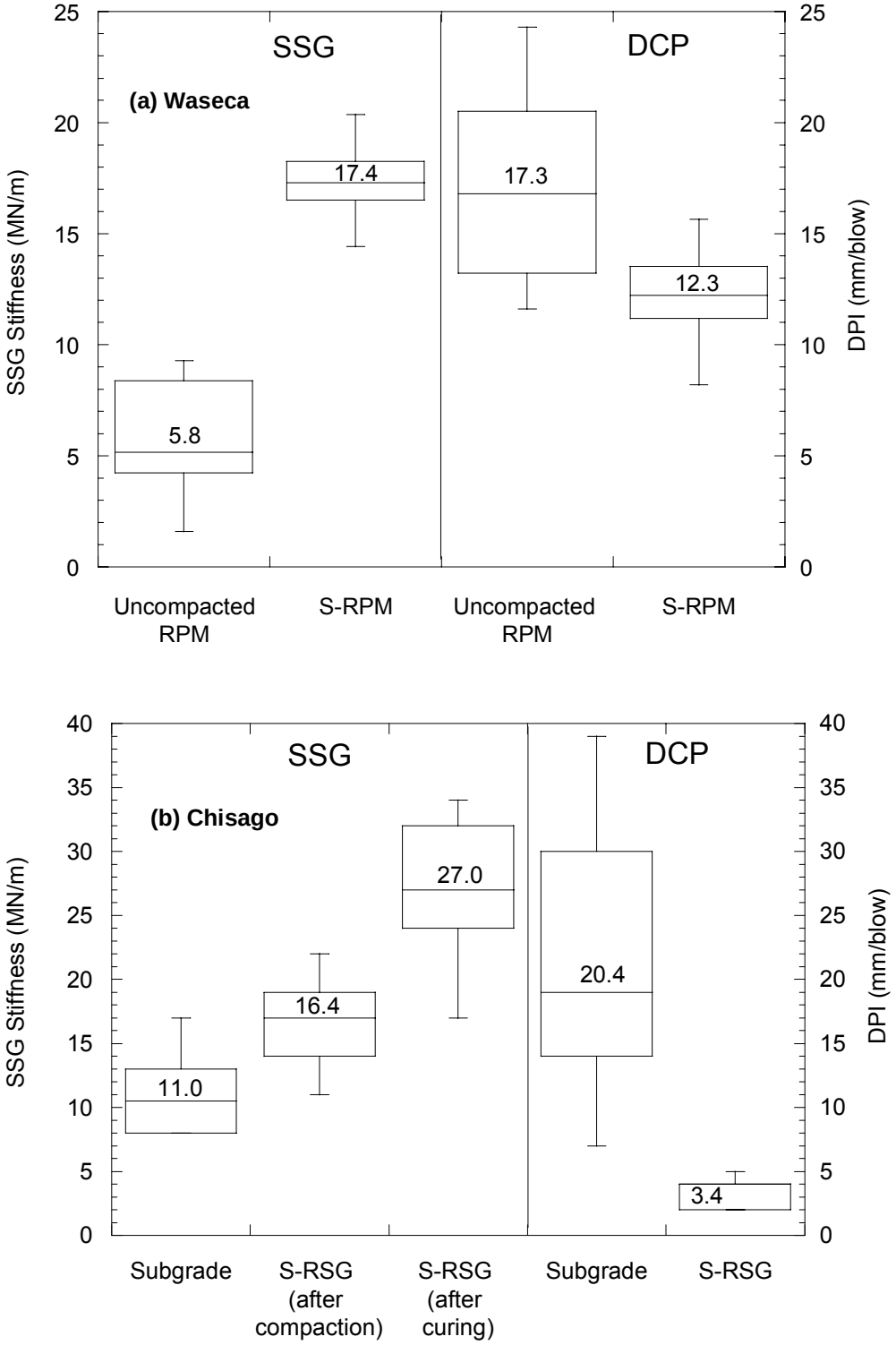

Fig. 2 Stiffness and DPI of base material and fly ash-stabilized recycled pavement material and road surface gravel (numbers on the boxes indicate mean value)

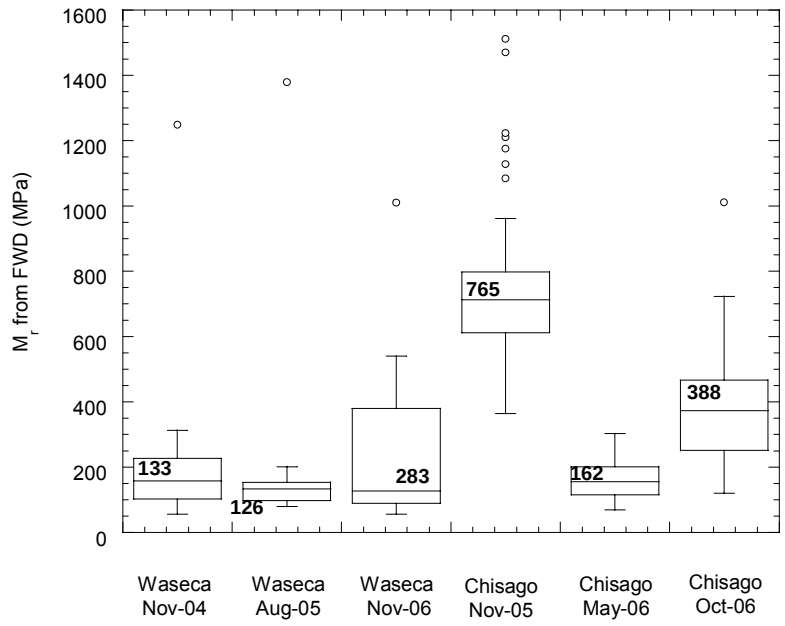

Fig. 3 Back-calculated Mr of fly ash-stabilized layer from FWD data at Waseca and Chisago projects (numbers on the boxes indicate mean modulus)

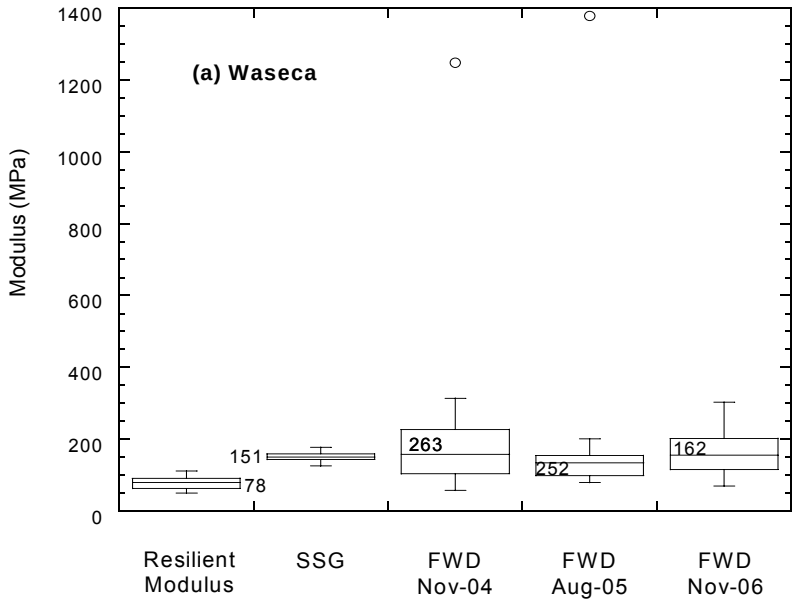

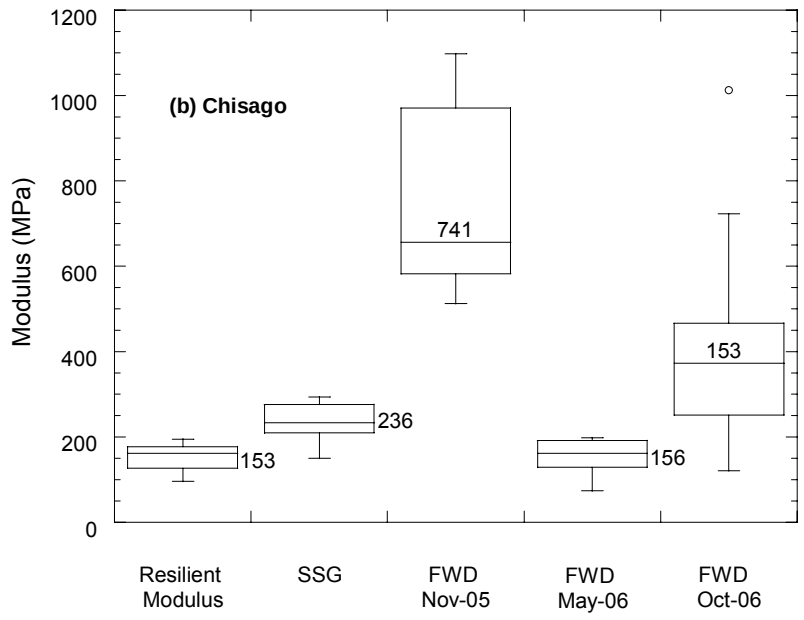

Fig. 4 Modulus as determined by different methods (numbers on the boxes indicate mean modulus)

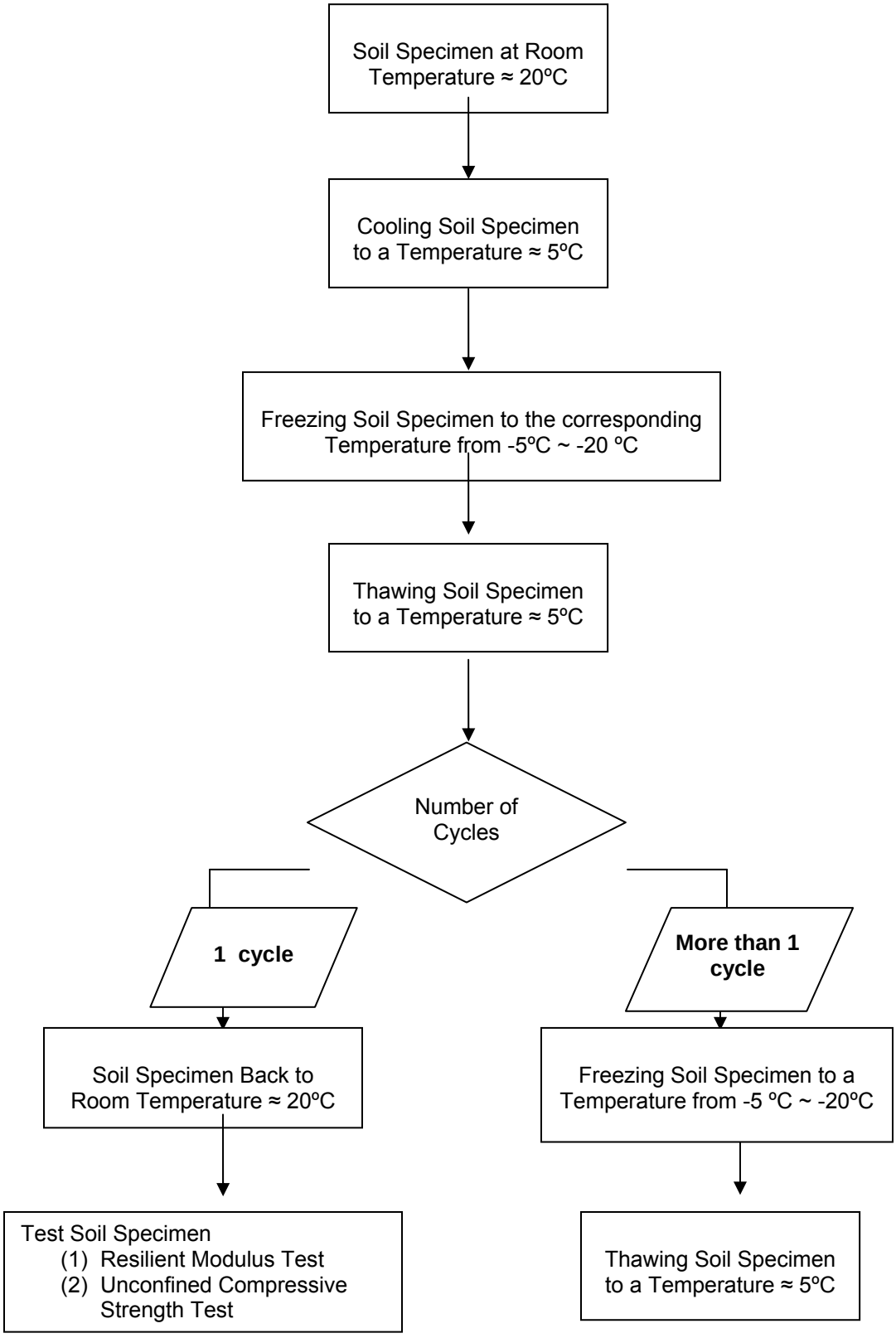

Fig. 5 Description of the process used for freeze-thaw cycling

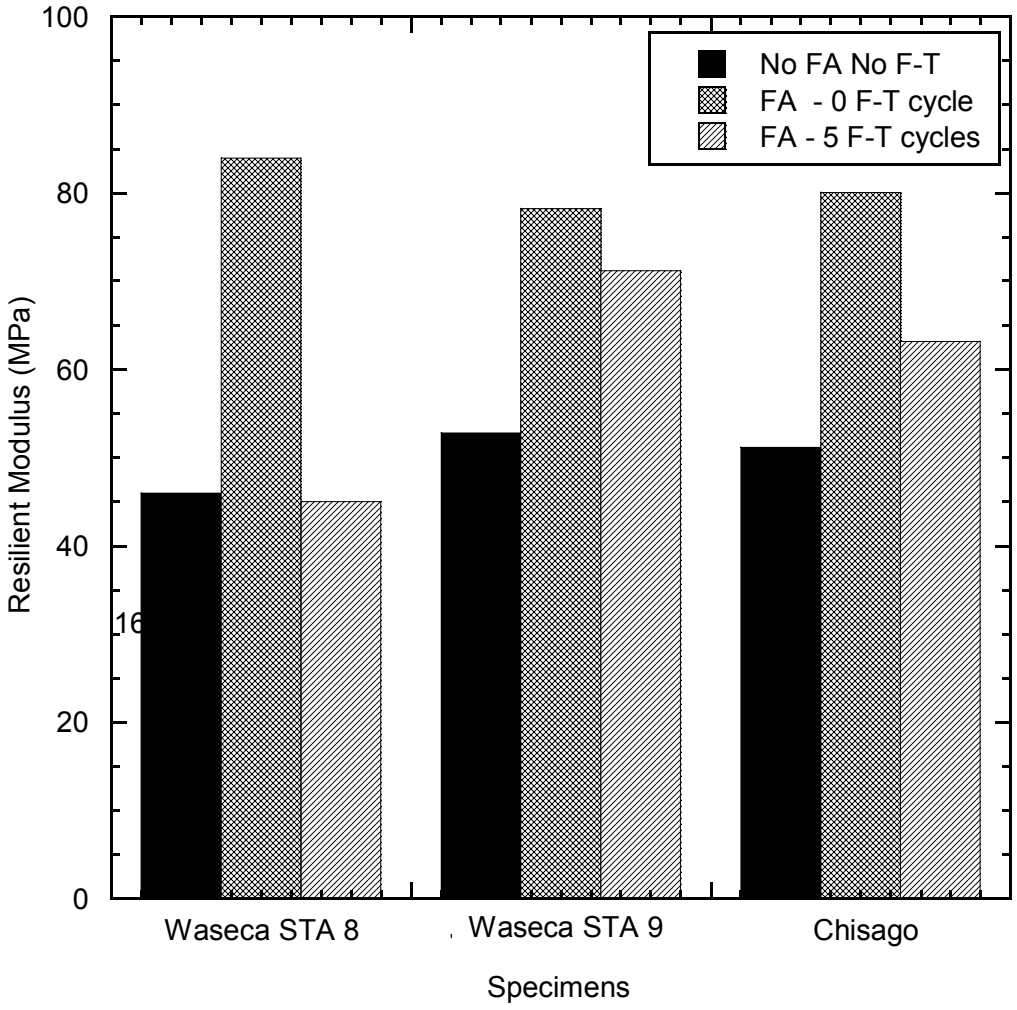

Fig. 6 Comparison of the resilient modulus values without fly ash and unfrozen with the resilient modulus of the fly ash-stabilized base materials after 5 of freeze-thaw

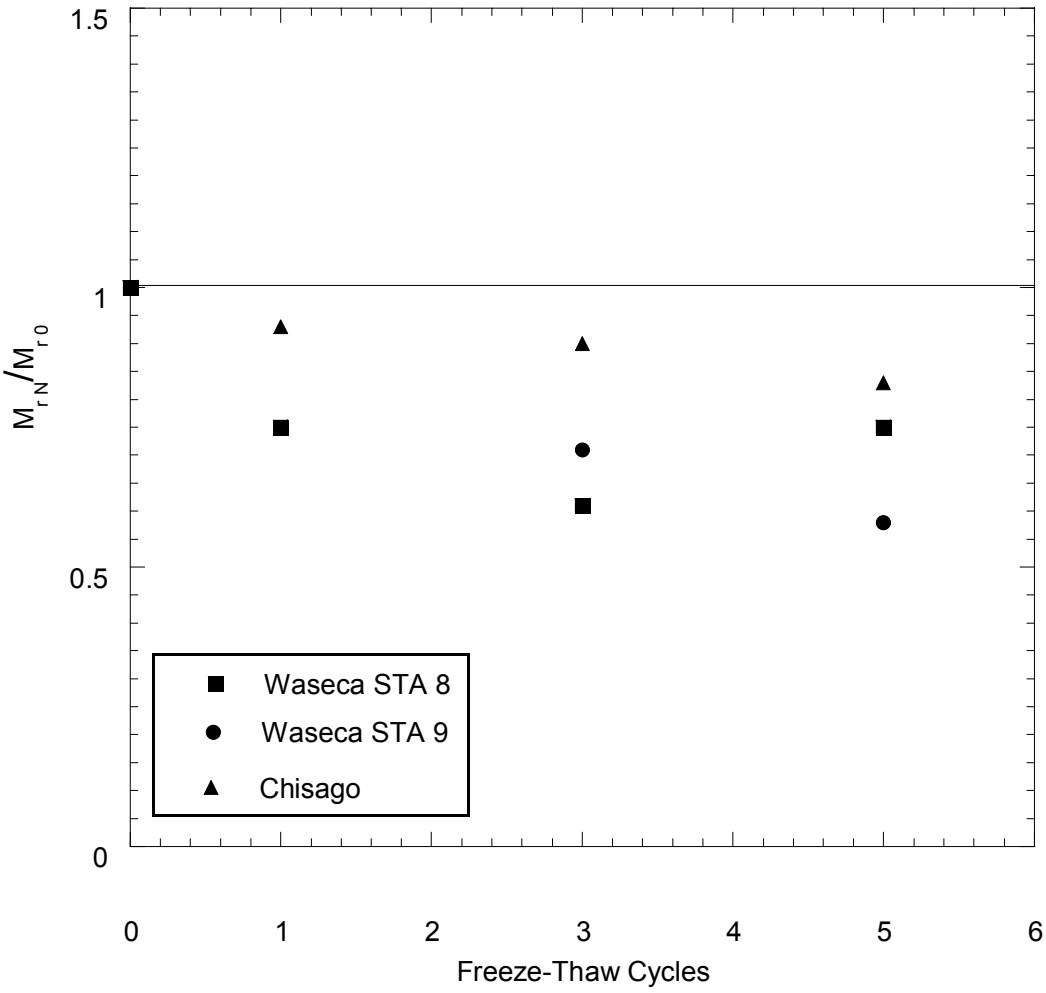

Fig. 7 Normalized resilient modulus vs. freeze-thaw cycles for fly ash-stabilized materials at Waseca and Chisago

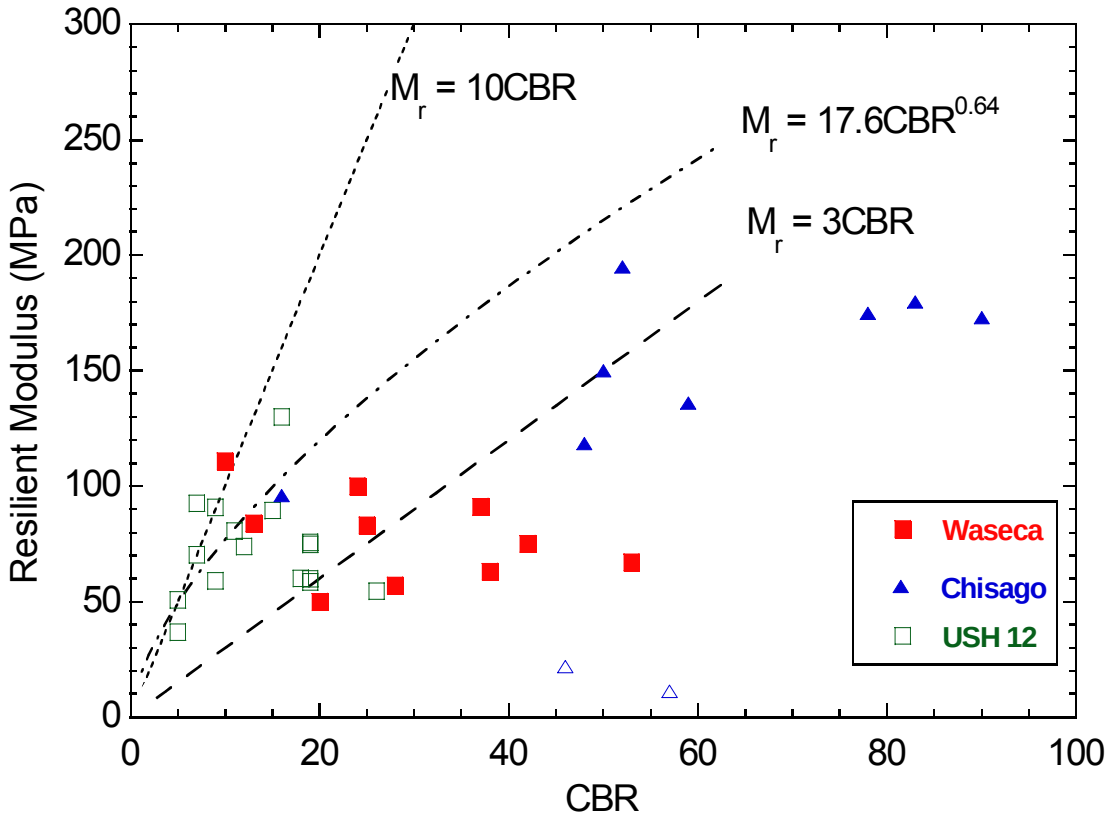

Fig. 8 Resilient Modulus versus CBR for fly ash-stabilized materials

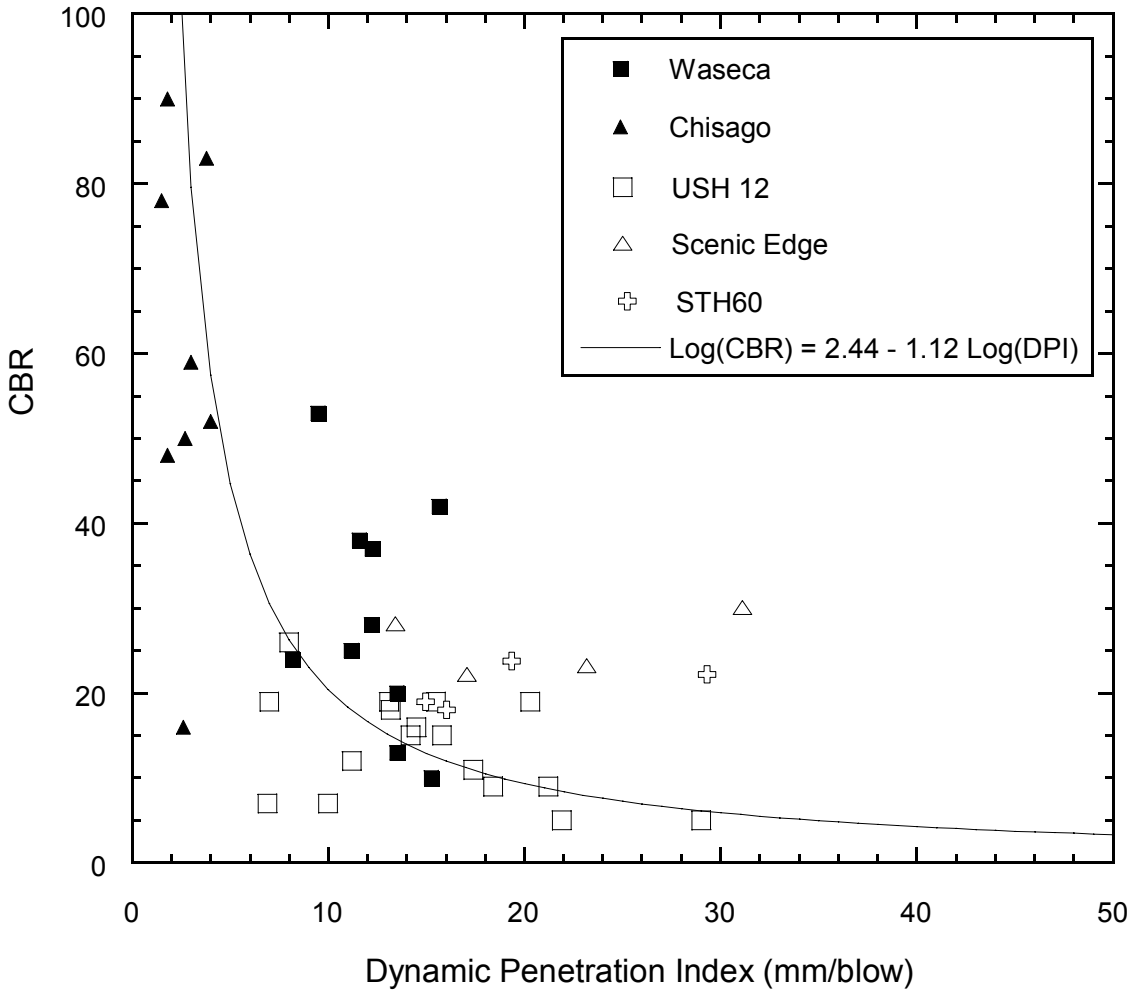

Fig. 9 CBR versus DPI for fly ash-stabilized materials

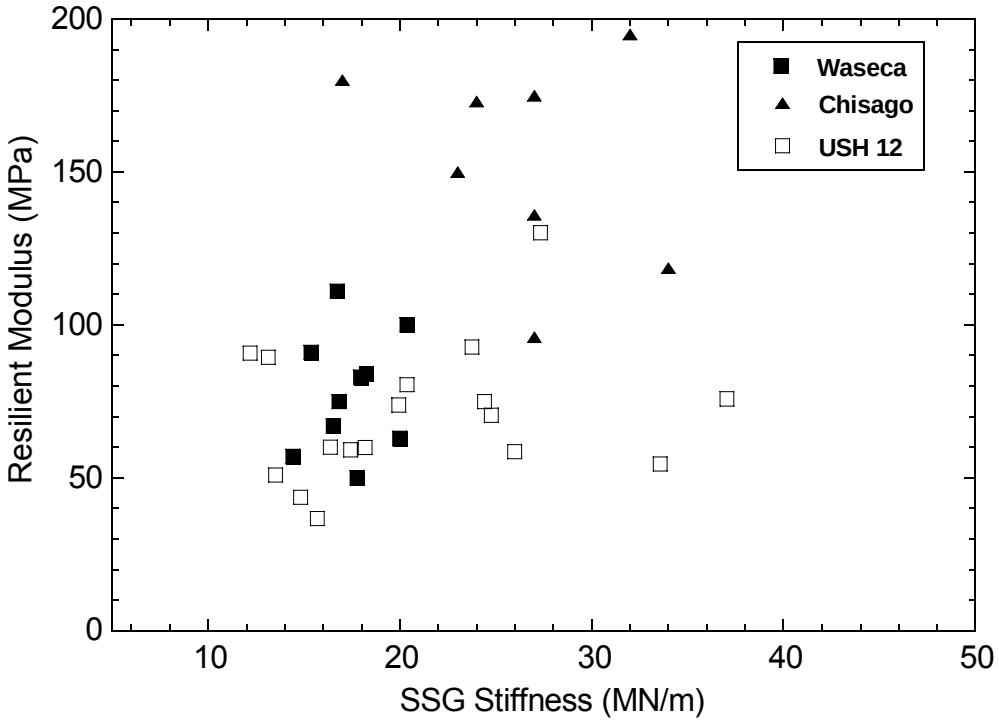

Fig. 10 Resilient modulus versus SSG stiffness for fly ash-stabilized materials

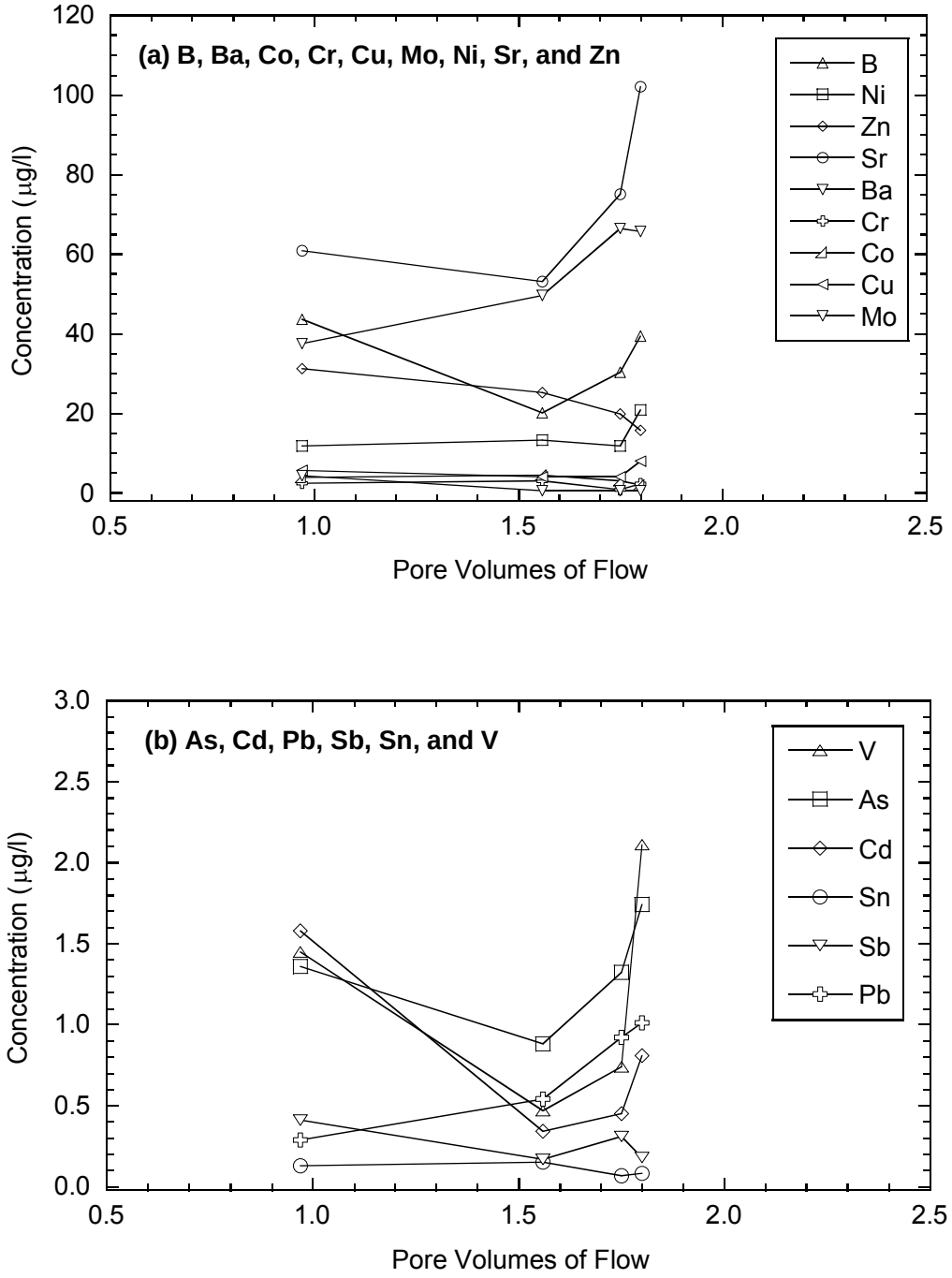

Fig. 11 Concentrations of trace elements in leachate collected in lysimeter in Waseca: (a) elements with peak concentrations between 3 and 102 g/L and (b) elements with peak concentrations less than 2.5 g/L.

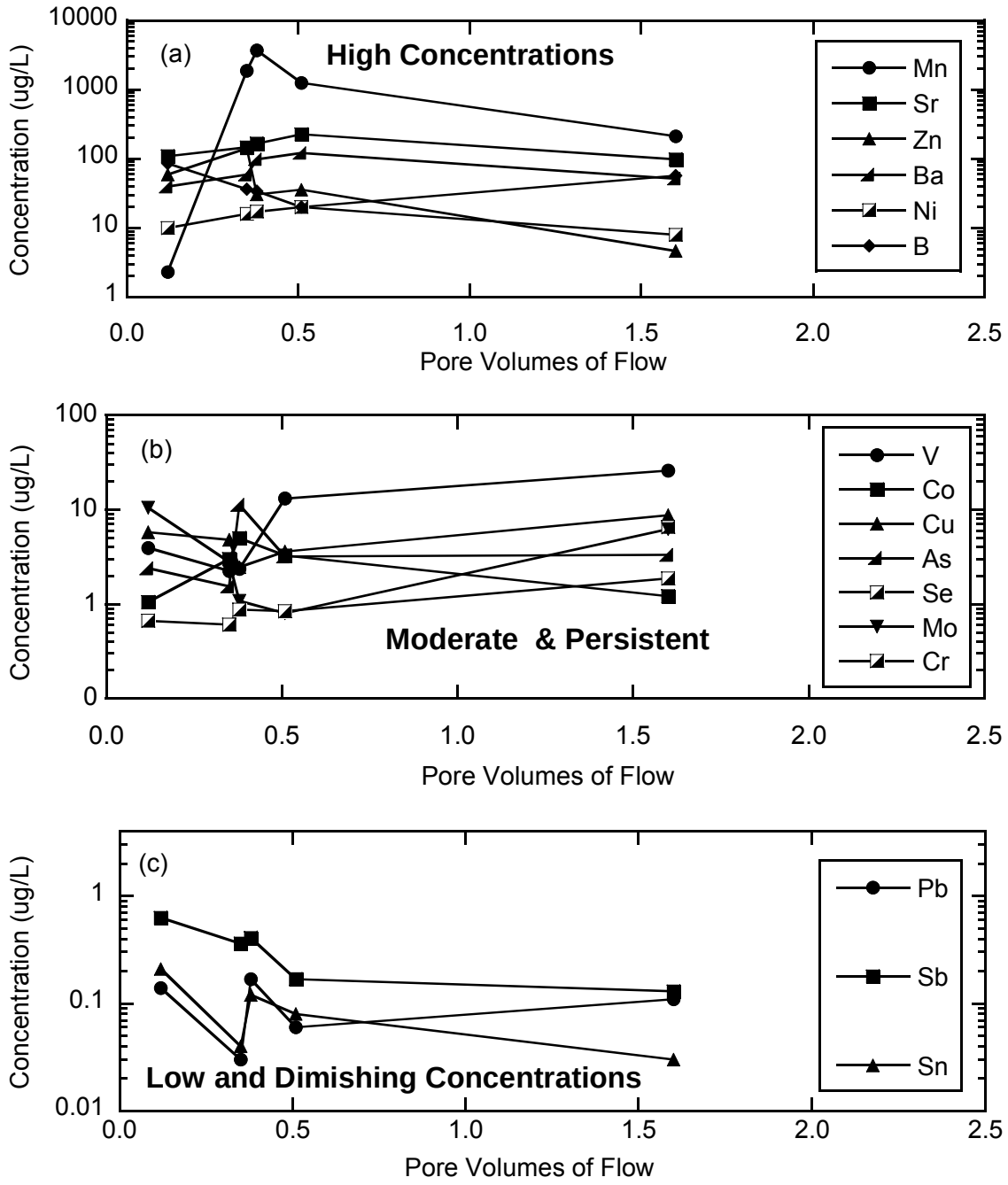

Fig. 12 Concentrations of trace elements in leachate collected in Chisago lysimeter: (a) elements with high concentrations, (b) elements with moderate and persistent concentrations and (c) elements with low and diminishing concentrations.

FLY ASH STABILIZATION OF RECYCLED ASPHALT PAVEMENT MATERIAL IN WASECA, MINNESOTA

by

Lin Li, Craig H. Benson, Tuncer B. Edil, and Bulent Hatipoglu

Geo Engineering Report No. 06-18

Department of Civil and Environmental Engineering
University of Wisconsin-Madison
Madison, Wisconsin 53706
USA

June 9, 2006

EXECUTIVE SUMMARY

This report describes a field site where Class C fly ash was used to stabilize recycled pavement material (RPM) during construction of a flexible pavement in Waseca, MN. The project consisted of pulverizing the existing hot-mix asphalt (HMA), base, and subgrade to a depth of 300 mm to form RPM, blending the RPM with fly ash (10% by dry weight) and water, compacting the RPM, and placement of a new HMA surface. California bearing ratio (CBR), resilient modulus (M_r), and unconfined compression (q_u) tests were conducted on the RPM alone and the fly-ash stabilized RPM (SRPM) prepared in the field and laboratory to evaluate how addition of fly ash improved the strength and stiffness. *In situ* testing was also conducted on the RPM and SRPM with a soil stiffness gauge (SSG), dynamic cone penetrometer (DCP), and falling weight deflectometer (FWD). A pan lysimeter was installed beneath the roadway to monitor the quantity of water percolating from the pavement and the concentration of trace elements in the leachate. A column leaching test was conducted in the laboratory for comparison.

Addition of fly ash improved the stiffness and strength of the RPM significantly. After 7 d of curing, the SRPM prepared in the laboratory using materials sampled during construction had CBR ranging between 70 and 94, M_r between 78 and 119 MPa, and unconfined compressive strengths between 284 and 454 kPa, whereas the RPM alone had CBR between 3 and 17 and M_r between 46 and 50 MPa. Lower CBR, M_r, and q_u were obtained for SRPM mixed in the field relative to the SRPM mixed in the laboratory (64% lower for CBR, 25% lower for M_r, and 50% lower for q_u). Moduli back-calculated from the FWD data were in good agreement with those obtained with the SSG, but were higher than moduli obtained from the M_r tests due to differences in the magnitude of the bulk stress and strain existing in situ and applied in the laboratory. Testing conducted approximately one year after construction showed no degradation in the modulus of the SRPM, even though the SRPM underwent a freeze-thaw cycle.

Percolation from the pavement was seasonally dependent, with peak flows occurring in summer and no flow occurring in winter. Approximately 2 pore volumes of flow (PVF) drained from the lysimeter during the monitoring period. Analysis of leachate collected in the lysimeter showed that concentrations of many trace elements were increasing toward the end of the study, indicating that longer-term monitoring of the lysimeter is needed to characterize the field leaching behavior of the SRPM. In contrast, for the laboratory column test, leachate concentrations peaked within approximately one PVF and then leveled-off or diminished. For leachate collected in the lysimeter, concentrations of all but one element (Mn) were below USEPA maximum contaminant levels (MCLs) and health-risk levels (HRLs) established by the Minnesota Dept. of Public Health (Mn exceeded the HRL). For the column test, these thresholds were exceeded for B (HRL exceeded), Pb (MCL and HRL exceeded), Se (MCL and HRL exceeded), Sr (HRL exceeded), and Mn (HRL exceeded).

ACKNOWLEDGEMENT

Financial support for this study was provided by the Minnesota Local Road Research Board (LRRB). The study was administered by the Minnesota Department of Transportation (Mn/Dot). The conclusions and recommendations in this report are solely those of the authors and do not reflect the opinions or policies of LRRB or Mn/DOT. Appreciation is expressed to the City of Waseca's Department of Engineering for supporting the field investigation, providing FWD testing, and for monitoring the lysimeter. Xiaodong Wang, Jacob Sauer, Maria Rosa, and Onur Tastan assisted with the project in the field and laboratory.

TABLE OF CONTENTS

LIST OF TABLES

LIST OF FIGURES

1. INTRODUCTION

In-place recycling of pavement materials is an attractive method to rehabilitate deteriorated flexible pavements due to lower costs relative to new construction and the long-term societal benefits associated with sustainable construction methods. One approach is to pulverize and blend the existing hot-mix asphalt, base, and some of the subgrade to form a broadly graded granular material referred to as recycled pavement material (RPM) that can be used in place as base course for a new pavement. Blending is typically conducted to a depth of approximately 300 mm and, in cases where the surface elevation is fixed, some of the blended material is removed and used for other applications. The RPM is compacted to form the new base course and is overlain with new hot-mix asphalt (HMA).

The residual asphalt and fines from the underlying subgrade may result in RPM having lower strength and stiffness compared to compacted virgin base material. Thus, methods to enhance the strength and stiffness of RPM are being considered, including the addition of stabilizing agents such as asphaltic oils, cements, and self-cementing coal fly ash (a residue from coal combustion that is normally landfilled). Stabilization is believed to increase the service life of the rehabilitated pavement or permit a thinner HMA layer (Turner, 1997; Crovetti, 2000; Mallick et al., 2002; Wen et al., 2003; Robinson et al., 2004). The use of fly ash for stabilization is particularly attractive because fly ashes traditionally have been disposed in landfills. Consequently, using fly ash for stabilization promotes sustainable construction and improves the pavement structure (Edil et al., 2002; Bin-Shafique et al., 2004; Trzebiatowski et al., 2004). However, the effectiveness of stabilizing RPM with coal fly ash is largely undocumented. Providing documentation was a primary objective of this study.

This report describes a project where self-cementing Class C fly ash from a coal-fired electric power plant was used to stabilize a RPM during rehabilitation of a 0.5-km section of flexible pavement along 7th Avenue and 7th Street in Waseca, MN (≈ 125 km south of Minneapolis). RPM was prepared by pulverizing the existing asphalt pavement and underlying materials to a depth of 300 mm below ground surface (bgs) using a CMI RS-650-2 road reclaimer. The uppermost 75 mm of the RPM was removed and then Class C fly ash (10% by dry weight) was spread uniformly on the surface using truck-mounted lay-down equipment similar to that described in Edil et al. (2002). The fly ash was mixed with the RPM to a depth of 150 mm using the road reclaimer, with water being added during mixing using a water truck (see photographs in Appendix A). This mixture, which contained 10% fly ash by dry weight, was compacted within 1-2 h by a tamping foot compactor followed by a vibratory steel drum compactor. The SRPM was cured for 7 d and then overlain with 75 mm of HMA.

2. MATERIALS

2.1 Subgrade and RPM

Disturbed samples of subgrade soil and recycled pavement material (RPM) (≈ 20 kg each) were collected at 10 stations during construction (Fig. 1). Tests were conducted on each sample to determine index properties, soil classification, water content, dry unit weight, compaction characteristics (RPM only), and CBR.

A summary of the properties of the subgrade is shown in Table 1. Particle size distribution curves for the subgrade are shown in Fig. 2. The subgrade consists of highly plastic organic clay (CH) or silt (MH), clayey sand (SC), or silty sand (SM) according to the Unified Soil Classification System. However, coarse silty gravel is present in one region (Station 3). According to the AASHTO Soil Classification System, most of subgrade soils at this site are A-7 with a group index (GI) larger than 20. Two of the coarse-grained subgrade soils classify as A-2-7 (Stations 3 and 8) and have GI < 2. CBR of the subgrade soils ranges from 2 to 11 (mean = 5), indicating that the subgrade is soft.

A summary of the properties of the RPM is shown in Table 2 and particle size distribution curves for the RPM are shown in Fig. 2. The blending during production of RPM results in a material that is spatially uniform in particle size distribution, compaction characteristics, and water content. The particle size distribution curves fall in a relatively narrow band (Station 1 excluded) and have the convex shape typically associated with crushed materials that are not post-processed. Most of the RPM consists of sand and gravel-size particles (> 75 μm), which reflects the presence of the pulverized asphalt and the original base course. The *in situ* water content of the RPM was approximately 4% dry of optimum water content based on standard compaction effort (ASTM D 698).

2.2 Fly Ash

Fly ash from Unit 7 of the Riverside Power Station in St Paul, MN was used for stabilization. Chemical composition and physical properties of the fly ash are summarized in Table 3 along with the composition of typical Class C and F fly ashes. The calcium oxide (CaO) content is 24%, the silicon dioxide (SiO_2) content is 32%, the CaO/SiO_2 ratio (indicative of cementing potential, Edil et al., 2006) is 0.75, and the loss on ignition is 0.9%. According to ASTM C 618, Unit 7 fly ash is a Class C fly ash.

2.3 SRPM

Water content and unit weight of the compacted SRPM were measured at each station using a nuclear density gage (ASTM D 2922) immediately after compaction was completed. Grab samples (≈ 20 kg) of SRPM were also collected at these locations and were immediately compacted into a CBR mold (114 mm inside diameter x 152 mm height) and a resilient modulus mold (102 mm inside diameter x 203 mm height) to the unit weight measured with the nuclear density gage. Three lifts were used for the CBR specimens and six lifts were used for the M_r specimens. After compaction, the specimens were sealed in plastic and stored at 100% humidity for curing (7 d for CBR specimens, 14 d for M_r and q_u specimens). These test specimens are referred to henceforth as 'field-mix' specimens. Because of the cementing effects of the fly ash, index testing was not conducted on the SRPM.

Undisturbed samples of SRPM were also collected after compaction using thin-wall sampling tubes. These samples were cured at 25 ^oC and 100% relative humidity for 14 d. However, disturbance incurred during sampling or extrusion rendered the undistributed samples

useless. Similar problems with samples collected with thin-wall tubes have been reported for fly-ash stabilized soils (Edil et al. 2002) and cement-stabilized wastes (Benson et al. 2002).

Specimens of SRPM were also prepared in the laboratory using samples of the RPM and fly ash collected during construction. These specimens, referred to henceforth as 'laboratory-mix' specimens, were prepared with 10% fly ash (dry weight) at the mean field water content (7.9%) and mean dry unit weight (19.1 kN/m^3). The laboratory-mix specimens were compacted and cured using the procedures employed for the field-mix specimens. A similar set of specimens was prepared with RPM only (no fly ash) using the same procedure, except for the curing phase.

3. LABORATORY TEST METHODS

3.1 CBR

The CBR tests were conducted in accordance with ASTM D 1883 after 7 d of curing (field-mix or laboratory-mix SRPM) or immediately after compaction (RPM). The specimens were not soaked and were tested at a strain rate of 1.3 mm/min. The 7-d curing period and the absence of soaking are intended to represent the competency of the RPM when the HMA is placed (Bin-Shafique et al., 2004). Data from the unsoaked CBR tests were not intend as a measure of stiffness of the SRPM and are not for use in pavement design with SRPM.

3.2 Resilient Modulus and Unconfined Compression Tests

Resilient modulus tests on the SRPM and RPM were conducted following the methods described in AASHTO T292 after 14 d of curing (SRPM) immediately after compaction (RPM). The 14-d curing period is based on recommendations in Turner (1997), and is intended to reflect the condition when most of the hydration is complete (Edil et al., 2006). The loading sequence for cohesive soils was used for the SRPM as recommended by Bin-Shafique et al. (2004) and Trzebiatowski et al. (2004) for soil-fly ash mixtures. RPM was tested using the loading sequence for cohesionless soils. Five specimens of field-mix SRPM split horizontally after curing. These specimens were trimmed to an aspect ratio of 1 prior to testing. All other specimens had an aspect ratio of 2.

Unconfined compressive strength was measured on specimens of SRPM after the resilient modulus tests were conducted. Only those specimens having an aspect ratio of 2 were tested. The strains imposed during the resilient modulus test may have reduced the peak

undrained strength of the SRPM. However, strains in a resilient modulus test are small. Thus, the effect on peak strength is believed to be negligible.

A strain rate of 0.21%/min was used for the unconfined compression tests following the recommendations in ASTM D 5102 for compacted soil-lime mixtures. No standard method currently exists for unconfined compression testing of materials stabilized with fly ash, including stabilized RPM.

3.3 Column Leaching Test

A column leaching test (CLT) was conducted on a specimen of field-mix SRPM collected from Station 9. The specimen was prepared in the field in a standard Proctor compaction mold (height = 116 mm, diameter = 102 mm) using the same procedure employed for the specimens of field-mix SRPM prepared for CBR testing. The specimen was cured for 7-d prior to testing.

The CLT was conducted following the procedure described in ASTM D 4874, except a flexible-wall permeameter was used instead of a rigid-wall permeameter. Flow was oriented upward and was driven by a peristaltic pump set to provide a Darcy velocity of 2 mm/d. The effective confining pressure was set at 15 kPa. A 0.1 M LiBr solution was used as the permeant liquid to simulate percolate in regions where salt is used to manage ice and snow (Bin-Shafique et al. 2006). Effluent from the column was collected in sealed Teflon bags to prevent interaction with the atmosphere. Leachate was removed from the bags periodically (≈ 30 ~ 60 mL of flow accumulation). Volume of the leachate removed was measured, the pH was recorded, and a sample was prepared for chemical analysis by filtering with a 0.45 μm filter and preservation with nitric acid to pH < 2.

All effluent samples were analyzed by inductively coupled plasma-mass spectrometry (ICP-MS) following the procedure described in USEPA Method 200.8. Analysis was conducted for the following elements (detection limits in μg/L in parentheses): Ag (0.02), As (0.1), B (0.2), Ba (0.02), Be (0.02), Ca (5), Cd (0.08), Co (0.01), Cr (0.04), Cu (0.07), Hg (0.2), Mo (0.08), Mn (0.03), Ni (0.05), Pb (0.01), Sb (0.02), Se (2.0), Sn (0.04), Sr (0.01), Tl (0.006), V (0.06), and Zn (0.2).

4. FIELD METHODS

4.1 Environmental Monitoring

The environmental monitoring program consists of monitoring the volume of water draining from the pavement, concentrations of trace elements in the leachate, temperatures and water contents within the pavement profile, and meteorological conditions (air temperature, humidity, and precipitation). Monitoring of the pavement began in October 2004 and is still being conducted.

Leachate draining from the pavement was monitored using a pan lysimeter installed near the intersection of 7th Street and 7th Avenue (adjacent to Station 9, Fig. 1). The test specimen for the CLT (Section 3.3) was collected near the lysimeter so that a direct comparison could be made between leaching measured in the field and laboratory. The lysimeter is 4 m wide, 4 m long, and 200 mm deep and is lined with 1.5-mm-thick linear low density polyethylene geomembrane. The base of the lysimeter was overlain by a geocomposite drainage layer (geonet sandwiched between two non-woven geotextiles). SRPM was placed in the lysimeter and compacted using the same method employed when compacting SRPM in other portions of the project. Photographs showing the lysimeter are in Appendix B.

Water collected in the drainage layer is directed to a sump plumbed to a 120-L polyethylene collection tank buried adjacent to the roadway. The collection tank is insulated with extruded polystyrene to prevent freezing. Leachate that accumulates in the collection tank is removed periodically with a pump. The volume of leachate removed is recorded with a flow meter, a sample for chemical analysis is collected, and the pH and Eh of the leachate are recorded. The sample is filtered, preserved, and analyzed using the same procedures employed

for the CLT (Section 3.3). Personnel from the City of Waseca collected the samples from the lysimeter.

Air temperature and relative humidity (RH) are measured with a HMP35C temperature/RH probe manufactured by Campbell Scientific Inc. (CSI). A tipping bucket rain gage (CSI TE 525) with snowfall adaptor (CSI CS 705) is used to measure precipitation. Subsurface temperatures and water contents are monitored at three depths: 150 mm below ground surface (bgs) (mid-depth of the SRPM) and 425 and 675 mm bgs (subgrade). Type-T thermocouples are used to monitor temperature and CSI CS616 water content reflectometers (WCRs) are used to monitor volumetric water content. The WCRs were calibrated for the materials on site following the method in Kim and Benson (2002). Data from the meteorological and subsurface sensors are collected with a CSI CR10 datalogger powered by a 12-V deep-cycle battery and a solar panel. Data are downloaded from the datalogger via telephone modem. Photographs of the instrumentation are included in Appendix B.

4.2 Mechanical Evaluation of Pavement Materials

Strength and stiffness of the SRPM were measured with a soil stiffness gauge (SSG), a dynamic cone penetrometer (DCP), a rolling weight deflectometer (RWD), and a falling weight deflectometer (FWD). Photographs of the testing are included in Appendix A. Testing with the SSG, DCP, and RWD was conducted directly on the SRPM after 7 d of curing. FWD testing was conducted two times after the HMA was placed (November 2004 and August 2005). The RWD testing was unsuccessful due to problems with the instrumentation and will not be discussed further.

The SSG tests were conducted in accordance with ASTM D 6758 using a Humboldt GeoGauge. Two measurements were made at each station within a 0.1-m radius. These measurements deviated by less than 10%. Thus, the mean of the two stiffness measurements is reported herein. DCP testing was conducted at each station in accordance with ASTM D 6951 using a DCP manufactured by Kessler Soils Engineering Products Inc. The dynamic penetration index (DPI) obtained from the DCP was computed as the mean penetration (mm per blow) over a depth of 150 mm.

FWD tests were conducted at each station by Braun Intertec Inc. in November 2004 (3 months after construction) and in August 2005 (one year after construction) using a Dynatest™ 8000E FWD following the method described in ASTM D 4694. Moduli were obtained from the FWD deflection data by inversion using MODULUS 5.0 from the Texas Transportation Institute. Analysis of the FWD data was conducted at the University of Wisconsin-Madison.

5. ENVIRONMENTAL DATA

5.1 Meteorological and Subsurface Conditions

Air and soil temperatures between October 2004 and April 2006 are shown in Fig. 3. Data are not shown between April 2005 and May 2005 due to an instrument malfunction. The air temperature ranged from -28 and 32 ^{o}C during the monitoring period, with sub-freezing temperatures occurring between October and April each year. Temperature of the SRPM and the subgrade ranged between -12 ^{o}C and 32 ^{o}C and varied seasonally with the air temperature. The magnitude and frequency of variation diminishes with depth, which reflects the thermal damping provided by the pavement materials.

Frost penetrated to approximately 0.5 m bgs each year, as illustrated by the drop in temperature below 0 ^{o}C at depths T1 and T2 and the drops in volumetric water content at T2 when the soil temperature falls below 0 ^{o}C (volumetric water contents are not reported in Fig. 3 for periods when freezing was established). These apparent drops in water content reflect freezing of the pore water. The water content measured by WCRs is determined by measuring the velocity of an electromagnetic wave propagated along the probe. The velocity of the wave varies with the apparent dielectric constant of the soil, which is dominated by the dielectric constant of the water phase. When the pore water freezes, the dielectric constant of the water phase drops significantly, which appears as a drop in water content in WCR data (Benson and Bosscher 1999).

Higher water contents were recorded in the fine-textured subgrade than the coarse-grained SRPM, which reflects the greater propensity of fine-textured soils to retain water. No spikes are present in the water content records, which reflects the ability of the HMA to impede infiltration during precipitation and snow melt events and to limit evaporation during drier

periods. The annual variation in water content is also small, with the water content of the SRPM varying between 21 and 26% and the water content of the subgrade varying between 35 and 45%. Higher water contents are recorded in the summer months, when greater precipitation occurs.

The seasonal variation in water content is also reflected in the seasonal variation in drainage collected in the lysimeter, as shown in Fig. 4. The drainage rate varies between 0-1 mm/d throughout the year, with drainage beginning in mid- to late spring (May to June) and the peak drainage rate occurring in mid-summer (July to August). The drainage rate then diminishes to zero by early fall, and remains nil until early spring. On an annual basis, the drainage rate is 0.15 mm/d or 56 mm/yr. A complete summary of the lysimeter data is in Appendix C.

5.2 Trace Elements in Lysimeter Drainage

Approximately 1.8 pore volumes of flow (PVF) have passed through the SRPM during the monitoring period. During this period, pH of the drainage has been near neutral (6.9 – 7.5) and oxidizing conditions have prevailed (Eh = 48-196 mV). A summary of the pH and Eh data along with the trace element concentrations is in Appendix C.

Concentrations of trace elements in drainage from the lysimeters are shown in Fig. 5 as a function of PVF. Elements with peak concentrations between 3 and 102 μg/L are shown in Fig. 5a, whereas those with peak concentrations less than 2.5 μg/L are shown in Fig. 5b. Elements not shown in Fig. 5 include those below the detection limit (Be, Ag, Hg, Se, and Tl) and elements not typically associated with health risks (Ca and Mn). All of the concentrations are below USEPA maximum contaminant levels (MCLs) and Minnesota health risk levels (HRLs). The exception is Mn (not shown in Fig. 5), which typically had concentrations between 1 and 2

mg/L. The Minnesota HRL for Mn currently is 100 μg/L, but plans exist to increase the HRL to 1.0-1.3 mg/L (www.pca.state.mn.us). USEPA does not have a MCL for Mn.

Most of the concentrations appear to be increasing, with a more rapid increase towards the end of the monitoring. Thus, higher concentrations are likely to be observed for many of the elements as the lysimeter is monitored in the future. However, concentrations of some elements appear to be decreasing (Mo and Sr) or remaining steady (Sb and Sn). The lack of a steady-state condition or clearly diminished concentrations for most of the trace elements highlights the need for longer term monitoring of the lysimeter.

5.3 Trace Elements in CLT Effluent

Effluent from the CLT had pH between 7.3 and 7.8, which is slightly higher than the pH observed in the leachate from the lysimeter. Concentrations of trace elements in the effluent from the CLT on the SRPM are shown in Fig. 6. Elements having peak concentrations less than 1 μg/L and elements not typically associated with health risks (Ca and Mn) are not shown in Fig. 6. Elements having peak concentrations exceeding 100 μg/L are shown in Fig. 6a, whereas those with peak concentrations less than 100 μg/L are shown in Fig. 6b. A compilation of the data is in Appendix D.

Comparison of Figs. 5 and 6 indicates that the trace element concentrations in the CLT effluent (Fig. 6) typically are higher than concentrations in the drainage collected in the field (Fig. 5). The poor agreement suggests that the CLT test method that was used may not be appropriate for evaluating leaching of trace elements from SRPM, unless a conservative estimate of the trace element concentrations is acceptable. Despite the higher concentrations obtained from the CLT, most of the elements have concentrations below USEPA MCLs and Minnesota

HRLs. The exceptions are for B (peak = 2196 μg/L, no MCL, HRL = 600 μg/L,), Pb (peak = 19 μg/L, MCL = 15 μg/L, HRL = 15 μg/L), Se (peak = 60 μg/L, MCL = 50 μg/L, HRL = 30 μg/L), and Sr (peak = 4023 μg/L, no MCL, HRL = 4000 μg/L). The peak Mn concentration (468 μg/L, not shown in Fig. 6) was also above the current Minnesota HRL for Mn, but is less than the proposed HRL.

The elution behavior observed in the CLT effluent follows two patterns: (i) delayed response, where the concentration initially increases and then falls, and (ii) persistent leaching, where the concentration initially increases and then remains relatively constant. Most of the elements with peak concentrations exceeding 100 μg/L (Fig. 6a) exhibit the persistent leaching pattern (B, Ba, Sr, and Mo), whereas those exhibiting delayed response typically have peak concentrations less than 100 μg/L (Fig. 6b) (Co, Cr, Pb, and Se). The exceptions are Cu and Zn, which have peak concentrations exceeding 100 μg/L and exhibited a delayed response, and As and V, which have peak concentrations less than 100 μg/L and exhibit the persistent leaching pattern.

6. PROPERTIES OF SRPM AND RPM

6.1 Laboratory Test Data

CBR, M_r, and q_u of the SRPM and RPM are summarized in Table 4. Tests were conducted on RPM and laboratory-mix SRPM using samples of RPM from Stations 1, 4 and 7. Samples from these stations were selected to bracket the range of gradation of the RPM (Stations 1 and 7) and to represent typical RPM (Station 4) (see Fig. 2). Tests were conducted on both RPM and SRPM to determine the benefits of adding fly ash to the mixture in terms of strength and stiffness.

CBR of the RPM and SRPM along the alignment of the project is shown in Fig. 7. Stations 1-8 correspond to locations along 7th Avenue and Stations 9 and 10 are along 7th Street (Fig. 1). There is no systematic variation in CBR of the RPM or SRPM along the alignment, suggesting that the variability in the CBR is more likely due to heterogeneity in the material rather than systematic variation in site conditions or construction methods. CBR of the RPM ranges from 3 to 17 (mean = 9), the laboratory-mix SRPM has CBR between 70 and 94 (mean = 84), and the field-mix SRPM has CBR between 13 and 53 (mean = 29). Thus, adding fly ash to the RPM increased the CBR appreciably, although the CBR in the field was 66% lower, on average, than the CBR of the laboratory-mix SRPM. The CBR of the field-mix SRPM also was more variable than the CBR of the laboratory-mix SRPM.

A similar difference between CBRs of mixtures prepared with fly ash in the laboratory and field is reported in Bin-Shafique et al. (2004) for fine-grained subgrade soils. They report that field mixtures of silty clay and Class C fly ash typically have a CBR that is one-third of the CBR of comparable mixtures prepared in the laboratory. Bin-Shafique et al. (2004) attribute

these differences in CBR to more thorough blending of soil and fly ash in the laboratory compared to the field, resulting in more uniform distribution of cements within the mixture.

Resilient moduli of RPM, field-mixed SRPM, and lab-mixed SRPM are shown in Fig. 8 and are summarized in Table 4. These M_r correspond to a deviator stress of 21 kPa, which represents typical conditions within the base course of a pavement structure (Tanyu et al. 2003, Trzebiatowski et al. 2004). Complete M_r curves are included in Appendix E. As observed for CBR, there is no systematic variation in M_r along the alignment. Comparison of the M_r for RPM and SRPM in Fig. 8 and Table 4 indicates that adding fly ash increased the M_r. For the RPM, the M_r ranges between 45 and 50 MPa (mean = 47 MPa), whereas the field-mix SRPM had M_r between 50 and 111 MPa (mean = 78 MPa) and the laboratory-mix SRPM had M_r ranging between 78 and 119 (mean = 104 MPa). As with CBR, M_r of the field-mix SRPM is lower (25%, on average) and more variable than the M_r of the laboratory-mix SRPM.

Unconfined compressive strengths are shown in Fig. 9 and Table 4 for the field-mix and laboratory-mix SRPM. Strengths are not reported for RPM because the RPM is essentially non-cohesive and therefore is not amenable to q_u testing. Data are missing at some of the stations for the field-mix SRPM because the specimens had an aspect ratio less than 2 and could not be tested to determine q_u. As with CBR and M_r, there is no systematic variation in q_u along the alignment. In addition, q_u of the field-mix SRPM is less than one-half of the q_u of the laboratory-mix SRPM, on average. Bin-Shafique et al. (2004) also found that q_u of their field-mix specimens ranged between one-half and two-thirds of the q_u of laboratory-mix specimens.

6.2 Field Test Data

In situ stiffness measured with the SSG and dynamic penetration index (DPI) measured with the DCP are shown in Fig. 10 for the RPM and the SRPM after 7 d of curing. Addition of the fly ash and compaction increased the strength and stiffness appreciably, with the DPI decreasing from 17 to 12 mm/blow, on average, and the stiffness increasing from 6 to 17 MN/m, on average. The DPI and stiffness of the SRPM are also less variable than those of the RPM.

Maximum deflections from the FWD tests for the 40-kN drop are shown in Fig. 11. Maximum deflection, which is measured at the center of the loading plate, is a gross indictor of pavement response to dynamic load. FWD tests were conducted in November 2004 and August 2005 to define the as-built condition and the condition after one year of winter weather. Similar deflections were measured during both surveys, suggesting that the SRPM had maintained its integrity even after exposure to freezing and thawing. The deflection at Stations 4-10 is slightly higher in 2005 than 2004. However, this difference is not caused by a decrease in modulus of the SRPM, as shown subsequently. A more likely cause is the higher temperature of the HMA in August relative to November.

Elastic moduli of the SRPM that were obtained by inversion of the FWD data are shown in Fig. 12a. For the inversion, a three-layer profile was assumed that consisted of asphalt (75-mm thick), SRPM (150-mm thick), and an infinitely thick subgrade. Modulus of the asphalt was allowed to vary between 345 and 11,750 MPa and the Poisson's ratio was set as 0.4. The SRPM was assumed to have a Poisson's ratio of 0.35 and the modulus was allowed to vary between 70-9400 MPa. The subgrade was assumed to have a Poisson's ratio of 0.35.

The modulus of the SRPM varies between 57 and 1248 MPa (mean = 262 MPa) in November 2004 and between 79 and 1379 MPa (mean = 252 kPa) in August 2005. Most of the

moduli are less than 200 MPa. The most significant exception is the very high modulus at Station 3. This modulus is believed to be an anomaly caused by the coarse gravel subgrade near Station 3 (Fig. 2), which was not included in the inversion.

Comparison of the moduli in November 2004 and August 2005 in Fig. 12a suggests that the SRPM was not affected by exposure to freezing and thawing. The close agreement between the mean moduli in November 2004 and August 2005 (262 vs. 252 MPa) also suggests that freeze-thaw cycling did not affect the SRPM. To test this assertion, the data from 2004 and 2005 were compared with a t-test at a significance level of 0.05. The t-test yielded a t-statistic of 0.060 and p of 0.952, confirming that the moduli measured in November 2004 and August 2005 are not statistically different (i.e., $p = 0.952 >> 0.05$).

Moduli obtained from the FWD inversion are compared with those obtained from the resilient modulus tests on field-mix specimens and the moduli computed from the stiffness measured with the SSG in Fig. 12b. Elastic modulus (E) was computed from the SSG stiffness (K_{SSG}) using (Sawangsuriya et al., 2003):

$$E = \frac{K_{SSG}(1-\upsilon^2)}{1.77\,R} \tag{1}$$

where R is the outside radius of the SSG foot (0.057 m) and υ is Poisson's ratio (assumed to be 0.35). Moduli obtained from the SSG and the FWD are comparable, whereas those from the resilient modulus tests are approximately one-half of those from the SSG and the FWD. Tanyu et al. (2003) and Trzebiatowski et al. (2004) report similar differences between moduli measured determined with FWD, SSG, and resilient modulus test, and attribute the differences in the

moduli to differences in the strain imposed in each test (shear strain ≈ 0.07% for SSG and FWD vs. 0.07% ~ 0.15% for M_r, Sawangsuriya et al., 2003).

7. CONCLUSIONS AND RECOMMENDATIONS

A case history has been described where Class C fly ash (10% by weight) was used to stabilize recycled pavement material (RPM) during construction of a flexible pavement. California bearing ratio (CBR), resilient modulus (M_r), and unconfined compression (q_u) tests were conducted on the RPM alone and fly-ash stabilized RPM (SRPM) mixed in the field and laboratory to evaluate how addition of fly ash improved the strength and stiffness. *In situ* testing was also conducted on the RPM and SRPM with a soil stiffness gauge (SSG), dynamic cone penetrometer (DCP), and falling weight deflectometer (FWD). A pan lysimeter was installed beneath the pavement to monitor the rate of drainage and trace element concentrations in the leachate. A column leaching test was also conducted on a sample of SRPM collected during construction.

SRPM mixed in the laboratory using materials sampled during construction had significantly higher CBR, M_r, and unconfined compressive strength than RPM that was not stabilized with fly ash. This finding suggests that fly ash stabilization of RPM should be beneficial in terms of increasing pavement capacity and service life. However, the CBR, M_r, and unconfined compressive strength for SRPM mixed in the field were lower than those for SRPM mixed in the laboratory (64% lower for CBR, 25% lower for M_r, and 50% lower for q_u). Similar biases between mixtures prepared in the laboratory and field has been observed by others. Given that mixtures prepared in the laboratory are likely to be used for materials characterization for design, additional study is needed to determine how this bias should be considered in design calculations and how the bias may affect pavement performance in the long term.

Moduli back-calculated from the FWD data were in good agreement with those obtained with the SSG, but were higher than moduli obtained from the M_r tests due to differences in the

magnitude of the bulk stress and strain existing in situ and applied in the laboratory. More importantly, analysis of FWD data collected after a freeze-thaw cycle showed no degradation in the modulus. Nevertheless, longer-term monitoring is needed to confirm that the modulus of SRPM will persist after multiple winter seasons.

Percolation from the pavement occurred only in late spring, summer, and early fall with an average drainage rate of 56 mm/yr. Chemical analysis of the draining leachate showed that equilibrium was not established, with the concentrations of many trace elements increasing toward the end of the study. Thus, longer-term monitoring is needed to fully understand the potential for SRPM to leach trace elements during the service life of a pavement. However, during the monitoring period, none of the trace elements normally associated with health risks exceeded USEPA maximum contaminant levels (MCLs) or health-risk levels (HRLs) established by the Minnesota Dept. of Public Health. Additional study is also needed to define laboratory leach testing protocols that can more accurately simulate leaching of trace elements from SRPM.

8. REFERENCES

Benson, C.H. (2002), Containment systems: Lessons learned from North American failures, Environmental Geotechnics (4th ICEG), Swets and Zeitlinger, Lisse, pp. 1095-1112.

Benson, C.H. and Bosscher, P.J., 1999. Time-domain reflectometry in geotechnics: a review. In: W. Marr and C. Fairhurst (Editors), Nondestructive and Automated Testing for Soil and Rock Properties, ASTM STP 1350. ASTM International, West Conshohocken, PA, pp. 113-136.

Bin-Shafique, S., Benson, C.H., Edil, T.B. and Hwang, K., 2006. Leachate concentrations from water leach and column leach tests on fly-ash stabilized soils. Environmental Engineering 23(1), pp. 51-65.

Bin-Shafique, S., Edil, T.B., Benson, C.H. and Senol, A., 2004. Incorporating a fly-ash stabilised layer into pavement design. Geotechnical Engineering, Institution of Civil Engineers, United Kingdom, 157(GE4), pp. 239-249.

Crovetti, J.A., 2000. Construction and performance of fly ash-stabilized cold in-place recycled asphalt pavement in Wisconsin, Issues in Pavement Design and Rehabilitation. Transportation Research Record, pp. 161-166.

Edil, T.B., Acosta, H.A. and Benson, C.H., 2006. Stabilizing soft fine-grained soils with fly ash. Journal of Materials in Civil Engineering, 18(2), pp. 283-294.

Edil, T.B. et al., 2002. Field evaluation of construction alternatives for roadways over soft subgrade. Transportation Research Record, No. 1786: National Research Council, Washington DC, pp. 36-48.

FHWA, 2003. Fly Ash Facts for Highway Engineers. Federal Highway Administration, US Department of Transportation, Washington D.C., FHWA-IF-03-019.

Kim, K. and Benson, C.H. (2002), Water content calibrations for final cover soils, Geo Engineering Report 02-12, Geo Engineering Program, University of Wisconsin-Madison.

Mallick, R.B. et al., 2002. Evaluation of performance of full-depth reclamation mixes, Design and Rehabilitation of Pavements 2002. Transportation Research Record, pp. 199-208.

Robinson, G.R., Menzie, W.D. and Hyun, H., 2004. Recycling of construction debris as aggregate in the Mid-Atlantic Region, USA. Resource Conservation and Recycling, 42(3), pp. 275-294.

Sawangsuriya, A., Edil, T.B. and Bosscher, P.J., 2003. Relationship between soil stiffness gauge modulus and other test moduli for granular soils. Transportation Research Record, No. 1849: National Research Council, Washington D.C., pp. 3-10.

Tanyu, B., Kim, W., Edil, T., and Benson, C., 2003. Comparison of laboratory resilient modulus with back-calculated elastic modulus from large-scale model experiments and FWD tests on granular materials. Resilient Modular Testing for Pavement Components, American Society for Testing and Materials, West Conshohocken, PA. STP 1437, pp. 191-208.

Trzebiatowski, B., Edil, T.B. and Benson, C.H., 2004. Case study of subgrade stabilization using fly ash: State Highway 32, Port Washington, Wisconsin. In: A. Aydilek and J. Wartman (Editors), Beneficial Reuse of Waste Materials in Geotechnical and Transportation Applications, GSP No. 127. ASCE, Reston, VA, pp. 123-136.

Turner, J.P., 1997. Evaluation of western coal fly ashes for stabilization of low-volume roads, Testing Soil Mixed with Waste or Recycled Materials. American Society for Testing and Materials, West Conshohocken, PA. STP 1275, pp. 157-171.

Wen, H.F., Tharaniyil, M.P. and Ramme, B., 2003. Investigation of performance of asphalt pavement with fly-ash stabilized cold in-place recycled base course, Eighth International Conference on Low-Volume Roads 2003, Vol. 1 and 2. Transportation Research Record, pp. A27-A31.

TABLES

Table 1. Physical properties and classifications of subgrade soils.

Station	LL	PI	% Fines	GI	LOI (%)	Classification		CBR	w_N (%)	γ_d (kN/m^3)
						USCS	AASHTO			
1	61	41	72.2	29	2.1	CH	A-7	4	21.6	15.5
2	55	27	47.1	9	3.0	SC	A-7	11	13.6	18.2
3	69	30	8.5	0	13.0	GM	A-2-7	-	14.7	18.9
4	57	21	46.7	7	8.8	SM	A-7	2	25.8	14.6
5	122	53	70.2	45	18.3	MH	A-7	-	20.9	13.8
6	77	46	66.4	30	11.1	CH	A-7	5	26.8	14.9
7	69	49	73.8	36	3.4	CH	A-7	3	24.0	15.8
8	68	39	21.1	2	7.3	SC	A-2-7	2	25.7	15.4
9	62	35	67.9	23	3.2	CH	A-7	5	17.2	15.9
10	61	34	67.3	23	-	CH	A-7	-	50.1	12.0

Notes: LL = liquid limit, PI = Plasticity Index, % Fines = percentage passing No. 200 sieve, GI = group index, LOI = loss on ignition, USCS = Unified Soil Classification System, AASHTO = American Association of State Highway and Transportation Officials, CBR = California bearing ratio, w_N = in situ water content, γ_d = in situ dry unit weight, hyphen indicates test was not conducted.

Table 2. Particle size fractions, in situ water content, and compaction characteristics of RPM.

Station	% Gravel	% Sand	% Fines	w_N (%)	w_{opt} (%)	γ_{dmax} (kN/m^3)
1	14.5	69.1	16.4	7.1	11.6	19.6
2	33.6	54.0	12.4	6.6	-	-
3	41.1	55.6	3.3	6.7	-	-
4	33.3	58.0	8.7	7.6	12.0	19.6
5	23.8	65.1	11.1	6.5	-	-
6	40.7	53.1	6.3	6.8	-	-
7	46.7	47.9	5.4	7.3	11.2	20.1
8	30.1	62.6	7.3	ND	-	-
9	35.4	55.9	8.7	8.6	-	-
10	30.0	60.4	9.6	10.3	-	-

Notes: w_N = in situ water content, γ_d = in situ dry unit weight, w_{opt} = optimum water content, γ_{dmax} = maximum dry unit weight, hyphen indicates test was not conducted.

Table 3. Chemical composition and physical properties of Riverside 7 fly ash and typical Class C and F fly ashes.

Parameter	Percent of Composition		
	Riverside 7[+]	Typical Class C*	Typical Class F*
SiO_2 (silicon dioxide), %	32	40	55
Al_2O_3 (aluminum oxide), %	19	17	26
Fe_2O_3 (iron oxide), %	6	6	7
$SiO_2 + Al_2O_3 + Fe_2O_3$, %	57	63	88
CaO (calcium oxide), %	24	24	9
MgO (magnesium oxide), %	6	2	2
SO_3 (sulfur trioxide), %	2	3	1
CaO/SiO_2	0.75	-	-
$CaO/(SiO_2+Al_2O_3)$	0.47	-	-
Loss on Ignition, %	0.9	6	6
Moisture Content, %	0.17	-	-
Specific Gravity	2.71	-	-
Fineness, amount retained on #325 sieve, %	12.4	-	-

[+]provided by Lafarge North America, *from FHWA (2003).

Table 4. CBR, M_r, and q_u of RPM and SRPM.

Station	CBR			M_r (MPa)			q_u (kPa)	
	RPM	Field-Mix SRPM	Lab-Mix SRPM	RPM	Field-Mix SRPM	Lab-Mix SRPM	Field-Mix SRPM	Lab-Mix SRPM
1	17	28	70	50	57	NA	-	284
2	-	13	-	-	84	-	185	-
3	-	38	-	-	63	-	-	-
4	3	24	88	45	100	78	198	430
5	-	42	-	-	75	-	134	-
6	-	37	-	-	91	-	158	-
7	7	25	94	46	83	116	144	454
8	-	53	-	-	67	-	-	-
9	-	10	-	-	111	-	-	-
10	-	20	-	-	50	119	-	-

Notes: CBR = California bearing ratio, M_r = resilient modulus, q_u = unconfined compressive strength, hyphen indicates test not conducted, NA = not available because specimen damaged.

FIGURES

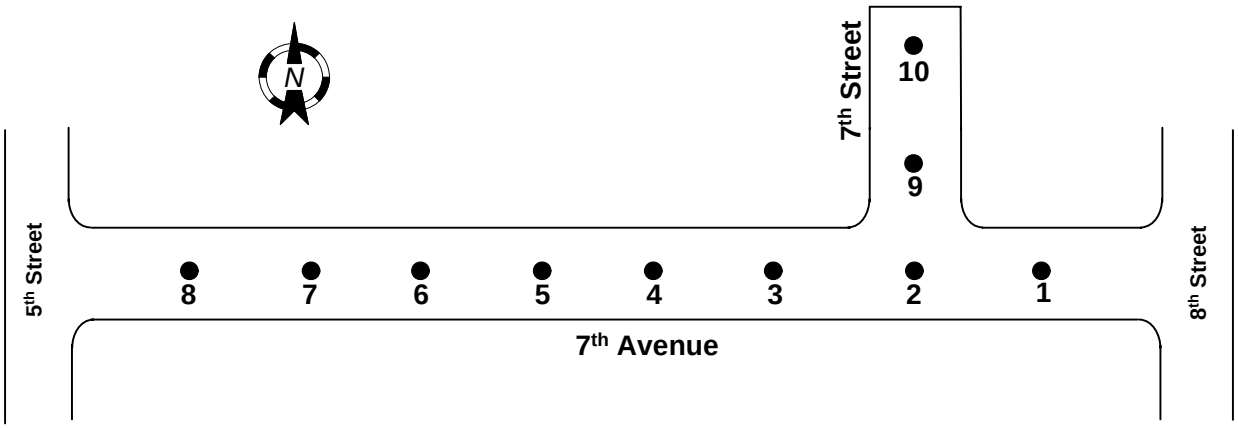

Fig. 1. Layout of stations along 7th Avenue and 7th Street in Waseca, MN.

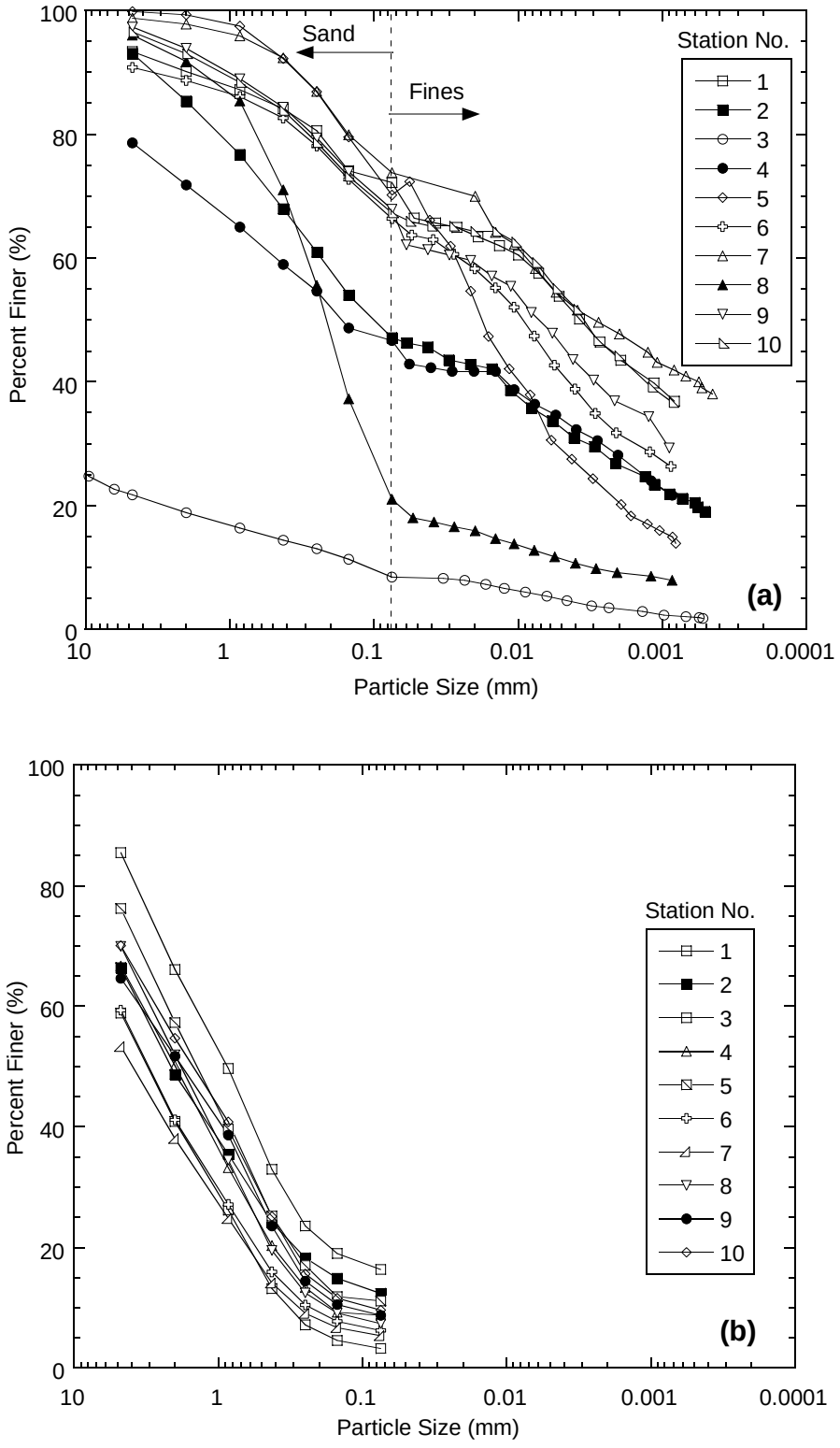

Fig. 2. Particle size distributions of the subgrade (a) and RPM (b).

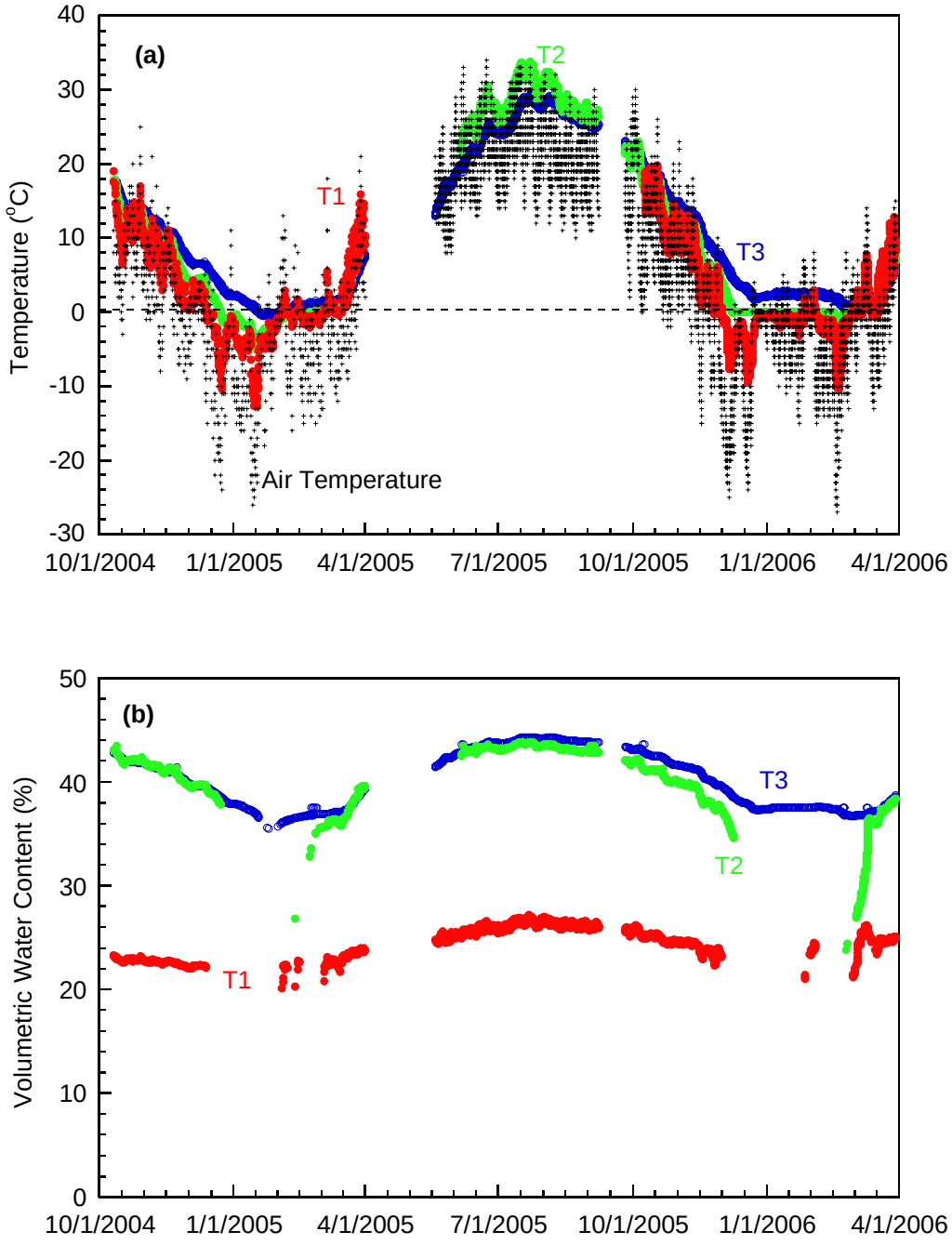

Fig. 3. Air and soil temperatures (a) and volumetric water content (b) of the SRPM and subgrade. Air temperature is shown in black. Soil temperature and water content measured at three depths: 150 mm bgs (mid-depth in SRPM) shown in red and designated as T1, 425 mm bgs (subgrade) shown in green and designated as T2, and 675 mm bgs (subgrade) shown in blue and designated as T3.

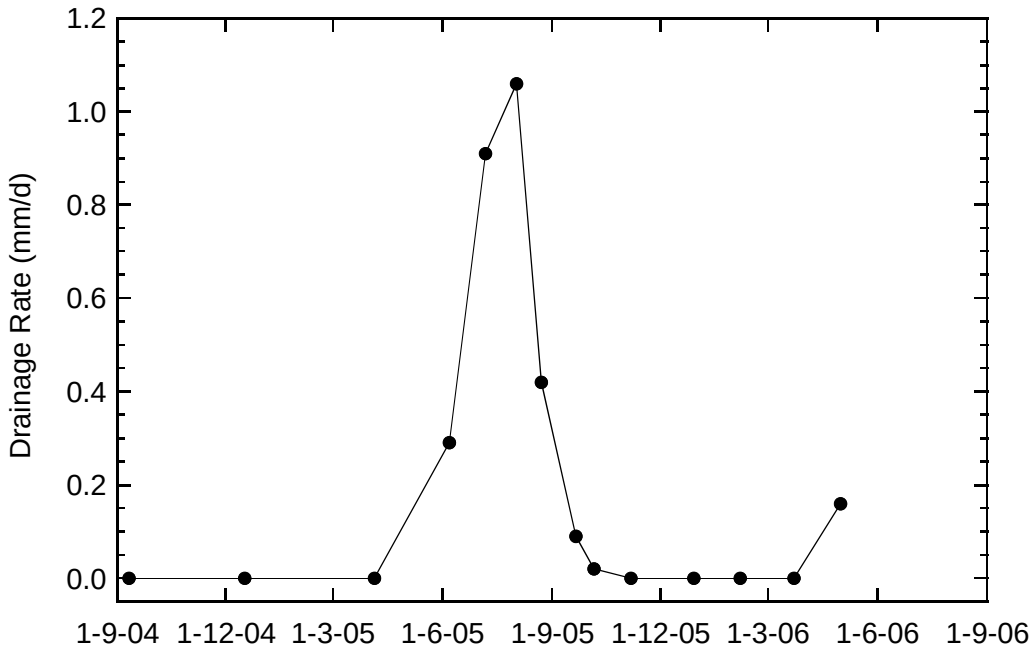

Fig. 4. Drainage from the pavement collected in the lysimeter. Base of lysimeter is located at the bottom of the SRPM layer.

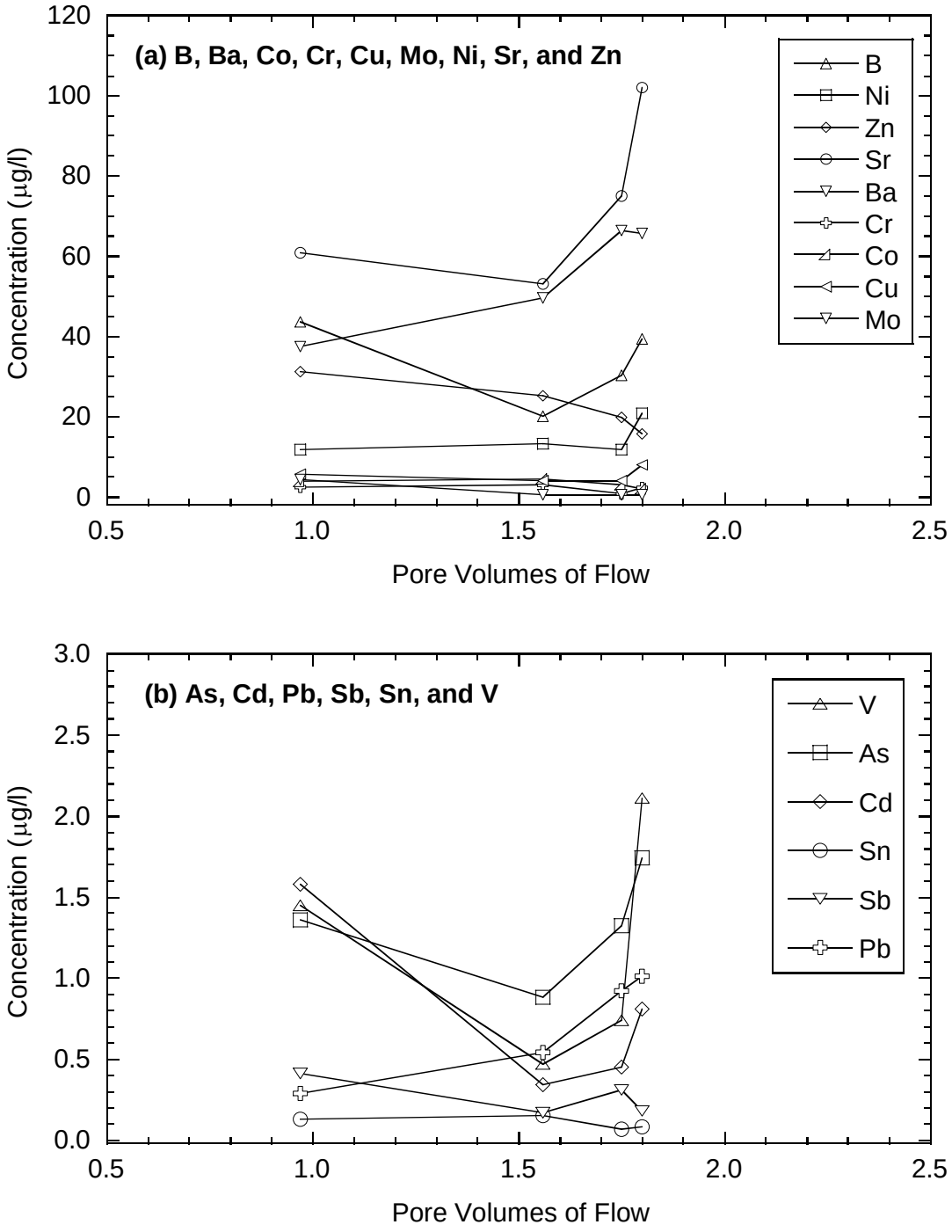

Fig. 5. Concentrations of trace elements in leachate collected in lysimeter: (a) elements with peak concentrations between 3 and 102 µg/L and (b) elements with peak concentrations less than 2.5 µg/L.

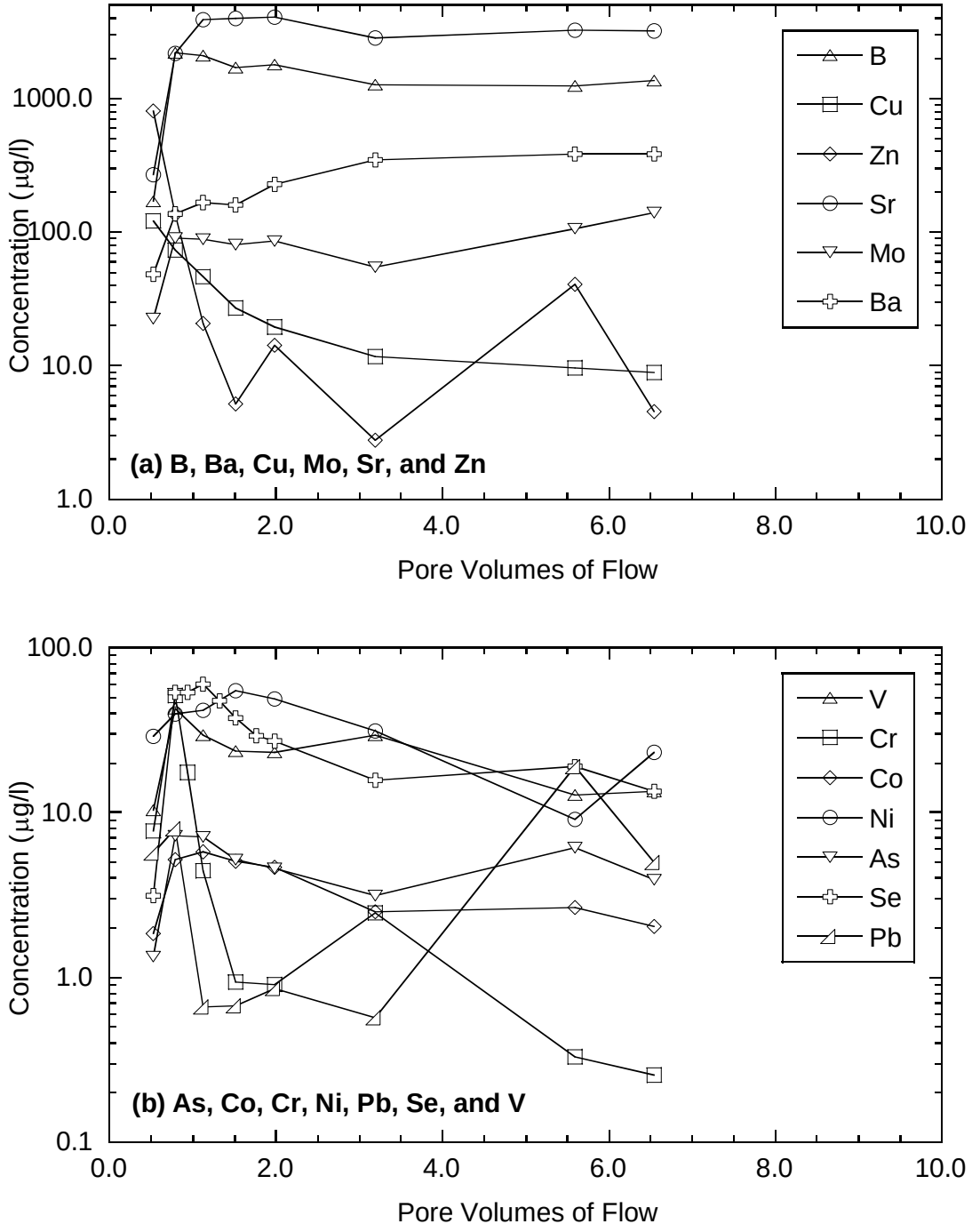

Fig. 6. Concentrations of trace elements in effluent from CLT on SRPM: (a) elements with peak concentrations exceeding 100 µg/L and (b) elements with peak concentrations less than 100 µg/L.

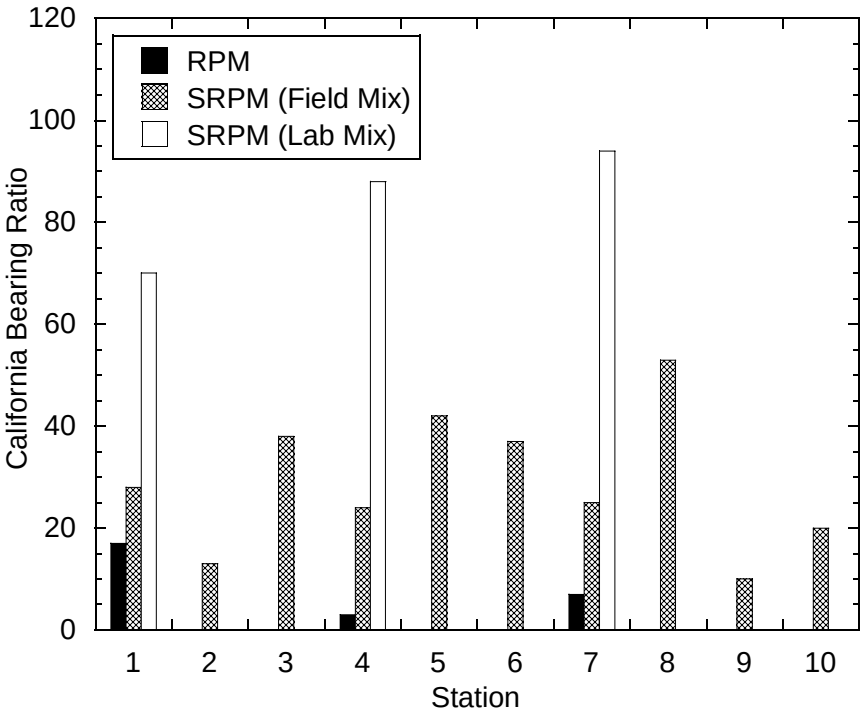

Fig. 7. California bearing ratio of RPM and SRPM (laboratory-mix and field-mix) after 7 d of curing.

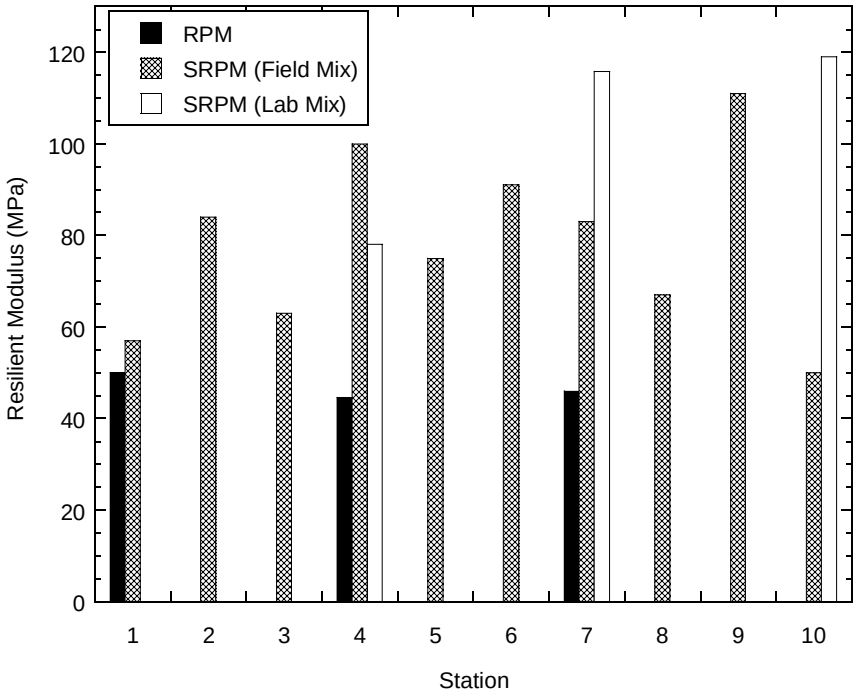

Fig. 8. Resilient modulus of RPM and SRPM (laboratory-mix and field-mix) after 14 d of curing.

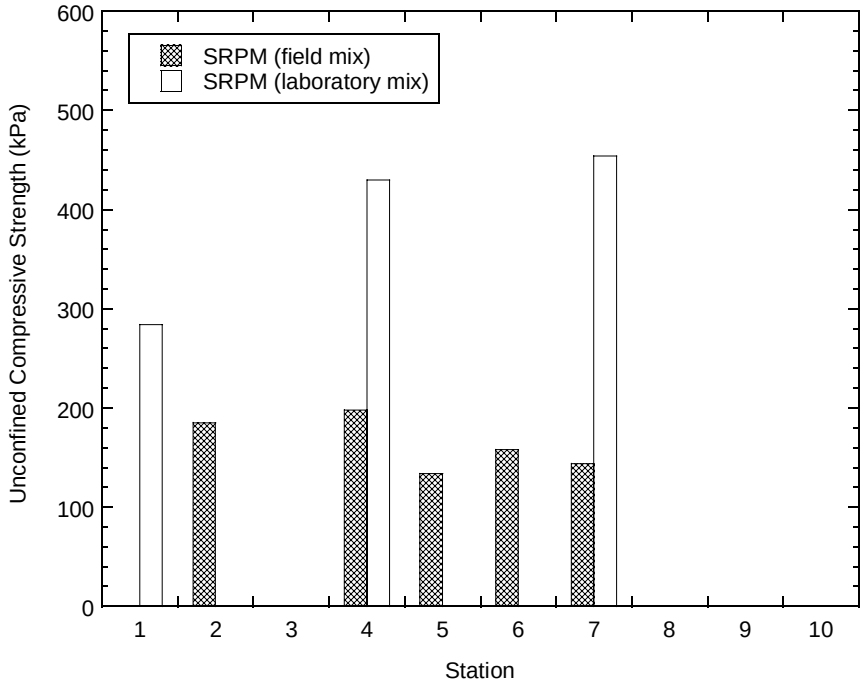

Fig. 9. Unconfined compressive strength (q_u) of SRPM (laboratory-mix and field-mix) after 7 d of curing.

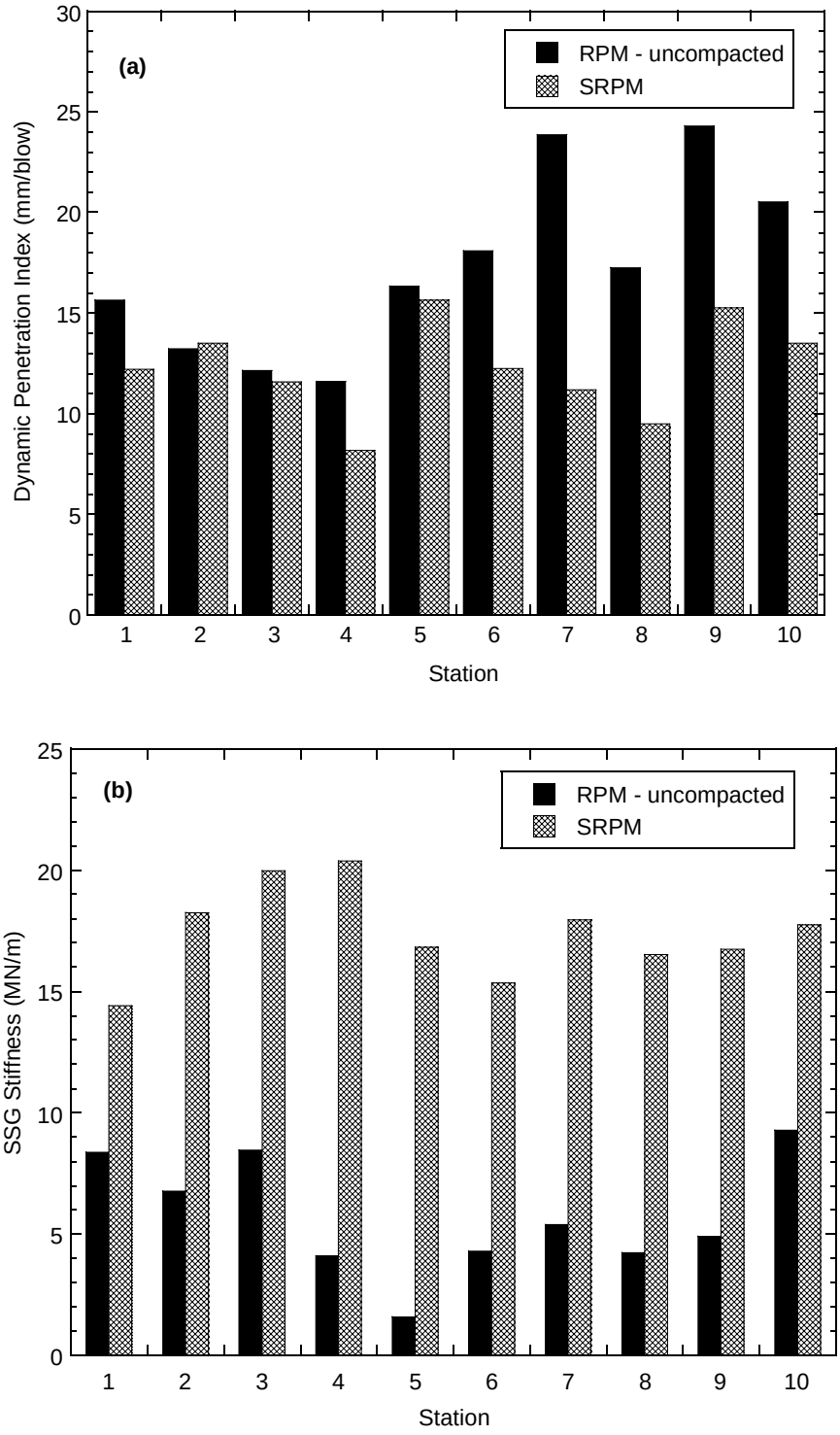

Fig. 10. Dynamic penetration index (DPI) and stiffness of uncompacted RPM and SRPM after compaction and 7 d of curing. DPI was measured with a DCP and stiffness was measured with a SSG.

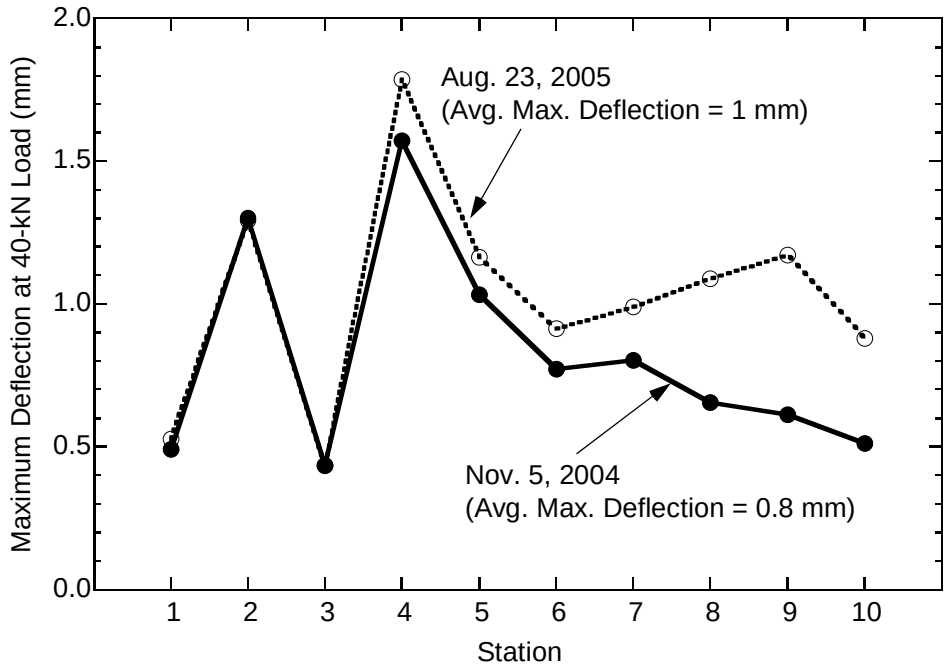

Fig. 11. Maximum deflection from the 40-kN drop for FWD tests conducted in November 2004 and August 2005.

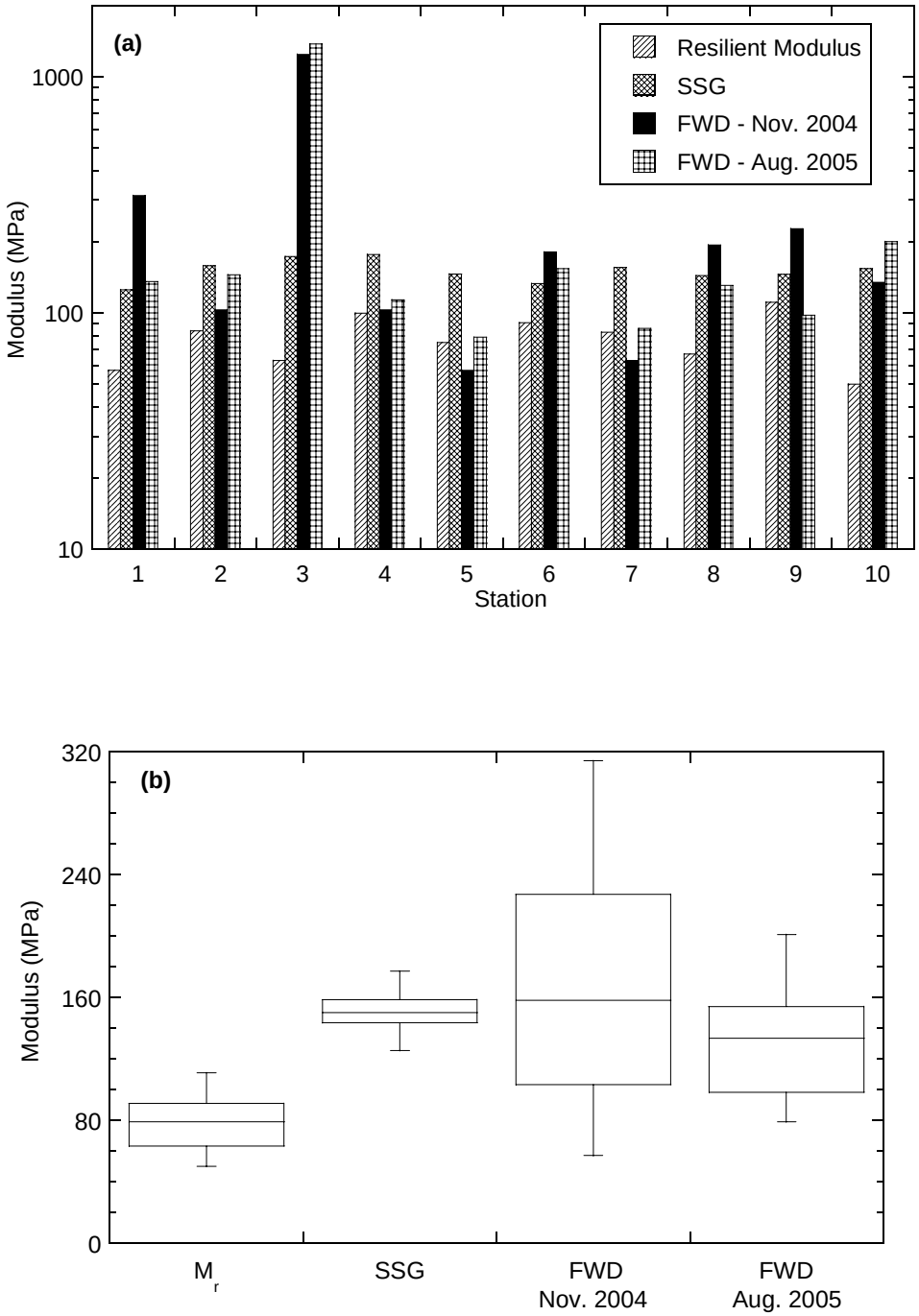

Fig. 12. Modulus of SRPM obtained by inverting FWD data, from SSG measurements, and from resilient modulus tests conducted in the laboratory: (a) modulus along the alignment and (b) box plots of each set of modulus measurements.

APPENDICES

APPENDIX A

CONSTRUCTION PHOTOGRAPHS

Fig. A1. RPM before placement of fly ash.

Fig. A2 Lay-down truck placing fly ash on SRPM.

Fig. A3. Water truck and road-reclaimer blending fly ash, water, and RPM.

Fig. A4. Surface of SRPM after compaction.

Fig. A5. Mid-section of road-reclaimer showing tines used to blend fly ash, water, and RPM.

Fig. A6. Collecting a sample of fly ash for use in laboratory testing.

Fig. A7. Collecting a sample in a thin-wall tube using a drive-tube hammer.

Fig. A8. Measuring water content and unit weight of SRPM after compaction.

Fig. A9. One of principal investigators (T. Edil) hard at work in the field.

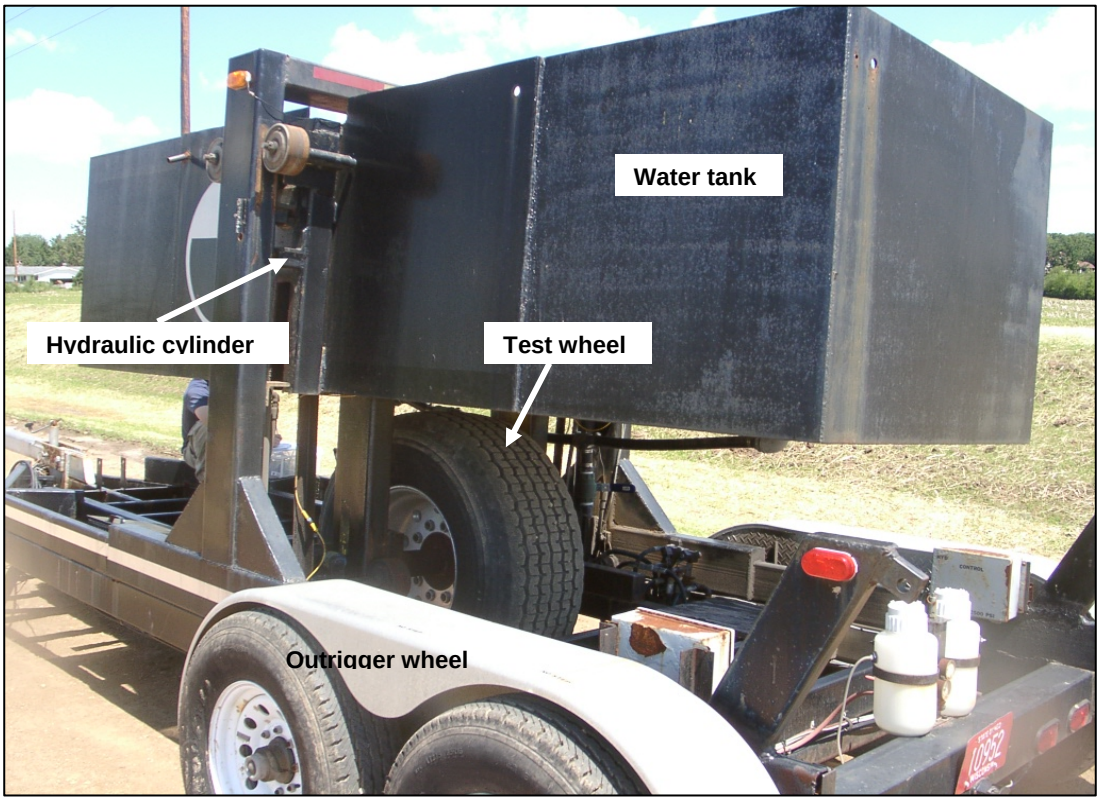

Fig. A10. RWD test apparatus.

APPENDIX B

PHOTOGRAPHS OF
LYSIMETER CONSTRUCTION
AND
INSTALLATION OF INSTRUMENTS

Fig. B1. Installing geomembrane for lysimeter.

Fig. B2. Installing collection tank for lysimeter.

Fig. B3. Installing water content reflectometer in subgrade.

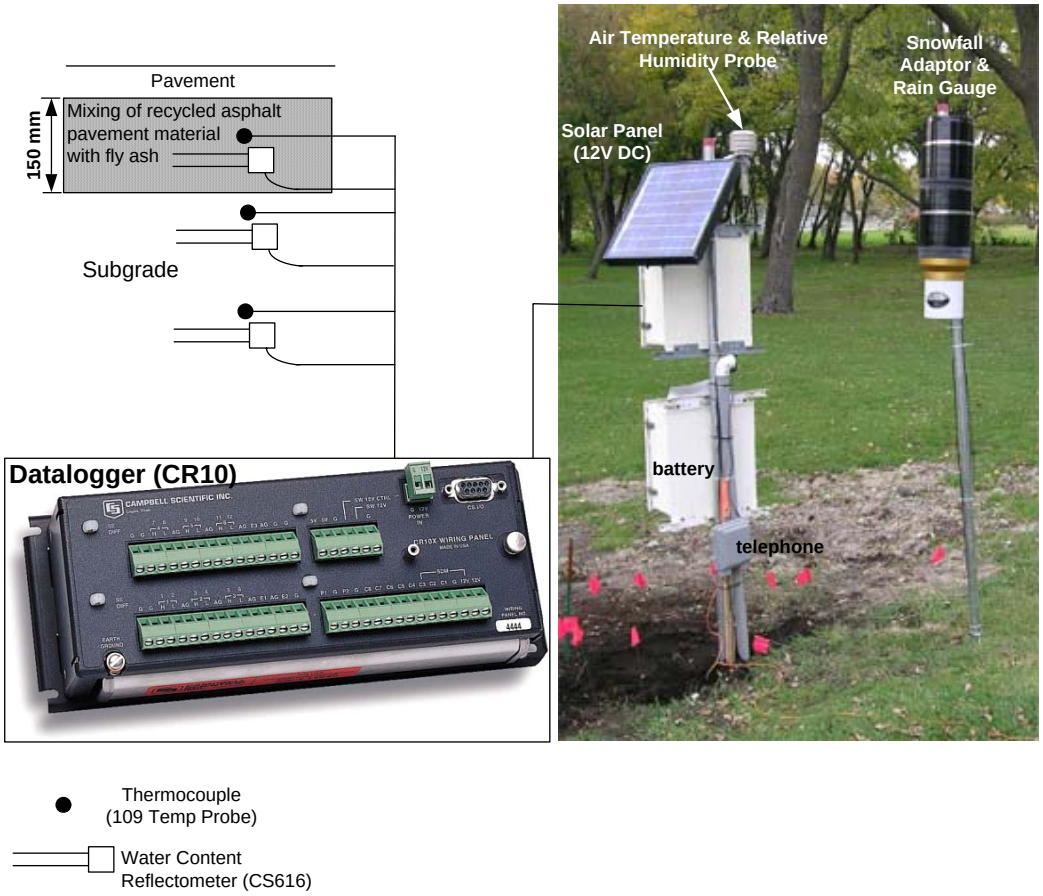

Fig. B4. Layout of field instrumentation.

APPENDIX C

LYSIMETER MONITORING DATA

Table C1. Summary of lysimeter data (except concentrations).

LYSIMETER DATA				**Dry Density =**		17.90	**kN/m^3**		**Porosity =**	**0.31**					
Site: Waseca, MN				**Water Content =**		8.00	**%**		**PV =**	**747.5**	**L**				
Lysimeter Size:		**16**	**m^2**	**Depth =**		0.15	**m**								
									Pump Volume Meter (g)						
Date	**Sample ID**	**pH field**	**pH lab**	**Eh (mv)**	**EC (us/cm)**	**Comments**	**Weather**	**Air Temp**	**Start (gall)**	**End (gall)**	**Vol (L)**	**Cum Vol (L)**	**PVF**	**Drain (mm/d)**	**Comments**
9/11/2004	-	-	-			start			0	0	0	0	0.00		
12/17/2004	-	-	-			no water	Sunny	1/9/1900	39.1	39.1	0	0.0	0.00	0.00	
4/5/2005	-	-	-			no water	-	-	0	0	0	0.0	0.00	0.00	
6/7/2005	W-06-07-05-	7.3	6.7	196		first water	-	-	400	477.5	290.6	290.6	0.39	0.29	
7/7/2005	W-07-07-05-	7.5	6.16	144.2			cloudy	65	477.5	593.5	435.0	725.6	0.97	0.91	
8/2/2005	W-08-02-05-	6.9	6.2	110.7			clear		594.5	712	440.6	1166.3	1.56	1.06	
8/23/2005	W-08-23-05-	7.1					clear	55	712	749.5	140.6	1306.9	1.75	0.42	
9/21/2005	W-09-21-05-	7.3	6.9	47.8	477		clear	70	749.5	760.1	39.8	1346.6	1.80	0.09	
10/6/2005	No analysis						cold	40	760.1	761.4	4.875	1351.5	1.81	0.02	
11/6/2005	No analysis						-	-	761.4	761.4	0	1351.5	1.81	0.00	Tank empty
12/29/2005	No analysis						-	-			0	1351.5	1.81	0.00	Tank empty
2/6/2006	No analysis						-	-			0	1351.5	1.81	0.00	Ice in Tank
3/23/2006	No analysis						-	-			0	1351.5	1.81	0.00	Tank empty
5/1/2006	W-05-01-06	7				water	clear	-	761.4	788.8	102.75	1454.3	1.95	0.16	

Table C2. Summary of concentrations in drainage from lysimeter.

Sample		Be	B	Ca	Tl	V	Cr
ID	PVF	ppb	ppb	ppb	ppb	ppb	ppb
W-07-07-05	0.97	< 0.1	43.57	47927	< 0.02	1.45	2.46
W-08-02-05	1.56	<0.06	20.06	35737	< 0.02	0.47	3.02
W-08-23-05	1.75	<0.06	30.32	53000	<0.02	0.74	0.75
W-09-21-05	1.80	<0.06	39.4	61253	0.03	2.11	2.26
Sample	**Mn**	**Co**	**Ni**	**Cu**	**Zn**	**As**	**Se**
ID	**ppb**	**ppb**	**ppb**	**ppb**	**ppb**	**ppb**	**ppb**
W-07-07-05	1414	3.84	11.83	5.70	31.23	1.36	<2
W-08-02-05	1645	4.53	13.21	4.00	25.16	0.88	<2
W-08-23-05	2200	2.94	11.76	4.04	19.77	1.32	<2
W-09-21-05	1365	1.89	20.8	7.96	15.7	1.74	<2
Sample	**Se**	**Sr**	**Mo**	**Ag**	**Cd**	**Sn**	**Sb**
ID	**ppb**	**ppb**	**ppb**	**ppb**	**ppb**	**ppb**	**ppb**
W-07-07-05	<2	60.90	4.28	< 0.1	1.58	0.13	0.41
W-08-02-05	<2	53.13	0.47	<0.02	0.34	0.15	0.17
W-08-23-05	<2	74.97	0.55	<0.02	0.45	0.068	0.31
W-09-21-05	<2	102	0.50	<0.02	0.81	0.08	0.18
Sample	**Ba**	**Hg**	**Pb**				
ID	**ppb**	**ppb**	**ppb**				
W-07-07-05	37.44	< 1	0.29				
W-08-02-05	49.64	< 0.2	0.54				
W-08-23-05	66.45	<0.2	0.92				
W-09-21-05	65.6	<0.2	1.01				

APPENDIX D

COLUMN LEACH TEST DATA

Table D1. Summary of concentrations in effluent from CLT on SRPM.

Concentrations from CLT on Waseca SRPM. All in units of μg/L

PVF	pH	Be	B	Ca	Tl	V	Cr	Mn	Co	Ni	Cu	Zn
0.5254	7.6	0.10	169	66922	0.03	10.30	7.70	19.8	1.84	29.0	121.0	802.8
0.7908	7.3	0.31	2196	160461	0.04	42.66	51.22	17.3	5.18	39.5	73.4	134.7
1.1285	7.5	0.28	2082	291257	0.06	29.46	4.40	317.2	5.76	41.5	46.1	20.8
1.5203	7.5	0.24	1694	300247	0.10	23.58	0.94	477.7	5.03	54.7	26.9	5.2
1.9905	7.3	0.30	1783	296740	0.10	23.19	0.90	426.6	4.65	48.8	19.5	14.2
3.1969	7.5	0.20	1259	188079	0.07	29.47	2.45	32.7	2.51	31.2	11.6	2.8
5.5932	7.3	0.17	1239	231	0.09	12.70	0.33	4.8	2.66	9.1	9.7	40.7
6.5471	7.8	0.19	1355	224460	0.05	13.40	0.25	184.6	2.03	23.0	8.9	4.5
	Detection Limits:	0.100	0.200	5.000	0.006	0.060	0.040	0.030	0.010	0.050	0.070	0.200

PVF	As	Se	Sr	Mo	Ag	Cd	Sn	Sb	Ba	Hg	Pb
0.5254	1.34	3.1	269	22.5	0.10	0.80	0.10	0.32	48.4	0.2	5.69
0.7908	7.21	53.5	2159	89.8	0.17	3.41	0.11	3.06	136.7	0.2	7.94
1.1285	7.08	59.8	3856	88.5	0.54	2.03	0.28	5.97	166.2	0.2	0.66
1.5203	5.20	37.5	3963	80.8	0.22	2.79	0.12	8.30	159.2	0.2	0.67
1.9905	4.59	27.1	4023	85.3	0.27	2.99	0.11	9.14	227.8	0.2	0.85
3.1969	3.13	15.7	2807	54.5	0.21	3.39	0.12	10.64	344.2	0.2	0.57
5.5932	6.1	19.0	3211	106.0	0.18	4.48	0.31	14.00	381.0	0.2	19.00
6.5471	3.91	13.4	3186	139.3	0.19	4.31	0.08	11.20	382.9	0.2	4.97
Detection Limits:	0.100	2.000	0.010	0.080	0.020	0.080	0.040	0.020	0.020	0.200	0.010

APPENDIX E

RESILIENT MODULUS CURVES FOR SRPM

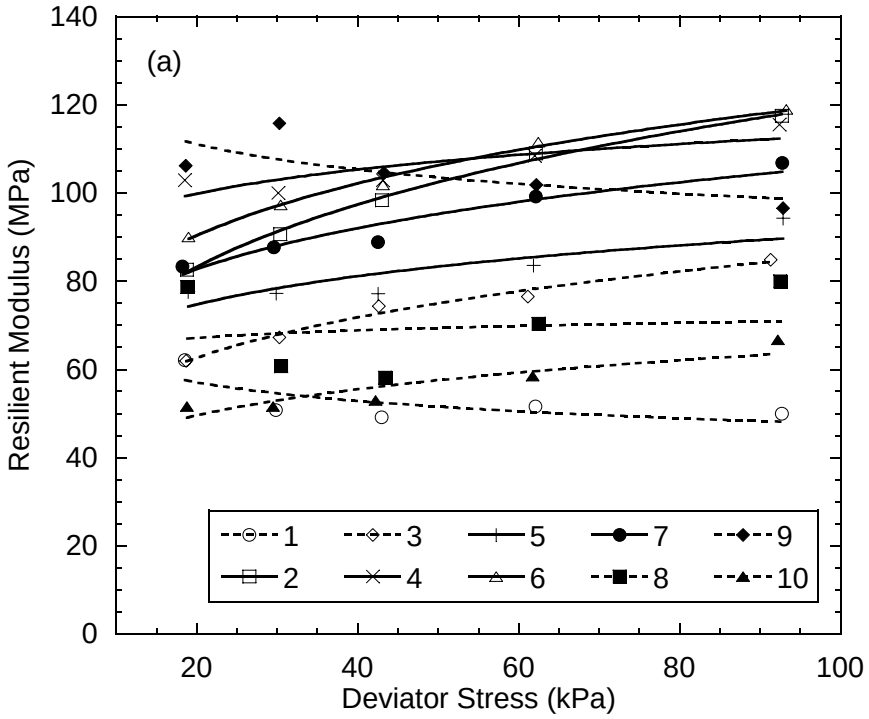

Fig. E1. Resilient modulus curves for SRPM.

FLY ASH STABILIZATION OF GRAVEL ROAD AS BASE FOR PAVEMENT AT CHISAGO COUNTY ROAD 53, MINNESOTA

by

Bulent Hatipoglu, Tuncer B. Edil, Craig H. Benson

Geo Engineering Report No. 06-19

Department of Civil and Environmental Engineering
University of Wisconsin-Madison
Madison, Wisconsin 53706
USA

November 28, 2006

EXECUTIVE SUMMARY

This report describes a field site where cementitious fly ashes (Class C and off-specification) were used to stabilize road-surface gravel (RSG) to form a base during construction of a flexible pavement in Chisago County, MN. The project involved conversion of a gravel road to a paved road. It consisted of mixing fly ash (10% by dry weight) and water into the gravel surface to a depth of 254 mm and compacting the mixture to form a firm base, and placement of an HMA surface. California bearing ratio (CBR), resilient modulus (M_r), and unconfined compression (q_u) tests were conducted on a composite sample of the RSG alone and the fly-ash stabilized RSG (S-RSG) samples prepared in the field and laboratory to evaluate how addition of fly ash improved the strength and stiffness. *In situ* testing was also conducted on the subgrade and S-RSG with a soil stiffness gauge (SSG), dynamic cone penetrometer (DCP), and falling weight deflectometer (FWD). A pan lysimeter was installed beneath the roadway to monitor the quantity of water percolating from the pavement and the concentration of trace elements in the leachate. Column leach tests were conducted in the laboratory for comparison.

Addition of fly ash improved the stiffness and strength of the RSG significantly. After 7 d of curing, the S-RSG prepared in the laboratory using materials sampled during construction had CBR mostly ranging between 48 and 90, M_r between 96 and 195 MPa, and unconfined compressive strengths between 197 and 812 kPa, whereas the RSG alone had CBR of 24 and M_r of 51 MPa. Moduli obtained from the FWD inversion were compared with those obtained from the resilient modulus tests on field-mix specimens and the moduli computed from the stiffness measured with the SSG. Moduli obtained from the resilient modulus test on field-mix samples are markedly lower than those obtained from November 2005 FWD but comparable to those from May 2006 FWD. SSG gives 50% higher moduli compared to the modulus obtained from the resilient modulus test. November 2005 FWD data appear anomalously high compared

to other data here and elsewhere. Longer-term monitoring is needed to confirm that the modulus of S-RSG will persist after multiple winter seasons. The CBRs of S-RSG mixed in the field were mostly lower than that for S-RSG mixed in the laboratory; however, the opposite was observed for M_r, and for q_u. This is in contrast with previous experience and being explored further. Laboratory freeze-thaw tests indicate 17% drop in resilient modulus of the S-RSG after 5 cycles of freeze-thaw.

Approximately 29.6 m^3 of leachate corresponding to 3,183 mm of total drainage occurred in the lysimeter during the monitoring period from November 2005 to June 2006. This corresponds to 48 pore volumes of flow by June 15, 2006. The low lying topography of the area and the heavy precipitation that occurred in Spring 2006 may have led to flooding of the lysimeter as these are very high numbers. All of the trace element concentrations (with the exception of Mn) are below USEPA maximum contaminant levels (MCLs) and Minnesota health risk levels (HRLs). Most of the concentrations appear to be stabilizing and persistent. Concentrations of some elements appear to be low and decreasing (e.g.,Pb, Sb and Sn). The trace element concentrations in the column leach test (CLT) effluent typically are higher than concentrations in the drainage collected in the field in the lysimeters. The poor agreement suggests that the CLT test method that was used may not be appropriate for evaluating leaching of trace elements from S-RSG, unless a conservative estimate of the trace element concentrations is acceptable. Despite the higher concentrations obtained from the CLT, most of the elements have concentrations below USEPA MCLs and Minnesota HRLs. The exceptions are B, Be, Cr, Ba, As, and Se. Additional study is also needed to define laboratory leach testing protocols that can more accurately simulate leaching of trace elements from S-RSG.

ACKNOWLEDGEMENT

Financial support for this study was provided by the Minnesota Local Road Research Board (LRRB). The study was administered by the Minnesota Department of Transportation (Mn/Dot). The conclusions and recommendations in this report are solely those of the authors and do not reflect the opinions or policies of LRRB or Mn/DOT. Appreciation is expressed to the Chisago County's Department of Public Works for supporting the field investigation, providing FWD testing, and for monitoring the lysimeter. Xiaodong Wang, Maria Rosa, and Jeremy Baugh assisted with the project in the field and laboratory. Financial Support of Dr. Bulent Hatipoglu was provided by Istanbul Technical University, The Scientific and Technological Research Council of Turkey and the University of Wisconsin – Madison.

TABLE OF CONTENTS

LIST OF TABLES

LIST OF FIGURES

1. INTRODUCTION

Utilization of byproducts is becoming a common method to improve the ride quality and structural capacity of roads. Use of self-cementitious fly ash in stabilizing the existing road-surface gravel to form a stable base for hot mixed asphalt layer was implemented in the conversion of a gravel road (CR 53) to a paved road in Chisago County, MN.

A study was conducted to evaluate both short and long term geo-mechanical and geo-environmental performance of the road constructed using fly ash stabilization by UW-Madison Geo Engineering Program. In the framework of the study resilient modulus, California Bearing Ratio (CBR), unconfined compressive strength, soil stiffness gauge (SSG), dynamic cone penetrometer (DCP), falling weight deflectometer (FWD) tests have been performed to evaluate the geo-mechanical characteristics. DCP and SSG were performed on both subgrade and stabilized base. Resilient modulus, CBR and unconfined compressive strength tests were conducted on fly ash mixed in the field prepared right after construction and cured for 7 d. A lysimeter was constructed for assessing ground water impacts associated with leaching of metals from fly-ash stabilized subgrade. Column leaching tests were performed to asses the leaching characteristics of fly ash stabilized road-surface gravel. An automated field monitoring system was installed to observe the climatic conditions and provide a basis to interpret the geo-mechanical and geo-environmental performance of the roadway. The field instrumentation measures and records air temperature, relative humidity and precipitation. Volumetric water content and temperature in base, subbase, and subgrade at six locations.

This report describes a project where self-cementing fly ashes from a coal-fired electric power plant were used to stabilize an existing gravel road to form a base for

HMA pavement during reconstruction as a paved road of a 3.5-km section of gravel County Road 53 in Chisago County, MN (≈ 88 km north of Saint Paul, MN). The area where fly ash stabilized material placed was cut and shaped in conformance with the lines and grades given on the plans. Then cementitious fly ash (10% by dry weight) was spread uniformly on the surface using truck-mounted lay-down equipment similar to that described in Edil et al. (2002). The fly ash was mixed with a CMI RS-650-2 road reclaimer into the gravel road to a depth of 254 mm, with water being added during mixing using a water truck (see photographs in Appendix A). This mixture, which contained 10% fly ash by dry weight, was compacted within 1-2 hr by a tamping foot compactor followed by a vibratory steel drum compactor. The S-RSG was overlain with 51 mm non-wearing course and 38 mm wearing course (total 89 mm) of HMA within 3 to 7 d after compaction of the fly ash stabilized base.

2. DESCRIPTION OF THE SITE AND CONSTRUCTION

2.1. Site Description

Chisago County Road 53 (CR 53) is located 88 km north of the Saint Paul, MN and runs north-south parallel to I-35. . The field study was conducted between stations 0+00 to 104+00 of CR 53 (Fig. 1). Road surface had not been covered by pavement and consisted of gravelly clayey sand before the construction. The purpose of the new construction work was to increase the strength of the road-surface gravel to form a base for the new asphalt pavement.

CR 53 lies on a flat topography in this area formed in Pine City ground moraine (primarily classified as lean clay). Twenty one borings (Appendix B) were performed along the length of the construction site that indicated presence of approximately 0.6-m thick sandy gravel fill forming the pavement structure. The gravel fill was underlain mostly by lean clay and occasionally poorly graded sand. The thickness of the gravel fill was less than 0.3-m when sand subgrade was encountered. Groundwater level is about 1 m below the existing gravel road.

2.2. Construction

Fly ash was spread uniformly in strips directly over the gravel road until the width of the whole road cross section was covered. The fly ash was spread by special truck-mounted lay-down equipment (Fig. 2a). Top 254 mm of working platform was mixed with fly ash using a CMI RS-650-2 road reclaimer. During the mixing process, water was added from a water tanker truck attached to the reclaimer to provide optimum water content. Immediately after the mixing process, a pad foot compactor and a vibratory compactor with steel drum were used to compact the mixture in sequence to complete

the stabilization process (Fig. 2b). Compaction was completed within 1 to 2h after mixing. The mixed material was compacted to a target relative compaction of 95% based on standard Proctor energy (ASTM D 698). The standard Proctor maximum dry unit weight was 21.9 kN/m^3 and the optimum water content of 6%. Working platform stabilized with fly ash was stiff and ready to be covered by asphalt concrete pavement. Construction started on August 23, 2005 and ended on August 26, 2005. The bituminous non wear course was paved on September 8, 2005 and the bituminous wear course was paved on September 9, 2005.

3. MATERIALS

3.1 Subgrade

In order to characterize the engineering properties of soil profile, ten sampling points were selected at construction stations of 10+00, 20+00, 27+30, 40+00, 50+00, 60+00, 70+00, 80+30, 90+00 and 104+00 in the middle of east bound lane. Disturbed samples of subgrade soil and road-surface gravel (RSG) (≈ 20 kg each) were collected at these 10 stations during construction (see the construction route from Station 0+00 to 115+00 in Fig. 1). A backhoe was used to obtain samples of RSG and expose the subgrade. On the exposed subgrade surface, in situ water content and dry unit weight were measured using a nuclear gauge, a stiffness measurement was made using the Soil Stiffness Gauge (SSG), and a dynamic penetration index (DPI) was determined using a Dynamic Cone Penetrometer (DCP) . The data obtained are given in Table 1 along with estimated California Bearing Ratio (CBR) and elastic modulus corresponding to weighted DPI over a depth of about 150 mm. CBR was estimated from the relationship given by the US Army Corps of Engineers as follows

$$CBR = 292 * DPI^{-1.12} \quad (1)$$

where CBR in percent, DPI in mm per blow. Elastic modulus was estimated from CBR using a well known UK Transportation Research Laboratory equation (Powell et al. 1984) as follows

$$E = 17.6 * CBR^{0.64} \quad (2)$$

where E is in MPa and CBR is in percent.

CBR of the subgrade soils ranges from 5 to 33 (mean = 14). Stations 20+00, 40+00 and 50+00 had CBR of 5-7 classifying as fair subgrade, all other stations had a CBR of 8

or more classifying as a medium to good subgrade. The elastic modulus of the subgrade ranges from 48 to 165 MPa (mean = 90 MPa). These values are reflective of the low water content of the subgrade at the time these measurements were made.

Subgrade samples were visually classified and grouped into five groups. Samples in each group were mixed together to create five composite samples and Atterberg limits and grain size distribution tests were performed on the composites. The Atterberg limits and percent fines are given in Table 2 along with group index and AASTHO and USCS classifications. The grain size distribution of each composite group is given in Fig. 3. The subgrade consists of silty sands (SM and SP-SM) or sandy low plasticity clays (CL and CL-ML) according to the Unified Soil Classification System. According to the AASHTO Soil Classification System, most subgrade soils at this site are A-2-4 with a group index (GI) of 0. Other subgrade soils classify as A-3, A-4, and A-5.

3.2 Road-surface gravel (RSG)

A summary of the textural characteristics of the RSG is shown in Table 3 and grain size distribution curves for the RSG are shown in Fig. 4. The grain size distribution curves fall in a relatively narrow band. The RSG samples consist of well-graded gravelly sand with fines in the range of 11 to 14% except Station 90+00 where fines content is 22%. The sand content is consistently around 60% and the gravel content is about 25%. Because of the very similar nature of the RSG along the construction route, a composite sample was prepared for conducting laboratory tests. It is classified as gravelly clayey sand according to Unified Soil Classification system (ASTM D2487).

Compaction tests were performed on a sample from Station 27+30 (near the pan lysimeter location) and on the composite sample as shown in Fig. 5. The optimum water

content is approximately 9% and the maximum dry unit weight is 20 kN/m^3 for both samples based on standard compaction effort. The effect of grains larger than #4 sieve on compaction is observable in Fig. 5b. (the optimum moisture content is lowered by 1% and the unit weight is increased by 1.4 kN/m^3). The compaction test performed by GME Consultants, Inc for Chisago County prior to construction indicated an optimum water content of approximately 6% and a maximum dry unit weight of 21.9 kN/m^3 based on standard compaction effort (ASTM D 698).

3.2 Fly Ash

Fly ashes from Riverside Unit 7 and Riverside Unit 8 power station at Saint Paul, MN were used for stabilization. Table 4 shows the types of fly ashes used in each station location. Chemical composition and physical properties of the fly ashes are given in Table 5 along with the composition of typical Class C and F fly ashes as well as the ASTM and AASHTO specifications for class C fly ash. Calcium oxide (CaO) contents of Riverside 7 and Riverside 8 fly ashes are 24% and 22% and silicon oxide (SiO_2) contents are 32% and 19% respectively. CaO/SiO_2 ratios, which are indicative of cementing potential are 0.75 and 1.18. Loss of ignition (LOI), which is the indication of the amount of unburned coal in the fly ash are 0.9% and 16.4%, respectively. According to ASTM C 618, Unit 7 fly ash is a Class C fly ash whereas Unit 8 fly ash is an off-specification (i.e., does not meet Class C or F specifications) self-cementing fly ash. In this project, 10% fly ash by weight was mixed with RSG.

3.3 Stabilized Road-surface gravel (S-RSG)

Water content and unit weight of the compacted S-RSG were measured at each station using a nuclear density gage (ASTM D 2922) immediately after compaction was

completed. Grab samples (≈ 20 kg) of S-RSG were also collected at these locations and were compacted in the field into a CBR mold (114 mm inside diameter x 152 mm height) and a resilient modulus mold (102 mm inside diameter x 203 mm height) to the unit weight measured with the nuclear density gage. Three lifts were used for the CBR specimens and six lifts were used for the M_r specimens. After compaction, the specimens were sealed in plastic and stored at 100% humidity for curing for approximately 7 d. These test specimens are referred to henceforth as 'field-mix' specimens. Because of the cementing effects of the fly ash, index testing was not conducted on the S-RSG.

Specimens of S-RSG were also prepared in the laboratory using the composite sample prepared by mixing samples of RSG collected during construction with River Side Unit 8 fly ash. These specimens, referred to henceforth as 'laboratory-mix' composite specimens, were prepared with 10% fly ash (dry weight) at the mean field water content (6.4%) and mean dry unit weight (19.3 kN/m^3). The laboratory-mix specimens were compacted and cured using the procedures employed for the field-mix specimens. Similarly a specimen was prepared with the composite RSG only (no fly ash) at a dry unit weight of 19.3 kN/m^3 in an air-dry condition.

4. LABORATORY TEST METHODS

4.1 CBR

The CBR tests were conducted in accordance with ASTM D 1883 after 7 d of curing (field-mix or laboratory-mix S-RSG) or immediately after compaction (RSG). The specimens were not soaked and were tested at a strain rate of 1.3 mm/min. The 7-d curing period and the absence of soaking are intended to represent the competency of the RSG when the HMA is placed (Bin-Shafique et al., 2004). Data from the unsoaked CBR tests were not intend as a measure of stiffness of the S-RSG and are not for use in pavement design with S-RSG.

4.2 Resilient Modulus and Unconfined Compression Tests

Resilient modulus tests on the S-RSG and RSG were conducted following the methods described in AASHTO T292 after approximately 7 d of curing (S-RSG) immediately after compaction (RSG). Turner (1997) recommended a 14-d curing period, intended to reflect the condition when most of the hydration is complete (Edil et al., 2006). However, here only 7 d of curing was employed to compare with the field measurements done after a similar period. The loading sequence for cohesive soils was used for the S-RSG as recommended by Bin-Shafique et al. (2004) and Trzebiatowski et al. (2004) for soil-fly ash mixtures. RSG was tested using the loading sequence for cohesionless soils. Unconfined compressive strength was measured on specimens of S-RSG after the resilient modulus tests were conducted. A strain rate of 0.21 % per min. was used for the unconfined compression tests following the recommendations in ASTM D 5102 for compacted soil-lime mixtures. No standard method currently exists for unconfined compression testing of materials stabilized with fly ash, including stabilized RSG.

Freeze-thaw effects were also investigated in the laboratory through resilient modulus and post-resilient modulus unconfined compression tests performed on composite RSG specimens stabilized with 10% Riverside 8 fly ash identically prepared and cured as described earlier. Four specimens were prepared in replicate. One set was tested immediately following the curing process. The remaining three sets were subjected to 1, 3, and 5 cycles of freeze and thaw and then tested. The procedure of freeze-thaw cycling is described by Rosa (2006). Her tests on a variety of fly ash stabilized and unstabilized materials showed that the freeze-thaw effects stabilize after 5 cycles, thus 5 cycles were applied. A freezing-point depression test following ASTM 5918 was performed on the RSG and S-RSG to determine the temperature at which to freeze the specimens. The freezing-point depression was 11 and 12 ^{o}C for RSG and S-RSG, respectively; so the specimens were frozen to 15 ^{o}C three-dimensionally during the freeze-thaw cycles. ASTM D 6035 was used as a guide for this procedure. This standard describes a method to determine the freeze-thaw effects on hydraulic conductivity. Specimens prepared for freeze-thaw cycles had a thermocouple embedded in the third layer. After curing, specimens were extruded from the molds. After extrusion from PVC molds, the specimens were soaked for five hours. The specimens were then wrapped in plastic to prevent changes in moisture content during freeze-thaw cycling and placed in a freezer to begin cycling. The embedded thermocouples were used to confirm freezing. Thawing took place at room temperature.

4.3 Column Leaching Test

Column leach tests (CLT) were conducted on samples of field-mix S-RSG collected from Stations 2 and 5 (20+00 and 40+00). The specimens were prepared in the field in a standard Proctor compaction mold (height = 116 mm, diameter = 102 mm)

using the same procedure employed for the specimens of field-mix S-RSG prepared for CBR testing. The specimens were cured for 7-d prior to testing.

The CLT was conducted following the procedure described in ASTM D 4874, except a flexible-wall permeameter was used instead of a rigid-wall permeameter as shown in Fig. 6. Flow was oriented upward and was driven by a peristaltic pump set to provide a Darcy velocity of 2 mm/d. The effective confining pressure was set at 15 kPa. A 0.1 M LiBr solution was used as the permeant liquid to simulate percolate in regions where salt is used to manage ice and snow (Bin-Shafique et al. 2006). Effluent from the column was collected in sealed Teflon bags to prevent interaction with the atmosphere. Leachate was removed from the bags periodically (≈ 30 ~ 60 mL of flow accumulation). Volume of the leachate removed was measured, the pH was recorded, and a sample was prepared for chemical analysis by filtering with a 0.45 μm filter and preservation with nitric acid to pH < 2.

All effluent samples were analyzed by inductively coupled plasma-mass spectrometry (ICP-MS) following the procedure described in USEPA Method 200.8. Analysis was conducted for the following elements (detection limits in μg/L in parentheses): Ag (0.02), As (0.1), B (0.2), Ba (0.02), Be (0.02), Ca (5), Cd (0.08), Co (0.01), Cr (0.04), Cu (0.07), Hg (0.2), Mo (0.08), Mn (0.03), Ni (0.05), Pb (0.01), Sb (0.02), Se (2.0), Sn (0.04), Sr (0.01), Tl (0.006), V (0.06), and Zn (0.2).

5. FIELD METHODS

5.1 Environmental Monitoring

The environmental monitoring program consists of monitoring the volume of water draining from the pavement, concentrations of trace elements in the leachate, temperatures and water contents within the pavement profile, and meteorological conditions (air temperature, humidity, and precipitation). Monitoring of the pavement began in November 2004 and is still being conducted.

Leachate draining from the pavement was monitored using a pan lysimeter installed at Station 27+30 (Fig. 1). The test specimens for the CLT (Section 4.3) were collected at Stations 2 and 5 (20+00 and 40+00) on either side of the pan lysimeter location, so that a comparison could be made between leaching measured in the field and laboratory. The lysimeter is 4 m wide, 4 m long, and 200 mm deep and is lined with 1.5-mm-thick linear low density polyethylene geomembrane. The base of the lysimeter was overlain by a geocomposite drainage layer (geonet sandwiched between two non-woven geotextiles). S-RSG was placed in the lysimeter and compacted using the same method employed when compacting S-RSG in other portions of the project. Photographs showing the lysimeter construction are in Fig. 7.

Water collected in the drainage layer is directed to a sump plumbed to a 120-L polyethylene collection tank buried adjacent to the roadway. The collection tank is insulated with extruded polystyrene to prevent freezing. Leachate that accumulates in the collection tank is removed periodically with a pump. The volume of leachate removed is recorded with a flow meter, a sample for chemical analysis is collected, and the pH and Eh of the leachate are recorded. The sample is filtered, preserved, and analyzed using the same procedures employed for the CLT (Section 4.3). Personnel from the Chisago County collected the samples from the lysimeter.

Conditions in the fly ash stabilized subbase and subgrade are being monitored continuously at station 27+30. The data being collected include air temperature and relative humidity; subsurface temperature and volumetric water content; quantity and quality of water percolating from the fly ash stabilized subbase layer into the pan lysimeter. Air temperature and relative humidity (RH) are measured with a thermistor and a capacitive relative humidity sensor (Fig. 8). The Campbell Scientific Inc. (CSI) HMP35C temperature/RH probe is housed in a radiation shield to eliminate the effects of solar radiation (Figure 8b). A Rain gage (CSI TE 525) is used to measure precipitation.

Subsurface volumetric water contents in the S-RSG and the subgrade soils are measured using CSI CS616 water content reflectometers (WCRs). Two of WCRs installed in the S-RSG layer at 216 and 241 mm depths from the pavement surface. The other two WCRs were placed in the subgrade soil at depths 445 and 700 mm from the pavement surface. Locations of the WCRs are shown in Fig. 8a. WCRs employ a time-domain reflectometry (TDR) methodology that relates the round-trip travel time of an electromagnetic pulse along a wave to the volumetric water content of the medium in which it is placed. The travel time is function of the dielectric content of the soil or S-RSG, which is strongly influenced by water content (Benson and Bosscher, 1999). Material-specific calibration curves are required to obtain accurate volumetric water contents.

Subsurface temperature is measured at 6 locations in the S-RSG and the subgrade using Type-T copper-constantan thermocouples. Thermo couples were wired to datalogger trough an AM25T type multiplexer. Locations of the duplex insulated thermocouples are shown in Fig. 8a.

Data from the meteorological and subsurface sensors are collected with a CSI CR 23X datalogger powered by a 12-V deep-cycle battery and a solar panel. Data are

downloaded from the datalogger via telephone modem. Photograph of the instrumentation are included in Fig. 8b.

5.2 Mechanical Evaluation of Pavement Materials

Strength and stiffness of the S-RSG were measured with a soil stiffness gauge (SSG), a dynamic cone penetrometer (DCP), and a falling weight deflectometer (FWD). Photographs of the testing are included in Appendix A. Testing with the SSG and DCP, was conducted directly on the S-RSG after approximately 7 d of curing. FWD testing was conducted two times after the HMA was placed (November 8, 2005 and May 9, 2006).

The SSG tests were conducted in accordance with ASTM D 6758 using a Humboldt GeoGauge. Two or three measurements were made at each station within a 0.1-m radius. These measurements deviated by less than 10%. Thus, the mean of these stiffness measurements is reported herein. DCP testing was conducted at each station in accordance with ASTM D 6951 using a DCP manufactured by Kessler Soils Engineering Products Inc. The dynamic penetration index (DPI) obtained from the DCP was computed as the weighted penetration (mm per blow) over a depth of 150 mm below the surface (subgrade or S-RSG) so it could be compared to SSG.

FWD tests were conducted at each station by Braun Intertec Inc. in November 2005 (2 months after construction) and in May 2006 (one year after construction) using a Dynatest^{TM} 8002E FWD following the method described in ASTM D 4694. Moduli were obtained from the FWD deflection data by inversion using MODULUS 6.0 from the Texas Transportation Institute. Analysis of the FWD data was conducted at the University of Wisconsin-Madison.

6. ENVIRONMENTAL DATA

6.1. Meteorological and Subsurface Conditions

Air temperature and relative humidity between November 2005 and May 2006 are shown in Fig. 9. The air temperature ranged from -27 and 34 ^{o}C during the monitoring period, with sub-freezing temperatures occurring between November and April.

Precipitation record at the site was obtained from the nearest weather station at Cambridge, MN. The cumulative precipitation is shown in Fig. 10 for the period from November 2005 to May 2006.

The air temperature and the subsurface temperatures and the volumetric water contents as measured by sensors 1, 2, 3, and 4 (see Fig. 8a) are plotted in Figs. 11 - 14. Additional subsurface temperatures were measured by sensors 5 and 6 at depths of 420 and 685 mm, respectively. They are plotted along with the air temperature in Fig. 15 for the period October 2005 to April 2006. Temperature of the S-RSG (Sensors 3 and 4) ranged between -10^{o}C and 35^{o}C (Figs. 11 and 12). This layer was frozen for about 3-4 months. The temperature of the unstabilized RSG ranged between -1 or -4^{o}C and 31^{o}C (Figs. 13 and 15). This layer also experienced subfreezing temperatures for about 3-4 months but the temperature was slightly below the freezing point. Furthermore, subfreezing temperatures penetrated for very short periods after major cold air temperature spells in December and February. The temperature of the subgrade ranged between -1 or -3^{o}C and 27^{o}C (Figs. 14 and 15). The subsurface temperatures varied seasonally with the air temperature. The magnitude and frequency of variation diminishes with depth, which reflects the thermal damping provided by the pavement materials. Overall, the main layer that experienced freezing was the S-RSG although

some penetration occurred below this layer. Main frost effects on the pavement would be expected to emanate from this layer.

The volumetric water contents are given in Figs. 11 and 12 for the S-RSG layer, in Fig. 13 for the RSG layer, and Fig. 14 for the subgrade. The volumetric water contents drop when the soil temperature begins to fall below 0^{o}C (volumetric water contents are not reported in these figures for periods when freezing was established). These apparent drops in water content reflect freezing of the pore water. The water content measured by WCRs is determined by measuring the velocity of an electromagnetic wave propagated along the probe. The velocity of the wave varies with the apparent dielectric constant of the soil, which is dominated by the dielectric constant of the water phase. When the pore water freezes, the dielectric constant of the water phase drops significantly and this appears as a drop in water content in WCR data (Benson and Bosscher 1999).

Higher volumetric water contents were recorded in the fine-textured subgrade (maximum of about 33.5%) than the coarse-grained RSG (maximum of 28%), which reflects the greater propensity of fine-textured soils to retain water. The volumetric water content of SRGS, however, was quite high (up to 44 to 54%). This may be partly due to calibration as we have not yet obtained the calibration curves for S-RSG but used the curves for SRPM from Waseca project. This will be revised. No spikes are present in the water content records, which reflects the ability of the HMA to impede infiltration during precipitation and snow melt events and to limit evaporation during drier periods. The annual variation in water content is relatively small in the subgrade and the RSG layer, with a larger variation in the S-RSG layer. Higher water contents are recorded in the spring, when greater precipitation occurs.

The seasonal variation in water content is also reflected in the drainage collected in the lysimeter, as shown in Fig. 10 when a significant rise is recorded in April 2006. There is not complete annual record of drainage drainage yet to make definitive conclusions. A complete summary of the lysimeter data is in Appendix C.

6.2 Trace Elements in Lysimeter Drainage

Approximately 29.6 m^3 of leachate corresponding to 3,183 mm of total drainage occurred during the monitoring period from November 2005 to June 2006 as shown in Fig. 16. This corresponds to 16 pore volumes of flow, PVF through the S-RSG by the end of March 2006. This amount has increased to 48 PVF by June 15, 2006. The low lying topography of the area and the heavy precipitation that occurred in Spring 2006 may have led to flooding of the lysimeter as these are very high numbers. For instance, in the City of Waseca only 1.8 PVF occurred over 20 months in a similar arrangement through a fly ash stabilized recycled pavement material. During this period, pH of the drainage has been near neutral (6.8 – 7.6) and Eh = 41-342 mV. A summary of the pH and Eh data along with the trace element concentrations is in Appendix C.

Concentrations of trace elements in drainage from the lysimeters are shown in Fig. 17 as a function of PVF. The figure is divided into three parts: high concentration, moderate and persistent, and low and diminishing concentration. Elements not shown in Fig. 17 include those below the detection limit (Be, Ag, Hg, and Tl) and elements not typically associated with health risks (e.g., Ca). All of the concentrations are below USEPA maximum contaminant levels (MCLs) and Minnesota health risk levels (HRLs). The exception is Mn, which had a maximum concentration of 3,682 ug/L and exceeded the Minnesoata HRL of 100 ug/L. However, the Minnesota Department of Health no longer recommends the HRL value and plans exist to increase the HRL to 1,000 to

1,300 ug/L (www.pca.state.mn.us). USEPA does not have a primary criterion for Mn although there is a secondary criterion. Most of the concentrations appear to be stabilizing and persistent. Concentrations of some elements appear to be low and decreasing (Pb, Sb and Sn).

6.3 Trace Elements in CLT Effluent

Two column tests were performed using material from Station 2 and 5 (20+00 and 40+00). Concentrations of trace elements in the effluent from the CLT on the S-RSG are shown in Figs. 18 and 19, respectively for Stations 2 and 5. Elements are plotted separately in 3 groups depending on their peak concentrations in Figs. 18 and 19: those having peak concentrations exceeding 1 mg/L, those having peak concentrations between 10 and 1,000 μg/L, and those having peak concentrations less than 10 μg/L. A compilation of the data is in Appendix D.

Comparison of Fig. 18 with Fig. 19 indicates that the trace element concentrations are comparable for the two samples obtained at two different stations as the same elements are grouped into the same concentration range in both plots. The only exception is Sr which has a peak concentration slightly over 10 μg/L in Station 5 and slightly lower than 10 μg/L in Station 2 sample. Comparison of Figs. 18 and 19 indicates that the trace element concentrations in the CLT effluent typically are higher than concentrations in the drainage collected in the field (Fig. 17). The poor agreement suggests that the CLT test method that was used may not be appropriate for evaluating leaching of trace elements from S-RSG, unless a conservative estimate of the trace element concentrations is acceptable. Despite the higher concentrations obtained from the CLT, most of the elements have concentrations below USEPA MCLs and Minnesota HRLs. The exceptions are for B (peak = 2,820 μg/L in St. 5, no MCL, HRL = 600 μg/L,),

Be (peak = 1 and 0.2 μg/L in St. 5 and St. 2 , MCL = 4 μg/L, HRL = 0.08 μg/L), Cr (peak = 801 and 543 μg/L in St. 5 and St. 2, MCL = 100 μg/L, HRL = 100 μg/L), Ba (peak = 4,460 and 4,490 μg/L in St. 5 and St. 2, MCL, HRL = 2,000 μg/L), As (peak = 50 and 37 μg/L in St. 5 and St. 2 , MCL = 10 μg/L, no HRL), and Se (peak = 45 and 48 μg/L in St. 5 and St. 2 , MCL = 50 μg/L, HRL = 30 μg/L). Although the leachates do not appear to exceed the new HRL limit of 2 μg/L for Sb, there are some concentrations that approach the limit in one of the CLT (Sta. 5, Table D3 in Appendix D).

The elution behavior observed in the CLT effluent follows two patterns: (i) first-flush response, where the concentration falls from an initially high value and then remains nearly constant, and (ii) persistent leaching, where the concentration initially increases and then remains relatively constant.

7. PROPERTIES OF S-RSG AND RSG

7.1 Laboratory Test Data

CBR, M_r, and q_u of the S-RSG and RSG are summarized in Table 6. Tests were conducted on the RSG and laboratory-mix S-RSG using the composite sample created by mixing the RSG samples from all of stations. Tests were conducted on both RSG and S-RSG to determine the benefits of adding fly ash to the mixture in terms of strength and stiffness gain but ultimately to assess these values for S-RSG and compare with traditional base course material.

CBR of the field mix S-RSG is given along the alignment of the project in Fig. 20 supplemented with CBR of the S-RSG estimated from DCP along with the laboratory CBR tests on RSG and S-RSG performed using the composite sample. There is no systematic variation in CBR of the RSG or S-RSG along the alignment, suggesting that the variability in the CBR is more likely due to heterogeneity in the material rather than systematic variation in site conditions or construction methods. A review of the type of fly ash used, Riverside Unit 7 or 8 (i.e., Class C versus off-specification fly ash) (see Table 4) in each station does not reveal any influence of fly ash. For instance, at Stations 27+30, 60, and 70 only Unit 8 (off-specification fly ash) was used whereas at Station 40 only Unit 7 (Class C fly ash) was used. There is no significant difference in CBR between these stations. After 7 d of curing, the S-RSG prepared in the laboratory using materials sampled during construction had CBR mostly ranging between 48 and 90, M_r between 96 and 195 MPa, and unconfined compressive strengths between 197 and 812 kPa, whereas the RSG alone had CBR of 24 and M_r of 51 MPa. At four stations, CBR of the field mix S-RSG varies between 50 and 80 and compares well with good quality gravel base course but lower than crushed rock base course (Hunt 1986). At three stations CBR of field mix S-RSG is around 80. At one station (Station 50), CBR

is much lower (i.e., 16) but this is not supported by the DCP data at that station. Therefore, it is likely due to some sampling error but not a systematic problem. The CBRs as estimated from the field DCP are mostly comparable to field mix CBR but occasionally higher and in no case lower. The curing period was 7 days both for field mix specimens tested in the laboratory and the DCP in the field. The CBR of the laboratory mix S-RSG was 154 and much higher than any of the S-RSG field specimens or tests. The CBR of the composite RSG sample was 24 and RSG is unqualified as a base course based on this CBR. However, adding fly ash to the RSG increased the CBR appreciably, although the CBR in the field was as much as 66% lower than the CBR of the laboratory-mix S-RSG. This is consistent with the observations made at for stabilized recycled pavement material in the City of Waseca (Li et al. 2006) and fine-grained subgrade stabilization (Bin-Shafique et al. 2004). Bin-Shafique et al. (2004) attribute these differences in CBR to more thorough blending of soil and fly ash in the laboratory compared to the field, resulting in more uniform distribution of cements within the mixture.

The CBR of the subgrade soils were estimated from DCP and given in Table 1 and plotted in Fig. 20. Subgrade CBR vary between 5 and 33 (mean = 14). Stations 20+00, 40+00 and 50+00 had CBR of 5-7 classifying as fair subgrade, all other stations had a CBR of 8 or more classifying as a medium to good subgrade.

Resilient moduli data of field mix S-RSG are shown in Fig. 21. Fig. 21a shows resilient modulus as a function of deviator stress. Resilient modulus does not show much dependence on deviator stress within the test range unlike typical cohesive soils. The resilient moduli along the alignment of the project are shown in Fig. 21b. These M_r correspond to a deviator stress of 21 kPa, which represents typical conditions within the base course of a pavement structure (Tanyu et al. 2003, Trzebiatowski et al. 2004). As

observed for CBR, there is no systematic variation in M_r along the alignment. The field-mix S-RSG had M_r between 96 and 195 MPa (mean = 153 MPa). The mean resilient modulus of field-mix S-RSG is markedly higher than the mean resilient modulus of field-mix recycled pavement materials (153 Mpa versus 78 MPa). It is also higher than the typical resilient modulus of crushed rock aggregate (48 to 103 MPa). Mr of the composite RSG and the laboratory mix S-RSG were measured to be about 51 and 112 MPa (the range for the laboratory mix S-RSG is 94 and 131) at typical pavement stresses (Table 6). Adding fly ash increased the M_r by two folds in the laboratory. M_r of the field-mix S-RSG was on average higher than the M_r of the laboratory-mix S-RSG (153 versus 112 MPa). This is not consistent with all other fly ash sites investigated.

Unconfined compressive strength measured on the resilient modulus specimens after the resilient modulus tests of the S-RSG along the alignment of the project are shown in Fig. 22. Strengths are not reported for RSG because the RSG is essentially non-cohesive and therefore is not amenable to q_u testing. As with CBR and M_r, there is no systematic variation in q_u along the alignment. The field-mix S-RSG had q_u between 197 and 812 kPa (mean = 408 kPa). The laboratory mix S-RSG had q_u between 207 and 448 kPa (mean = 322 kPa). q_u of the field-mix S-RSG follows the same trend as M_r in comparison to the laboratory-mix S-RSG i.e., higher.

Resilient modulus and unconfined compressive strength of the specimens that were subjected to freeze-thaw cycles were normalized by the resilient modulus and unconfined compressive strength of the specimen that was not subjected to any freeze-thaw cycles to determine the loss of property due to freze-thaw. The results are summarized in Table 7. Resilient modulus dropped by 17% after 5 cycles of freeze-thaw. Rosa (2006) performed freeze-thaw tests on a variety of materials including fine-grained soils alone and stabilized with fly ash. The degree of resilient modulus reduction

varied with the type of material but remained to be no more than 50%. S-RSG appears to show resistance to frost damage in the laboratory.

7.2 Field Test Data

A set of SSG measurements were made immediately after S-RSG was compacted in the field. Another set of SSG as well as a set of DCP measurements were made approximately after 7 to 10 d of curing. In situ stiffness measured with the SSG and dynamic penetration index (DPI) measured with the DCP are shown in Fig. 23 for the subgrade and the S-RSG. Subgrade has DPI vary between 7 and 39 mm/blow (mean = 20.4 mm/blow) whereas S-RSG DPI varies between 2 and 5 mm/blow (mean = 3.4 mm/blow) as shown in Fig. 23a.

As shown in Fig. 23b, subgrade SSG stiffness varies between 8 and 17 MN/mm (mean = 11 MN/mm). SSG stiffness of S-RSG varies between 11 and 22 MN/mm (mean = 16 MN/mm) after compaction. SSG stiffness increased with curing and varies between 17 and 34 MN/mm (mean = 27 MN/mm) after 7 d. The DPI and stiffness of the S-RSG are also less variable than those of the subgrade.

The SSG and DPI statistics for the subgrade and the S-RSG are shown in Fig. 24. In this type of box plot, each box encloses 50% of the data with the median value of the variable displayed as a line. The top and bottom of the box mark the limits of ± 25% of the variable population. The lines extending from the top and bottom of each box mark the minimum and maximum values within the data set that fall within an acceptable range. Any value outside of this range, called an outlier, is displayed as an individual point. The effect of stabilization and curing is evident in Fig. 24.

Maximum deflections from the FWD tests for the 40-kN drop are shown in Fig. 25a for November 2005 several months after construction and when the air and ground temperatures were dipping although there was no frost penetration and for May 2006 when ground temperatures but also the volumetric water contents both in RSG and S-RSG layers were significantly higher compared to November 2005 (see Figs. 11, 12, and 13). The volumetric water content of the subgrade layer was comparable between the two FWD testing dates (see Fig. 14). Maximum deflection, which is measured at the center of the loading plate, is a gross indicator of pavement response to dynamic load. Also given on Fig. 23b are the subgrade and S-RSG SSG surveys. There is a marked increase in deflections in May 2006. The deflections in May 2006 are particularly larger at Stations 60+00 to 80+00. The S-RSG stiffness as measured by SSG shows some variation but does not indicate any weakness around Station 60+00. The subgrade stiffness, however, tends to mimic the variation observed in the FWD maximum deflections. Additional data are needed to make reasonable conclusions.

Elastic moduli of the S-RSG that were obtained by inversion of the FWD data are shown in Fig. 26a. For the inversion, a three-layer profile was assumed that consisted of asphalt (89-mm thick), S-RSG (254-mm thick), and an infinitely thick subgrade. Modulus of the asphalt was allowed to vary between 345 and 11,750 MPa and the Poisson's ratio was set as 0.4. The S-RSG was assumed to have a Poisson's ratio of 0.35 and the modulus was allowed to vary between 70-9400 MPa. The subgrade was assumed to have a Poisson's ratio of 0.35.

The modulus of the S-RSG varies between 513 and 1098 MPa (mean = 741 MPa) in November 2005 and between 74 and 199 MPa (mean = 156 MPa) in May 2006. Most of the S-RSG moduli are 600-700 Mpa in November 2005. In May 2006, S-RSG moduli are 100 to 200 MPa at most stations but it is markedly low at Station 70+00. The subgrade

moduli also are lower in May 2006 in comparison to November 2005 but they appear to be fairly uniform along the roadway.

The statistics of elastic moduli as determined from the FWD test for the S-RSG and the subgrade are shown in Fig. 27 over the length of the construction route indicating the drop for both the S-RSG and the subgrade from November 2005 to May 2006. Additional monitoring is needed to understand the trends and the causes. While there is a dramatic drop in the S-RSG modulus, the median value of 162 MPa in May 2006 is comparable to or slightly higher than that of fly ash stabilized recycled pavement material in the City of Waseca as measured in August 2005 (Lin et al. 2006).

Moduli obtained from the FWD inversion are compared with those obtained from the resilient modulus tests on field-mix specimens and the moduli computed from the stiffness measured with the SSG in Fig. 28. Elastic modulus (E) was computed from the SSG stiffness (K_{SSG}) using (Sawangsuriya et al., 2003):

$$E = \frac{K_{SSG}(1-\upsilon^2)}{1.77\,R} \tag{3}$$

where R is the outside radius of the SSG foot (0.057 m) and υ is Poisson's ratio (assumed to be 0.35). Moduli obtained from the resilient modulus test on field-mix samples are markedly lower than those obtained from November 2005 FWD but comparable to those from May 2006 FWD. SSG gives 50% higher moduli than the moduli obtained from the resilient modulus test. November 2005 FWD data appear anomalously high compared to other data here and elsewhere.

8. CONCLUSIONS AND RECOMMENDATIONS

A case history has been described where Class C and off-specification cementitious fly ashes (10% by weight) were used to stabilize road-surface gravel (RSG) during construction of a flexible pavement. California bearing ratio (CBR) and resilient modulus (M_r) tests were conducted on the RSG alone and fly-ash stabilized RSG (S-RSG) mixed in the field and laboratory to evaluate how addition of fly ash improved the strength and stiffness. *In situ* testing was also conducted on the subgrade and S-RSG with a soil stiffness gauge (SSG) and dynamic cone penetrometer (DCP). Falling weight deflectometer (FWD) test were conducted after paving on two different occasions. A pan lysimeter was installed beneath the pavement to monitor the rate of drainage and trace element concentrations in the leachate. Two column leaching tests were also conducted on samples of S-RSG collected during construction.

After 7 d of curing, the S-RSG prepared in the laboratory using materials sampled during construction had CBR mostly ranging between 48 and 90, M_r between 96 and 195 MPa, and unconfined compressive strengths between 197 and 812 kPa, whereas the RSG alone had CBR of 24 and M_r of 51 MPa. Field-mix S-RSG had significantly higher CBR and M_r than RSG that was not stabilized with fly ash. This finding suggests that fly ash stabilization of RSG should be beneficial in terms of increasing pavement capacity and service life. The CBRs of S-RSG mixed in the field were mostly 50 to 80 and lower than that for S-RSG mixed in the laboratory (154); however, the opposite was observed for M_r, and for q_u. This is in contrast with previous experience and being explored further.

Moduli obtained from the FWD inversion are compared with those obtained from the resilient modulus tests on field-mix specimens and the moduli computed from the stiffness measured with the SSG. Moduli obtained from the resilient modulus test on

field-mix samples are markedly lower than those obtained from November 2005 FWD but comparable to those from May 2006 FWD. SSG gives 50% higher moduli compared to the modulus obtained from the resilient test . November 2005 FWD data appear anomalously high compared to other data here and elsewhere. Longer-term monitoring is needed to confirm that the modulus of S-RSG will persist after multiple winter seasons.

Chemical analysis of the draining leachate showed that the concentrations of many trace elements were reasonably steady toward the end of the monitoring period. Longer-term monitoring is needed to fully understand the potential for S-RSG to leach trace elements during the service life of a pavement. However, during the monitoring period, all of the concentrations (with the exception of Mn) were below USEPA maximum contaminant levels (MCLs) and Minnesota health risk levels (HRLs) established by the Minnesota Dept. of Public Health. The trace element concentrations in the CLT effluent typically are higher than concentrations in the drainage collected in the field in the lysimeters. The poor agreement suggests that the CLT test method that was used may not be appropriate for evaluating leaching of trace elements from S-RSG, unless a conservative estimate of the trace element concentrations is acceptable. Despite the higher concentrations obtained from the CLT, most of the elements have concentrations below USEPA MCLs and Minnesota HRLs. The exceptions are for B, Be, Cr, Ba,As, and Se. Additional study is also needed to define laboratory leach testing protocols that can more accurately simulate leaching of trace elements from S-RSG.

9. REFERENCES

Benson, C.H. and Bosscher, P.J., 1999. Time-domain reflectometry in geotechnics: a review. In: W. Marr and C. Fairhurst (Editors), Nondestructive and Automated Testing for Soil and Rock Properties, ASTM STP 1350. ASTM International, West Conshohocken, PA, pp. 113-136.

Bin-Shafique, S., Benson, C.H., Edil, T.B. and Hwang, K., 2006. Leachate concentrations from water leach and column leach tests on fly-ash stabilized soils. Environmental Engineering 23(1), pp. 51-65.

Bin-Shafique, S., Edil, T.B., Benson, C.H. and Senol, A., 2004. Incorporating a fly-ash stabilised layer into pavement design. Geotechnical Engineering, Institution of Civil Engineers, United Kingdom, 157(GE4), pp. 239-249.

Edil, T.B., Acosta, H.A. and Benson, C.H., 2006. Stabilizing soft fine-grained soils with fly ash. Journal of Materials in Civil Engineering, 18(2), pp. 283-294.

Edil, T.B. et al., 2002. Field evaluation of construction alternatives for roadways over soft subgrade. Transportation Research Record, No. 1786: National Research Council, Washington DC, pp. 36-48.

Hunt, Roy E. 1986. “Geotechnical Engineering Techniques and Practices.” McGraw Hill Book Company.

Li, L., Benson, C. H., Edil, T.B. and Hatipoglu, B. 2006. “Fly Ash Stabilization of Recycled Asphalt Pavement Material in Waseca, Minnesota.” Geo Engineering Report N0. 06-18, Department of Civil and Environmental Engineering, University of Wisconsin-Madison.

Powell, W. D., Potter, J. F., Mayhew, H. C., and Nunn, M. E. 1984. “The Structural Design of Bituminous Roads.” TRRL Laboratory Report 1132, Transportation and Road Research Laboratory, Crowthorne, Berkshire, 1984, 62 pp.

Rosa, M. “Effect of Freeze-Thaw Cycling on Soils Stabilized with Fly Ash.” M.S. Thesis, Department of Civil and Environmental Engineering, University of Wisconsin-Madison, 2006.

Tanyu, B., Kim, W., Edil, T., and Benson, C., 2003. Comparison of laboratory resilient modulus with back-calculated elastic modulus from large-scale model experiments and FWD tests on granular materials. Resilient Modular Testing for Pavement Components, American Society for Testing and Materials, West Conshohocken, PA. STP 1437, pp. 191-208.

Trzebiatowski, B., Edil, T.B. and Benson, C.H., 2004. Case study of subgrade stabilization using fly ash: State Highway 32, Port Washington, Wisconsin. In: A. Aydilek and J. Wartman (Editors), Beneficial Reuse of Waste Materials in

Geotechnical and Transportation Applications, GSP No. 127. ASCE, Reston, VA, pp. 123-136.

Turner, J.P., 1997. Evaluation of western coal fly ashes for stabilization of low-volume roads, Testing Soil Mixed with Waste or Recycled Materials. American Society for Testing and Materials, West Conshohocken, PA. STP 1275, pp. 157-171.

Table 1. Physical properties of subgrade soils.

Station	γ_d (kN/m^3)	w_n (%)	SSG Stiffness (MN/m)	DCP Index (DPI) (mm/blow)	CBR (%)	Elastic Modulus (MPa)*
10+00	19	12	12	14	15	100
20+00	17	3	8	31	6	57
27+30	18	15	14	19	11	81
40+00	18	6	8	30	7	61
50+00	21	8	13	39	5	48
60+00	19	12	17	19	11	81
70+00	22	7	12	7	33	165
80+00	20	8	9	9	25	138
90+00	19	5	8	16	13	91
104+00	19	5	9	20	10	78

Notes: SSG = Soil Stiffness Gauge, DCP = Dynamic Cone Penetrometer (DPI is the weighted average DPI over a depth of 150 mm), CBR = California Bearing Ratio (estimated from weighted DPI), w_n = in situ water content and γ_d = in situ dry unit weight (measured by nuclear gauge).
* Estimated from CBR

Table 2. Index properties and classification of subgrade soils.

Group	Stations	LL	PI	% Fines	GI	USCS		AASHTO
						Group Symbol	Group Name	
A	20+00 40+00	NP	NP	6.9	0	SP-SM	Poorly graded sand with silt	A-3
B	27+30 60+00	44	28	61.8	14	CL	Sandy lean clay	A-5
C	50+00 70+00 80+00 104+00	18	NP	21.1	0	SM	Silty sand	A-2-4
D	10+00	21	4	53.8	0	CL-ML	Sandy silty clay	A-4
E	90+00	NP	NP	16.5	0	SM	Silty sand	A-2-4

Note: LL = liquid limit. PI = plasticity index. GI = AASHTO group index. USCS = Unified Soil Classification System. AASHTO = American Association of State Highway and Transportation Officials.

Table 3. Grain size fractions, in situ water content, and compaction characteristics of RSG.

Station	% Gravel	% Sand	% Fines	D_{10} (mm)	C_u	C_c
10+00	27.8	58.6	13.6	0.03	38	1.6
20+00	18.4	69.5	12.0	0.05	17	1.6
27+30	28.1	60.8	11.2	0.06	30	0.8
40+00	22.4	64.9	12.8	0.06	19	1.1
50+00	25.9	62.1	12.0	0.06	21	1.1
60+00	20.8	64.4	14.8	0.04	21	1.8
70+00	19.5	68.4	12.1	0.05	16	1.7
80+30	32.8	55.4	11.8	0.10	5	1.1
90+00	20.1	57.5	22.4	0.03	13	1.7
104+00	16.8	69.7	13.5	0.03	25	1.6
Composite	24.5	64.3	11.2	0.06	20	0.9

Notes: D_{10} = effective grain diameter, C_u = uniformity coefficient, C_c = coefficient of curvature.

Table 4. Types of fly ashes used in each station.

Station	Fly Ash Type
10+00	Riverside 7, Riverside 8
20+00	Riverside 7, Riverside 8
27+30	Riverside 8
40+00	Riverside 7
50+00	Riverside 7, Riverside 8
60+00	Riverside 8
70+00	Riverside 8
80+30	Riverside 7, Riverside 8
90+00	-
104+00	-

Table 5. Chemical composition and physical properties of Riverside 7 and 8 fly ashes, typical Class C and F fly ashes, and specifications for Class C fly ash

Parameter	Percent of Composition				Specifications	
	Riverside 7[+]	Riverside 8[+]	Typical* Class C	Typical* Class F	ASTM C 618 Class C	AASHTO M 295 Class C
SiO_2 (silicon dioxide), %	32	19	40	55		
Al_2O_3 (aluminum oxide), %	19	14	17	26		
Fe_2O_3 (iron oxide), %	6	6	6	7		
$SiO_2 + Al_2O_3 + Fe_2O_3$, %	57	39	63	88	50 Min	50 Min
CaO (calcium oxide), %	24	22	24	9		
MgO (magnesium oxide), %	6	5.5	2	2		
SO_3 (sulfur trioxide), %	2	5.4	3	1	5 Max	5 Max
CaO/SiO_2	0.75	1.18				
$CaO/(SiO_2+Al_2O_3)$	0.47	0.68				
Loss on Ignition, %	0.9	16.4	6	6	6 Max	5 Max
Moisture Content, %	0.17	0.32	-	-	3 Max	3 Max
Specific Gravity	2.71	2.65	-	-		
Fineness, amount retained on #325 sieve, %	12.4	15.5	-	-	34 Max	34 Max

[+]Chemical analysis and physical analysis provided by Lafarge North America
*from Bin-Shafique et al. (2004)

Table 6. CBR, M_r, and q_u of RSG and S-RSG.

Station	CBR (%)			M_r (MPa)			q_u (kPa)	
	RSG (Lab)	Field-Mix S-RSG	Lab-Mix S-RSG	RSG	Field-Mix S-RSG	Lab-Mix S-RSG	Field-Mix S-RSG	Lab-Mix S-RSG
10+00	-	52	-	-	195	-	288	-
20+00	-	48	-	-	119	-	422	-
27+30	-	78	-	-	175	-	215	-
40+00	-	90	-	-	173	-	812	-
50+00	-	16	-	-	96	-	352	-
60+00	-	50	-	-	150	-	197	-
70+00	-	83	-	-	180	-	490	-
80+30	-	59	-	-	136	-	484	-
90+00	-	-	-	-	-	-	-	-
104+00	-	-	-	-	-	-	-	-
Composite	24	-	154	51[a]	-	112[b]		322

Notes: CBR = California bearing ratio, M_r = resilient modulus, q_u = unconfined compressive strength, hyphen indicates test not conducted, NA = not available because specimen damaged. [a] Tested as granular soil at bulk stress 70 kPa. [b] Reported at deviator stress of 21 kPa.

Table 7. Mr, and qu changes of S-RSG subjected to freeze-thaw cycles.

Freeze-Thaw Cycle	Normalized M_r	Normalized q_u
0	1	1
1	0.94	1.2
3	0.90	2.3
5	0.83	0.97

Notes: M_r = resilient modulus reported at deviator stress of 21 kPa (normalized by M_r of specimen not subjected to freeze-thaw). q_u = unconfined compressive strength (normalized by M_r of specimen not subjected to freeze-thaw). All tests in replicate.

Fig. 1 Location of County Road 53 and study area.

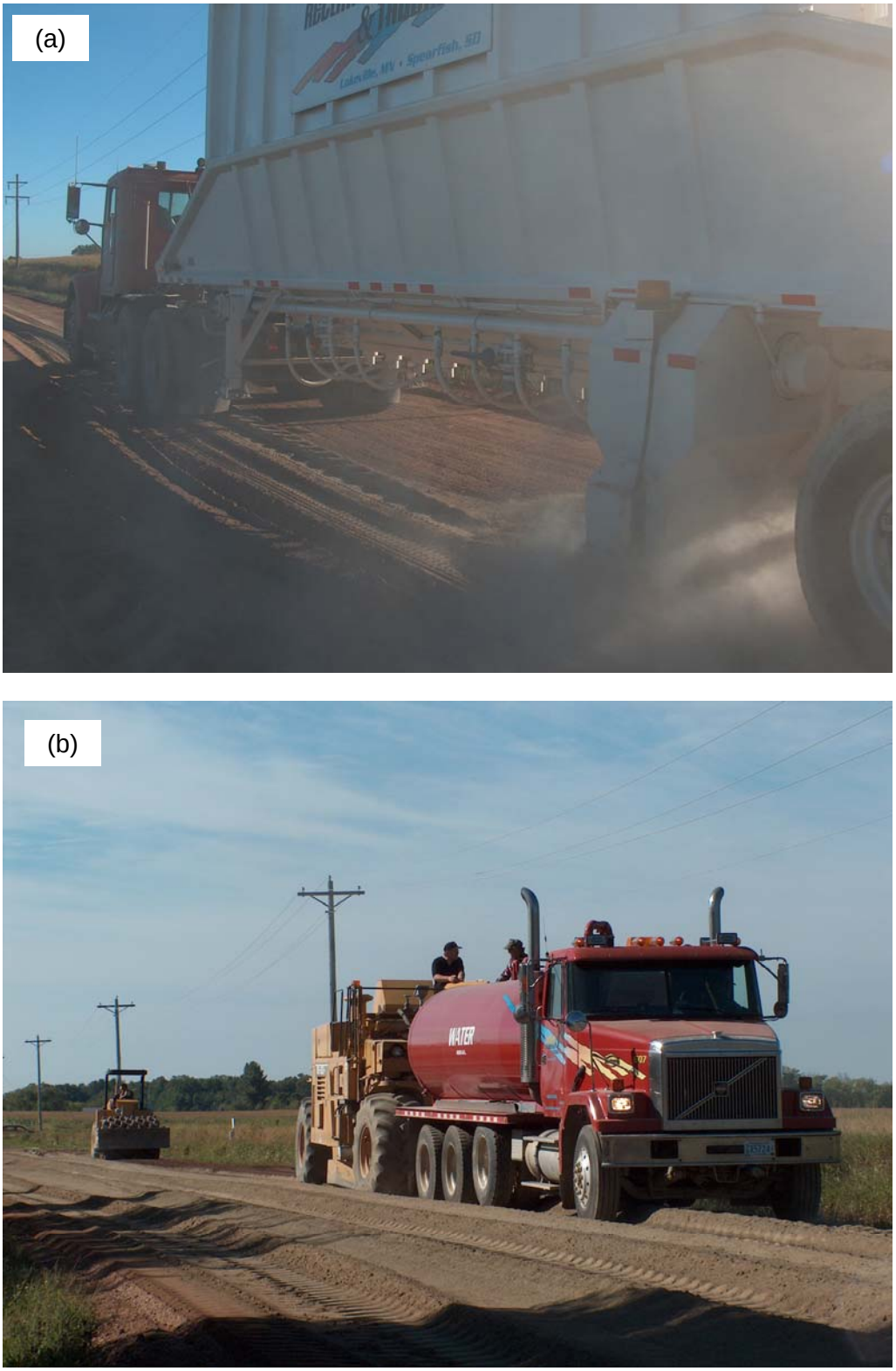

Fig. 2 (a) Spreading of fly ash on gravel road with lay-down equipment and (b) Mixing process of fly ash, road-surface gravel, and water by a reclaimer (compaction is performed right after mixing by tamp-foot compactor seen in the background).

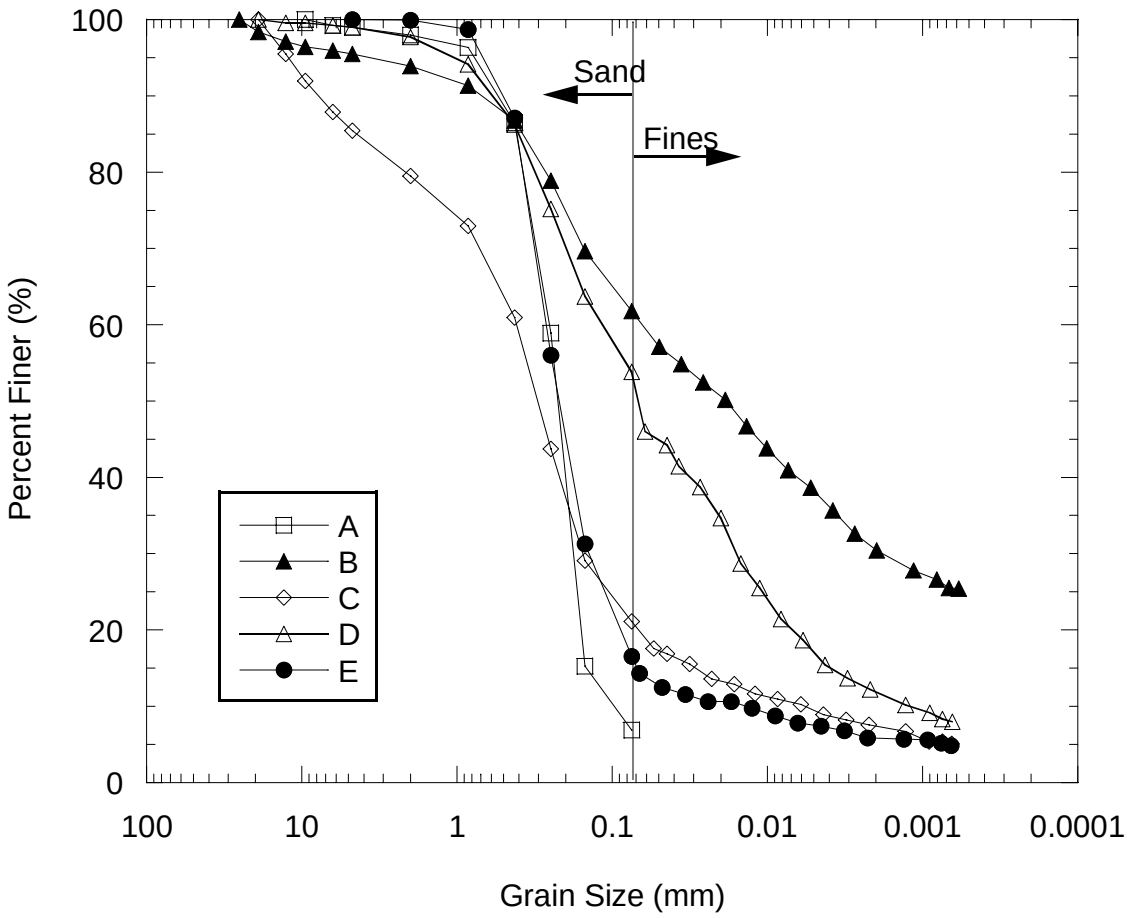

Fig. 3 Grain size distribution curves of grouped subgrade samples.

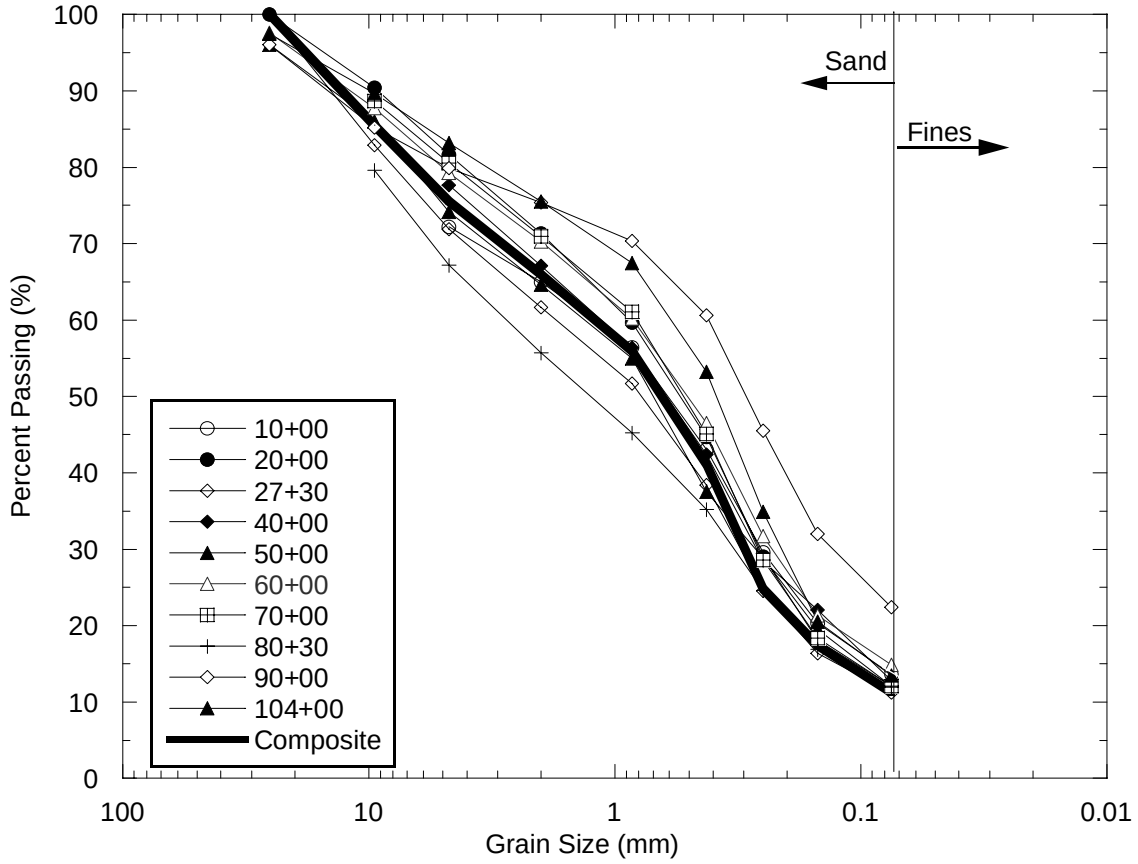

Fig. 4 Grain size distribution curves of RSG at sampling stations and composite of all stations.

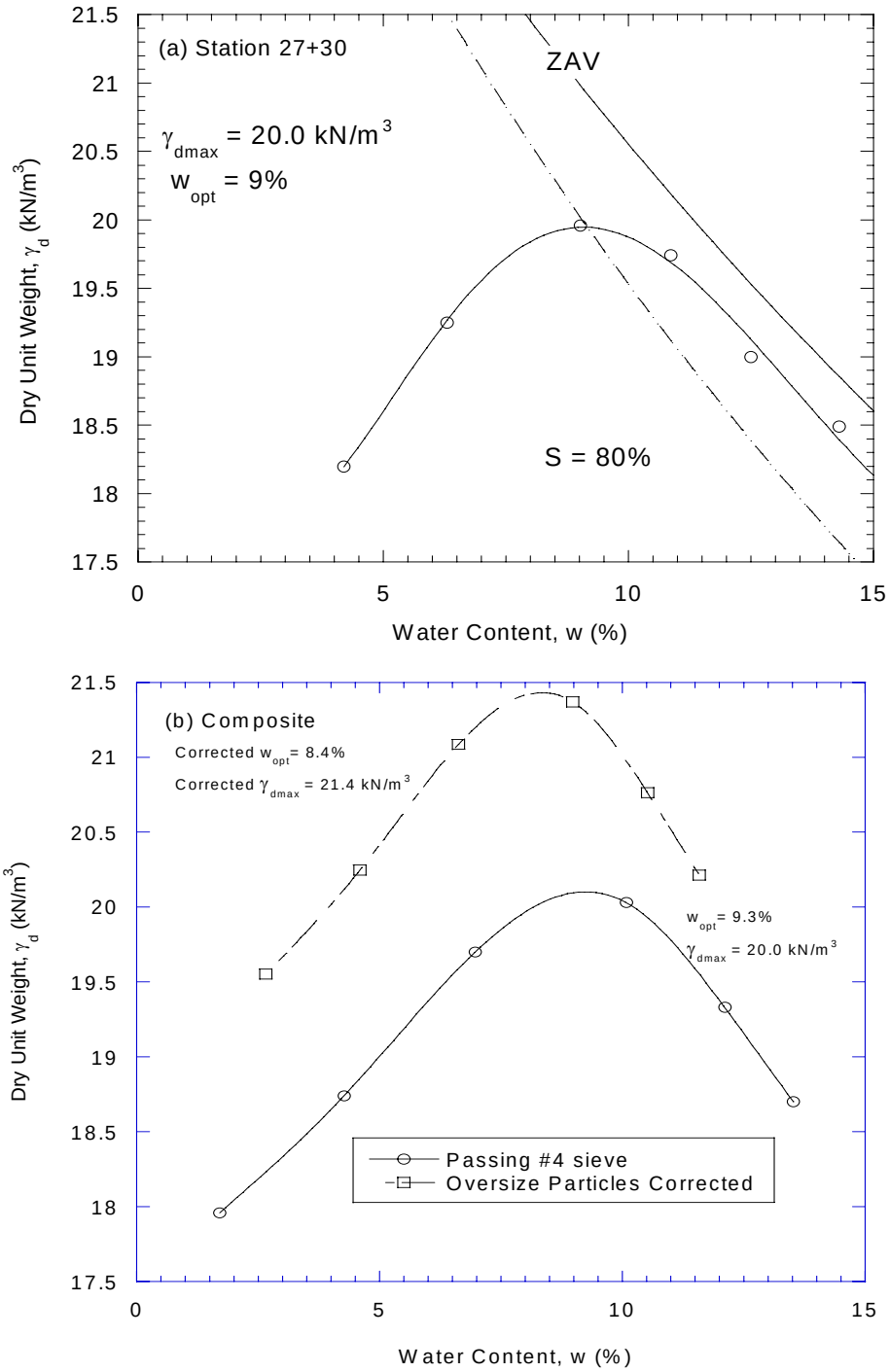

Fig. 5 Compaction curves: (a) for an RSG sample from Station 27+30 and (b) for the composite of RSG samples from of all stations.

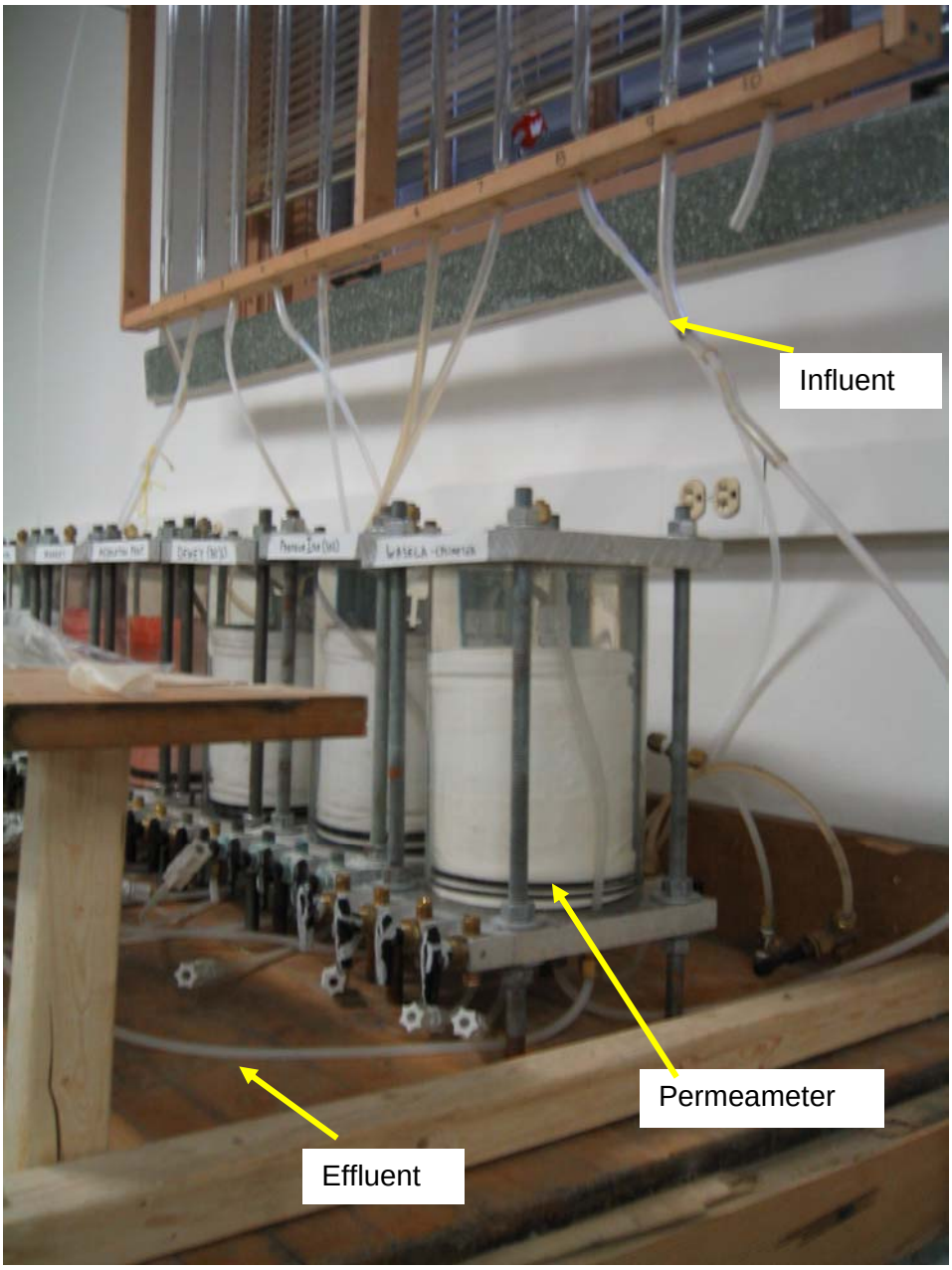

Fig. 6 Column leach test experimental setup

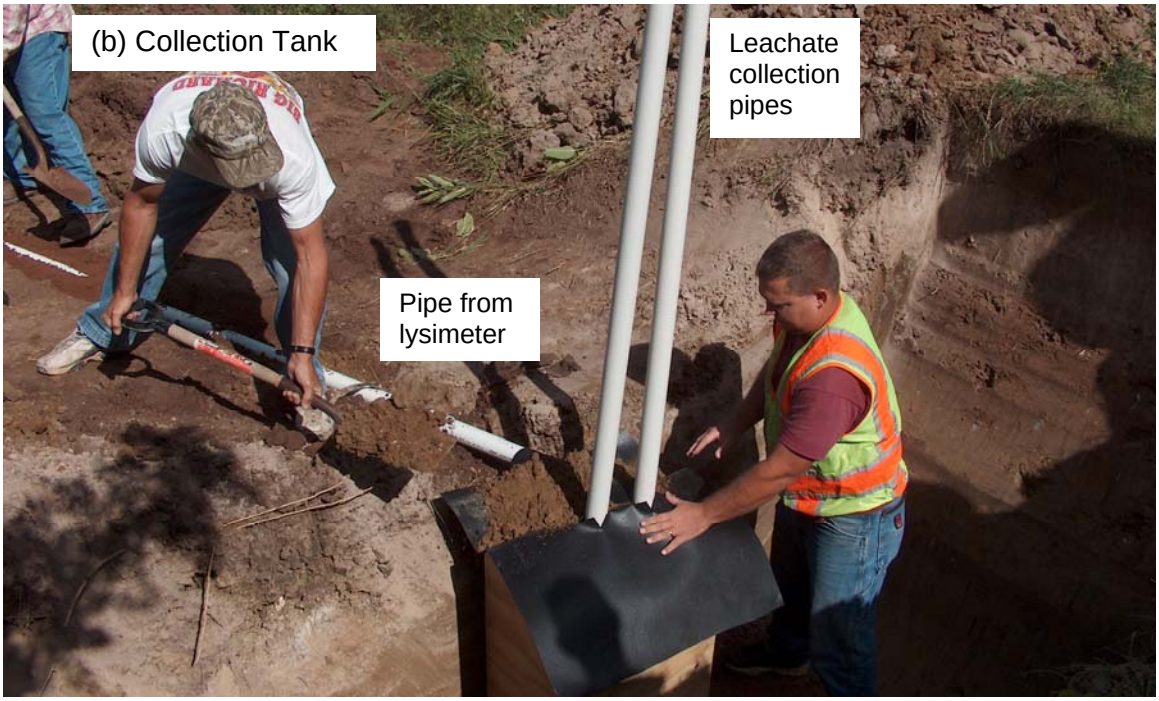

Fig. 7 Construction of Lysimeter (a) and leachate collection tank (b) at St. 27+30.

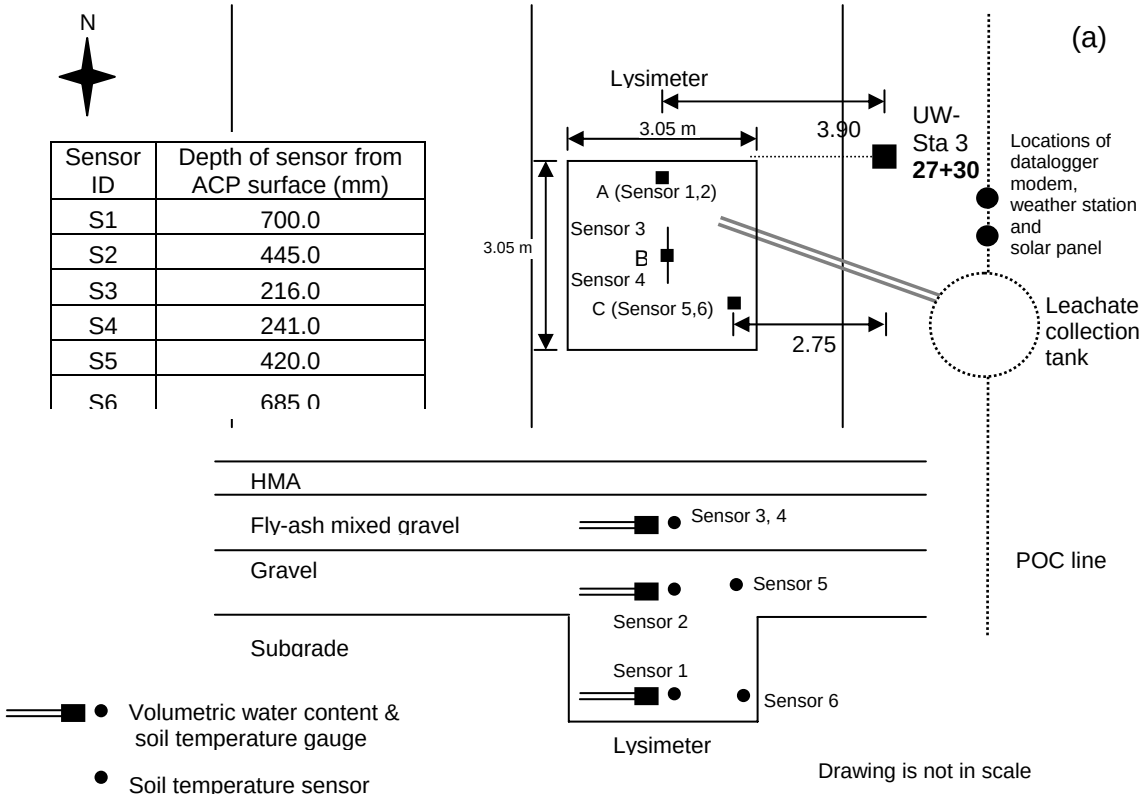

Sensor ID	Depth of sensor from ACP surface (mm)
S1	700.0
S2	445.0
S3	216.0
S4	241.0
S5	420.0
S6	685.0

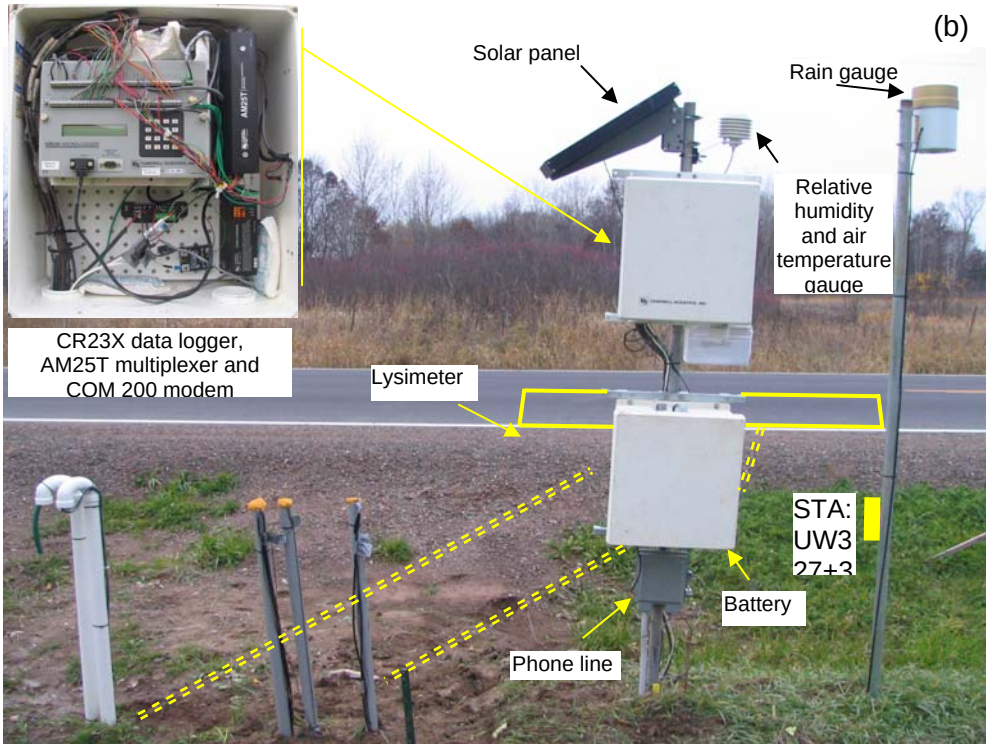

Fig. 8 (a) Layout (b) Photograph of completed field monitoring instrumentation system.

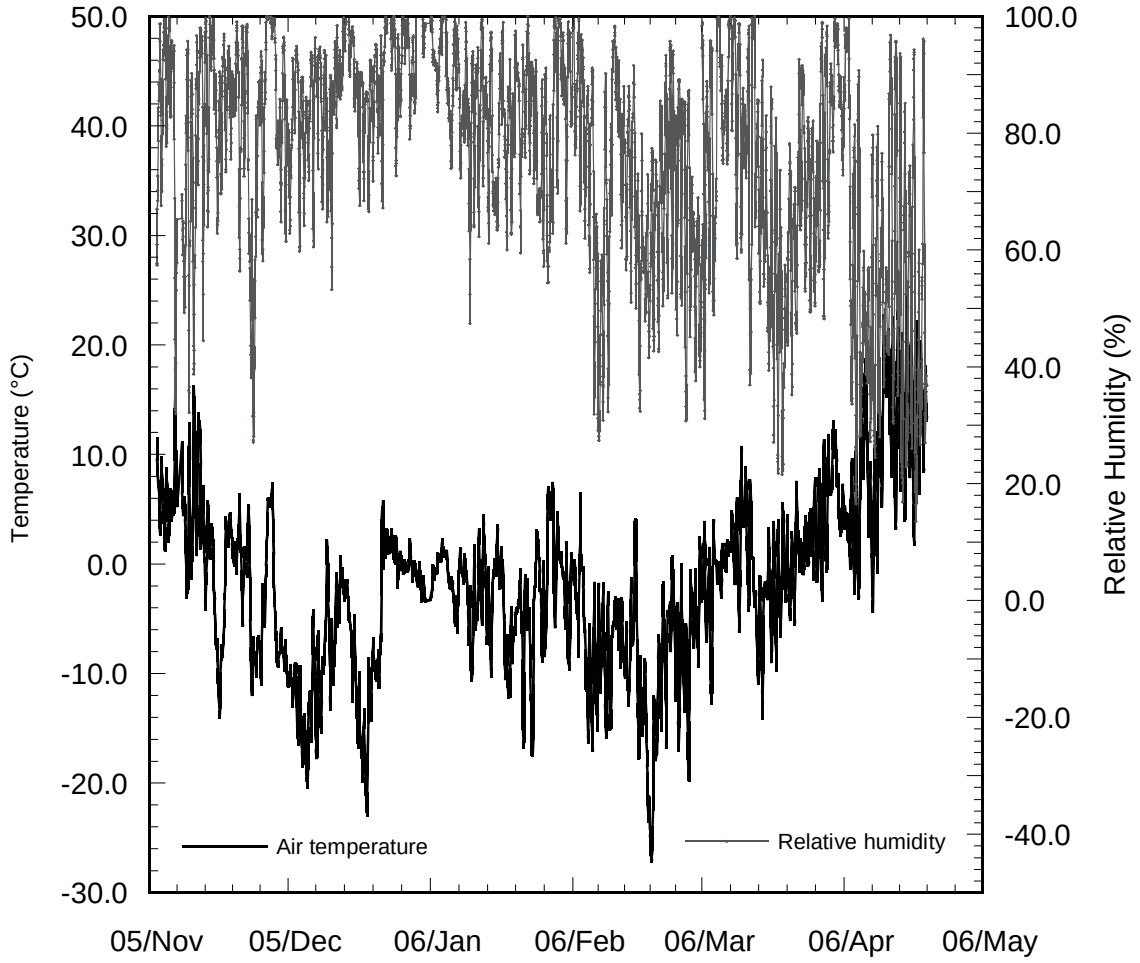

Fig. 9 Air temperature and relative humidity at CR 53.

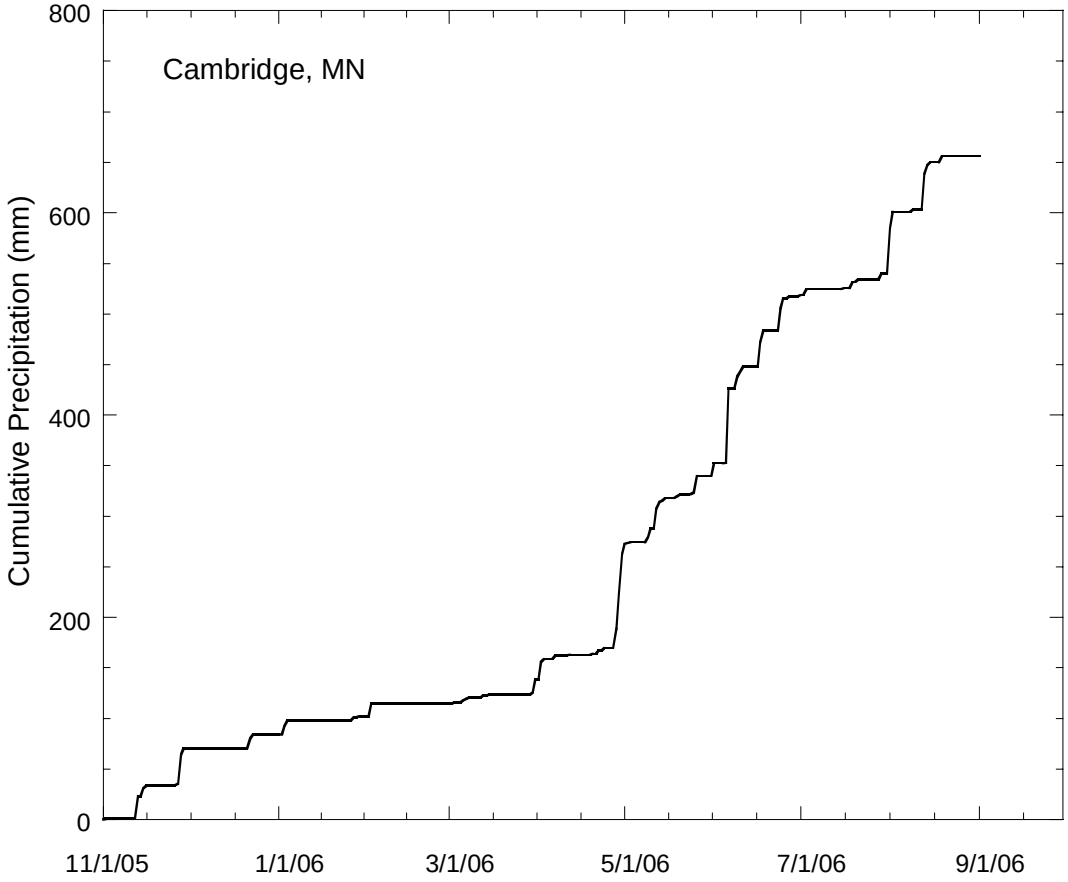

Fig. 10 Cumulative precipitation at Cambridge, MN (nearest NOAA Station to CR 53).

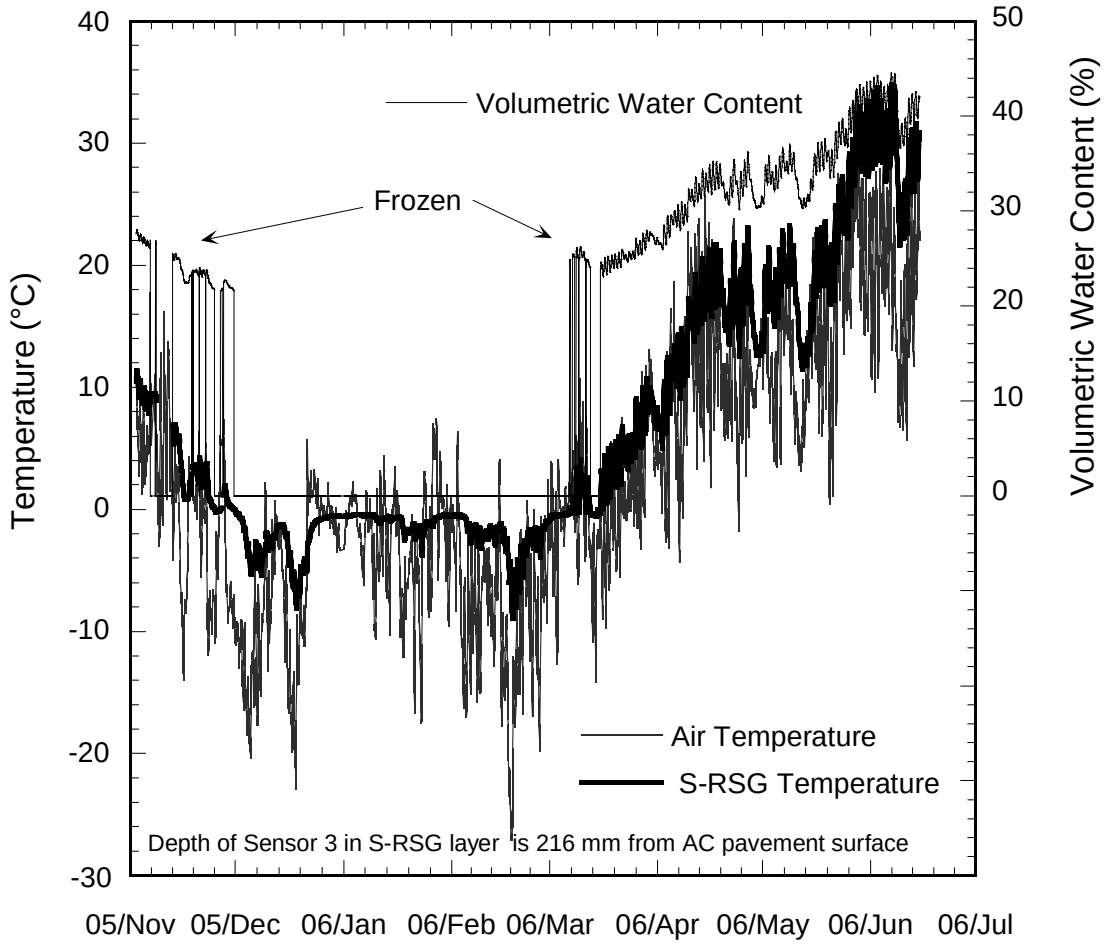

Fig. 11 Soil temperature and volumetric water content measurements in S-RSG layer at 216 mm depth from the AC pavement surface.

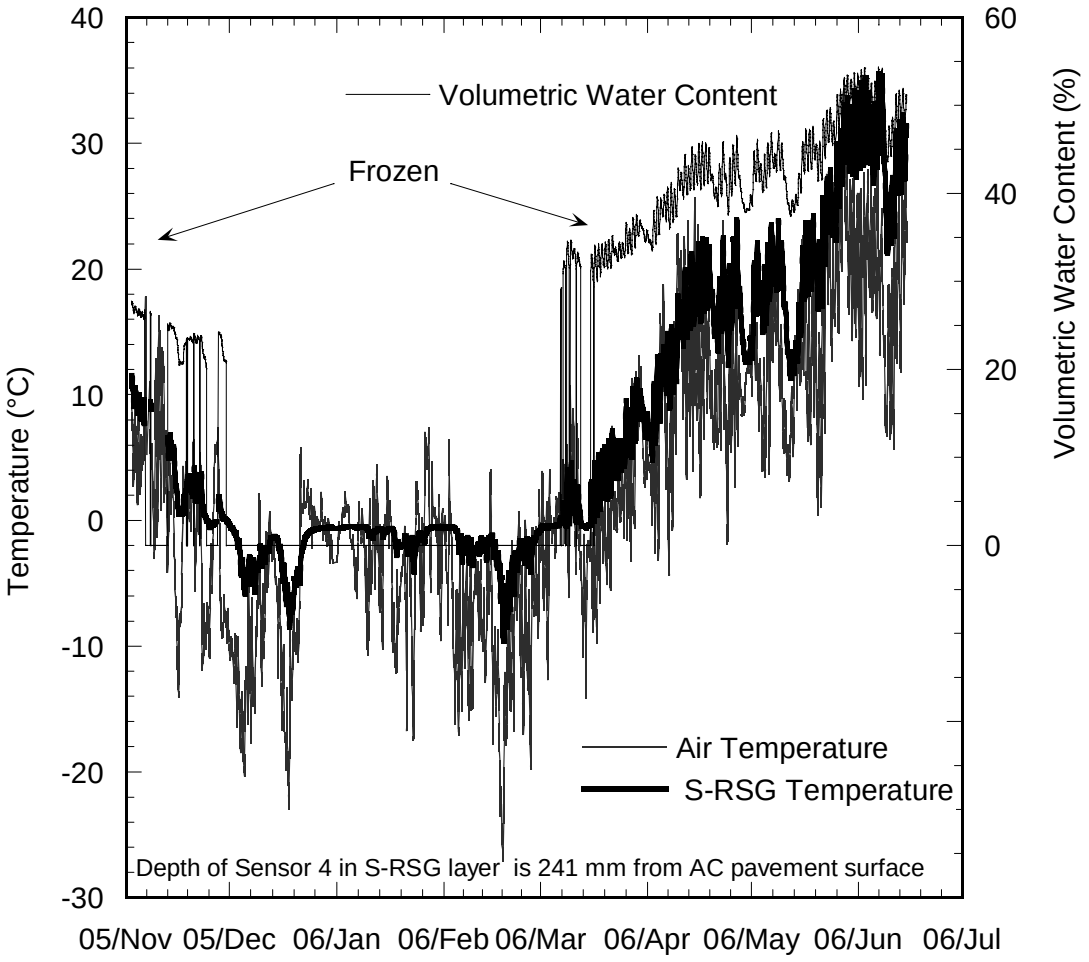

Fig. 12 Soil temperature and volumetric water content measurements in S-RSG layer at 241 mm depth from the AC pavement surface.

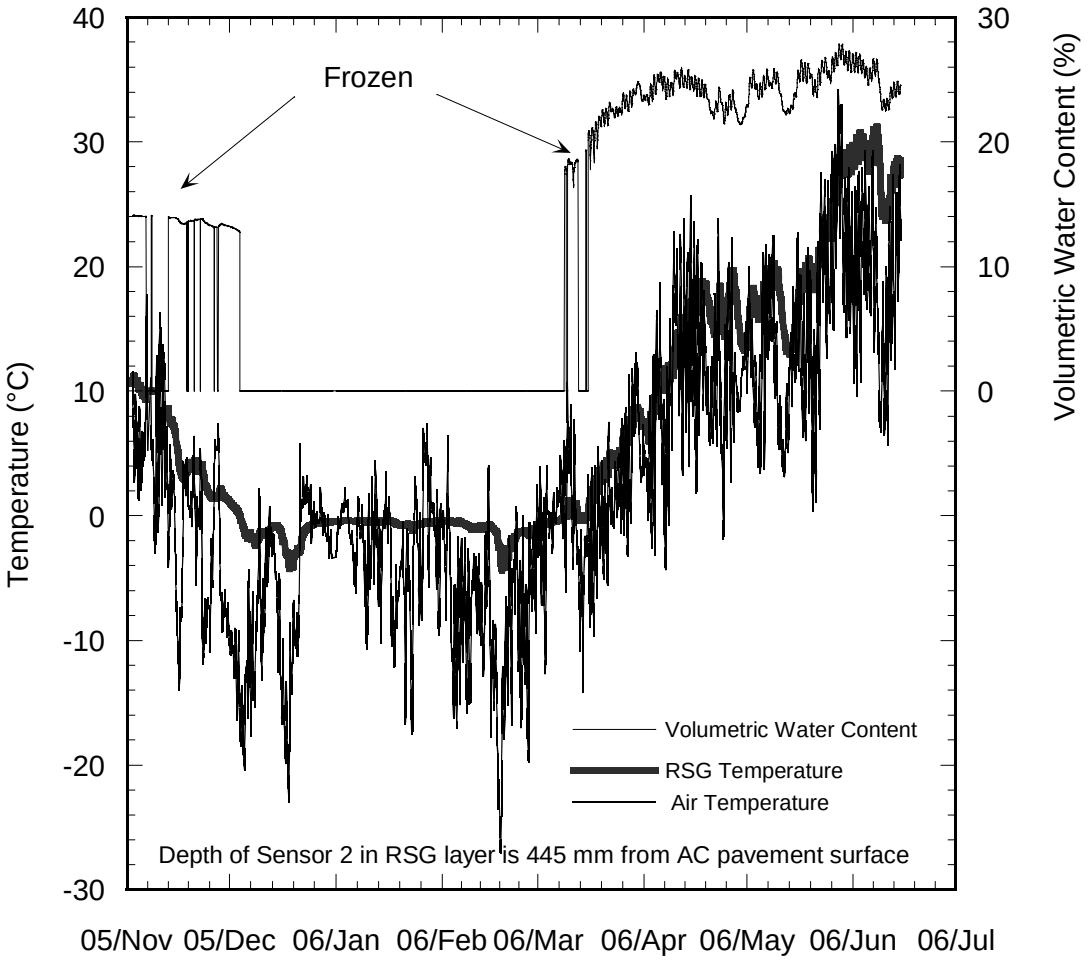

Fig. 13 Soil temperature and volumetric water content measurements in RSG at 445 mm depth from the AC pavement surface.

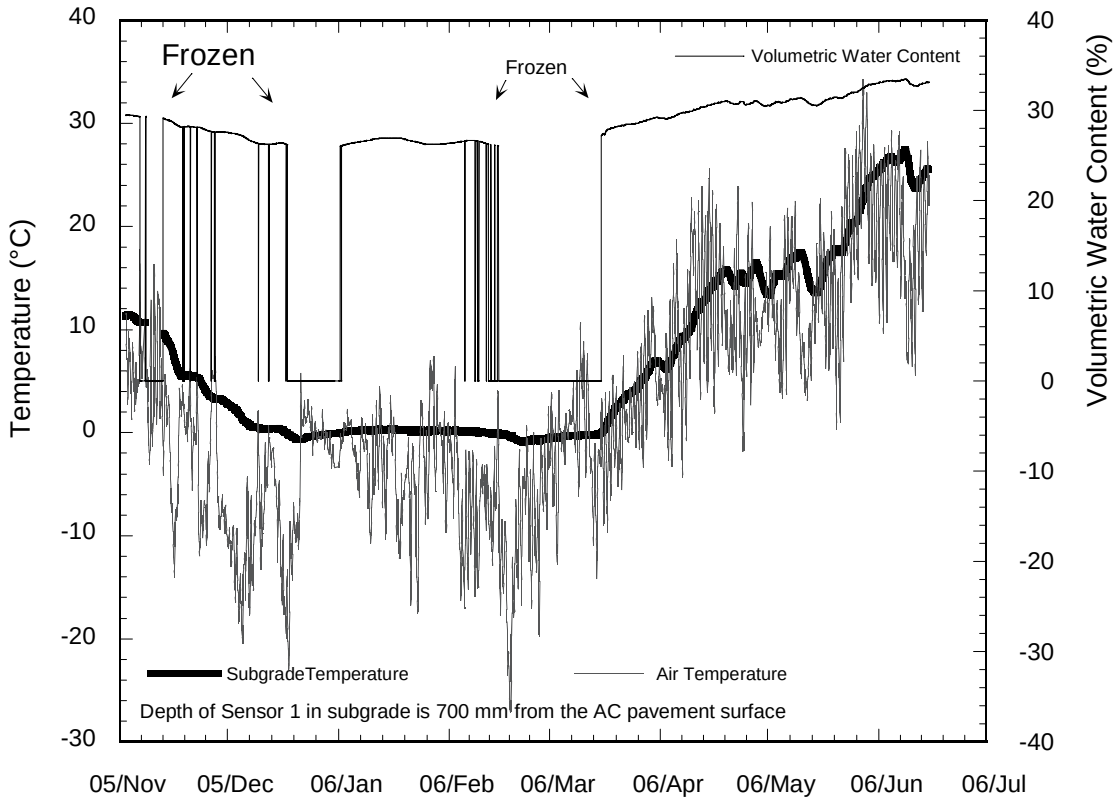

Fig. 14 Soil temperature and volumetric water content measurements in subgrade at 700 mm depth from the AC pavement surface.

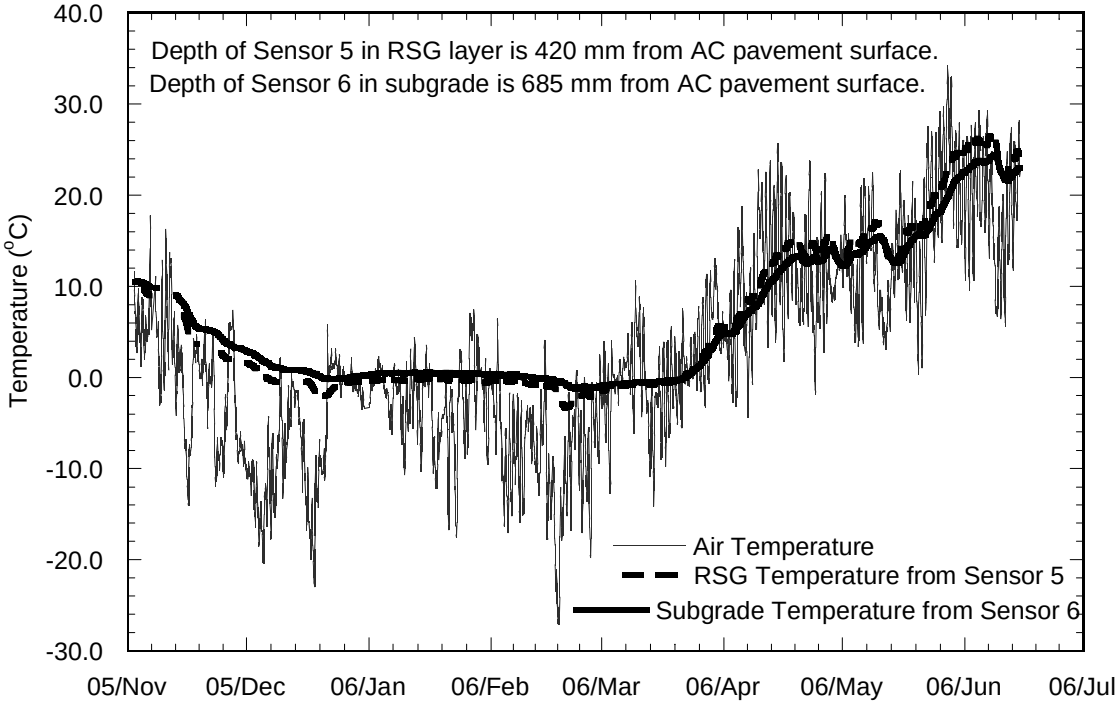

Fig. 15 Soil temperature measurements in RSG at 420 mm depth and in subgrade at 685 mm depth from the AC pavement surface.

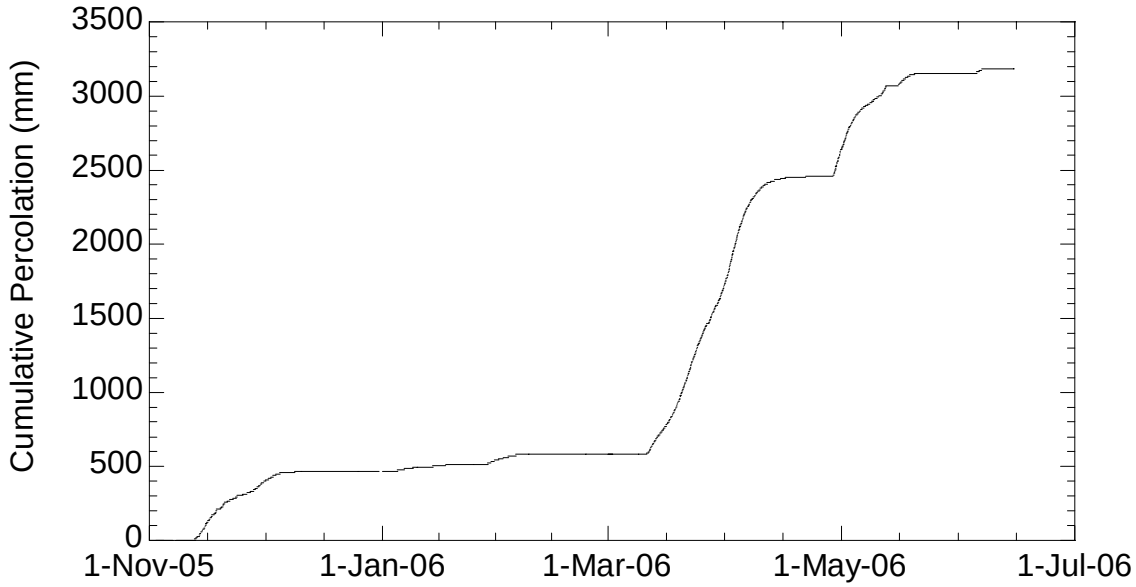

Fig. 16 Cumulative percolation into Lysimeter.

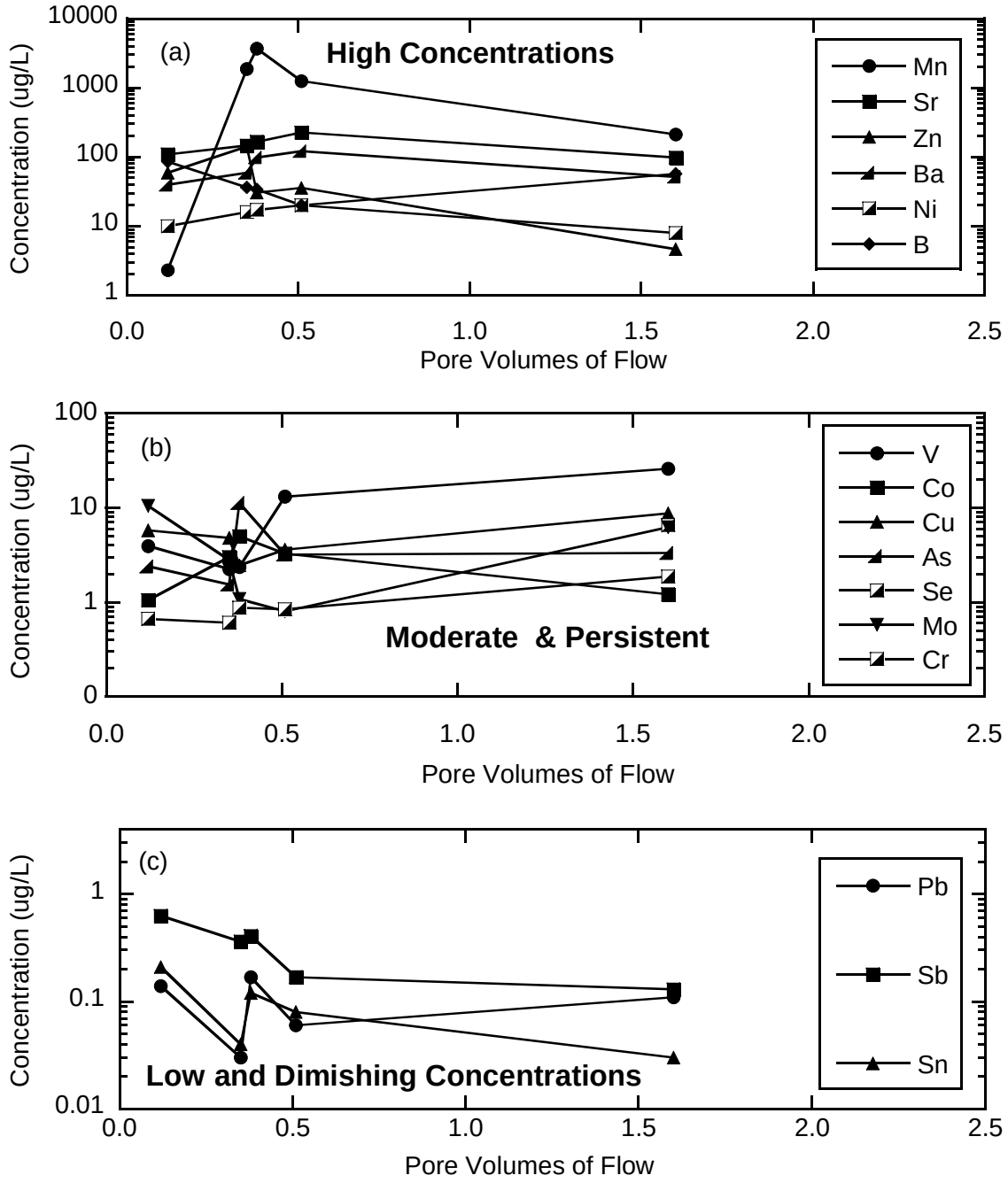

Fig. 17 Concentrations of trace elements in leachate collected in lysimeter: (a) elements with high concentrations, (b) elements with moderate and persistent concentrations and (c) elements with low and diminishing concentrations.

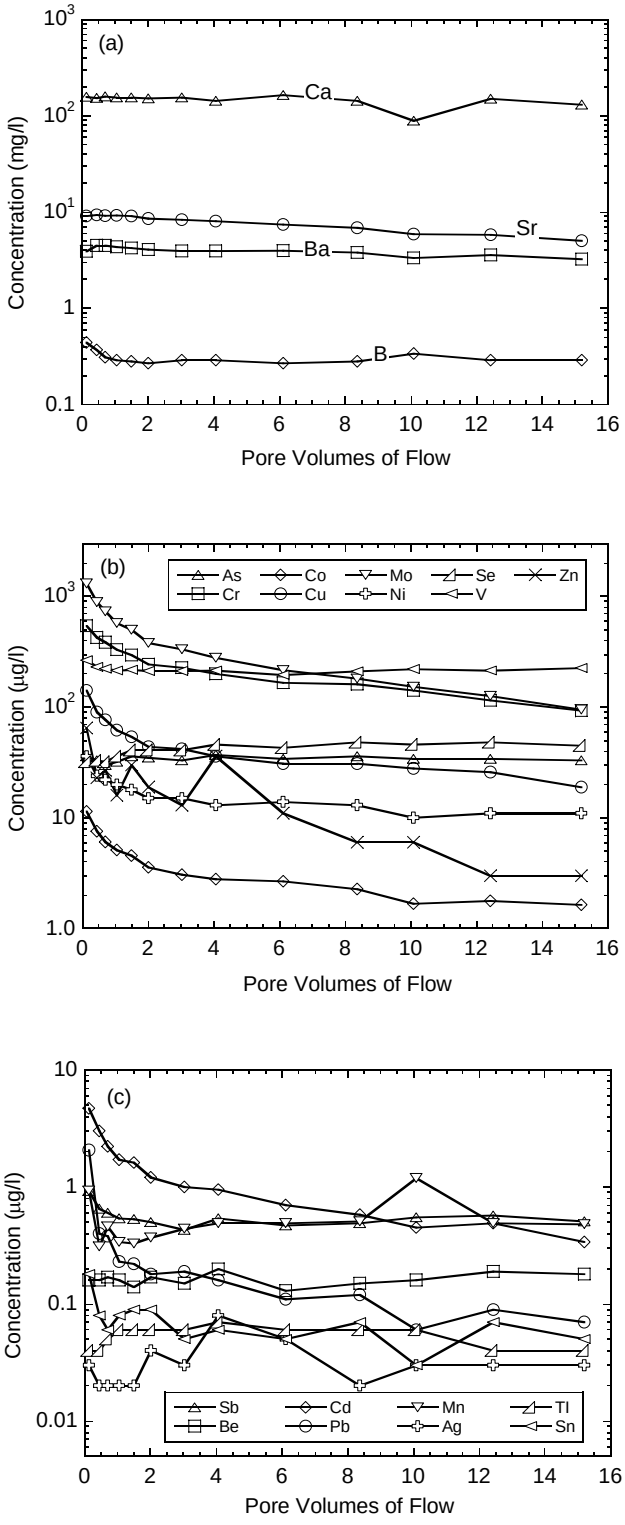

Fig. 18 Concentrations of trace elements in effluent from CLT on CH2 (Chisago Station 2): elements with peak concentrations (a) exceeding 1 mg/L, (b) elements with peak concentrations exceeding 10 μg/L, but less than 1 mg/L, and (c) elements with peak concentrations less than 10 μg/L.

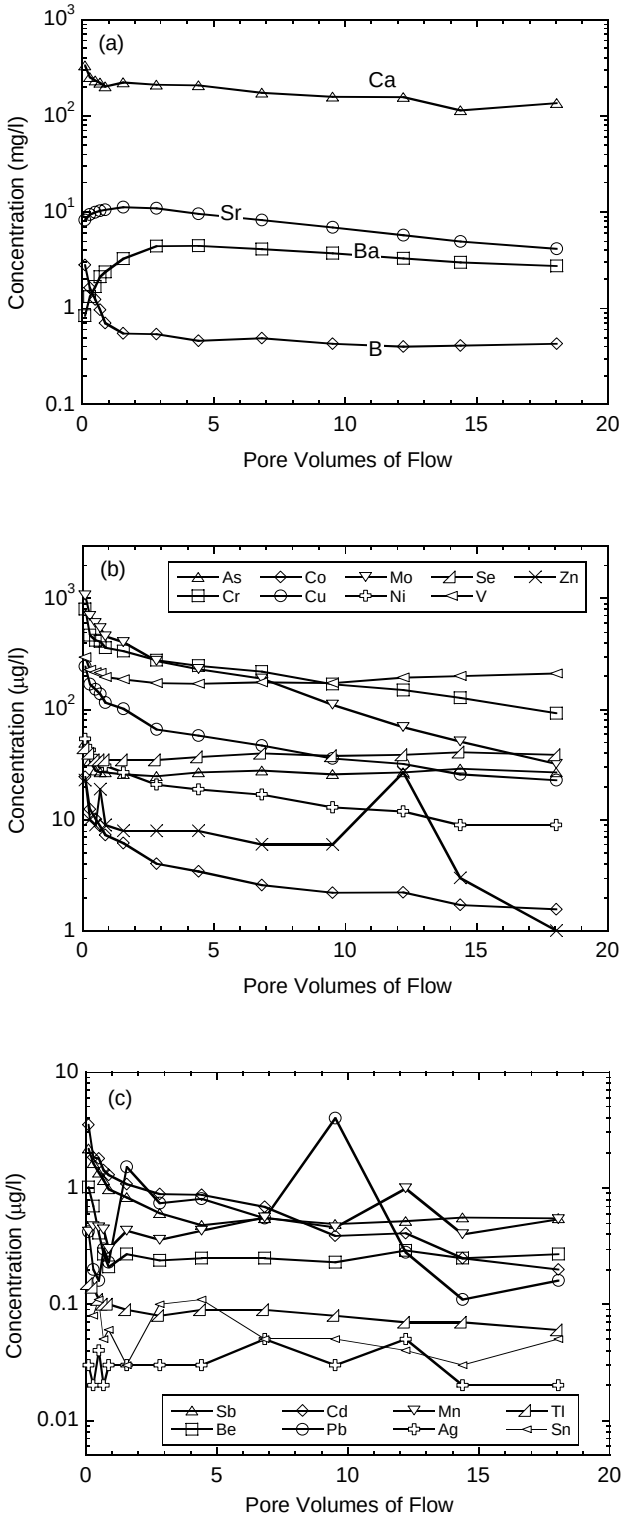

Fig. 19 Concentrations of trace elements in effluent from CLT on CH5 (Chisago Station 5): elements with peak concentrations (a) exceeding 1 mg/L, (b) exceeding 10 μg/L, but less than 1 mg/L, and (c) less than 10 μg/L.

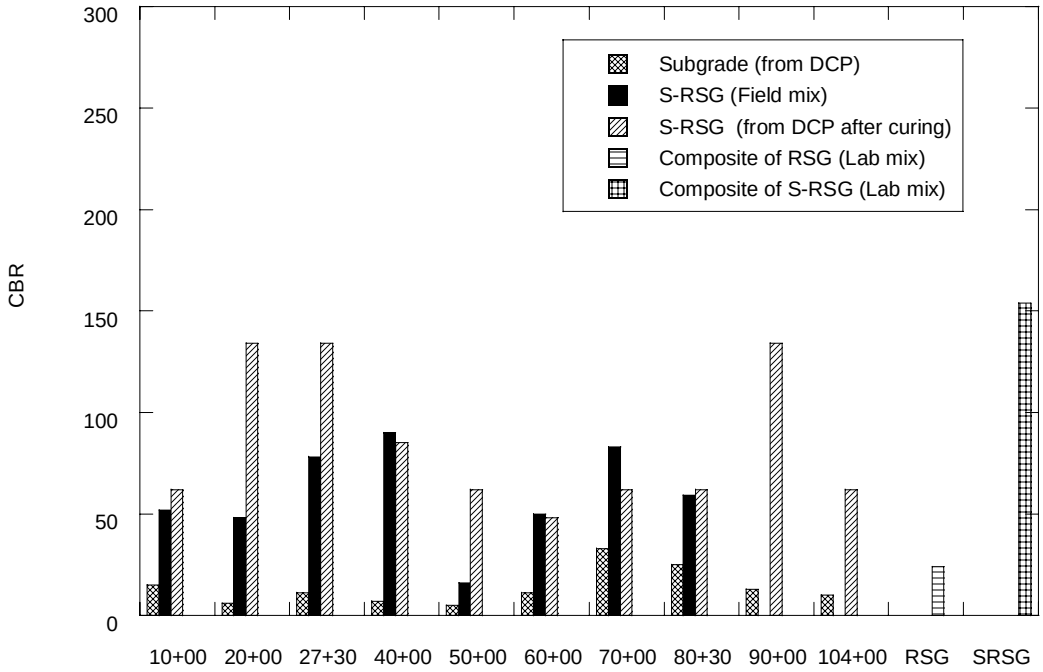

Fig. 20 California Bearing Ratio of S-RSG prepared in the field. Tests performed after 7 d of curing time.

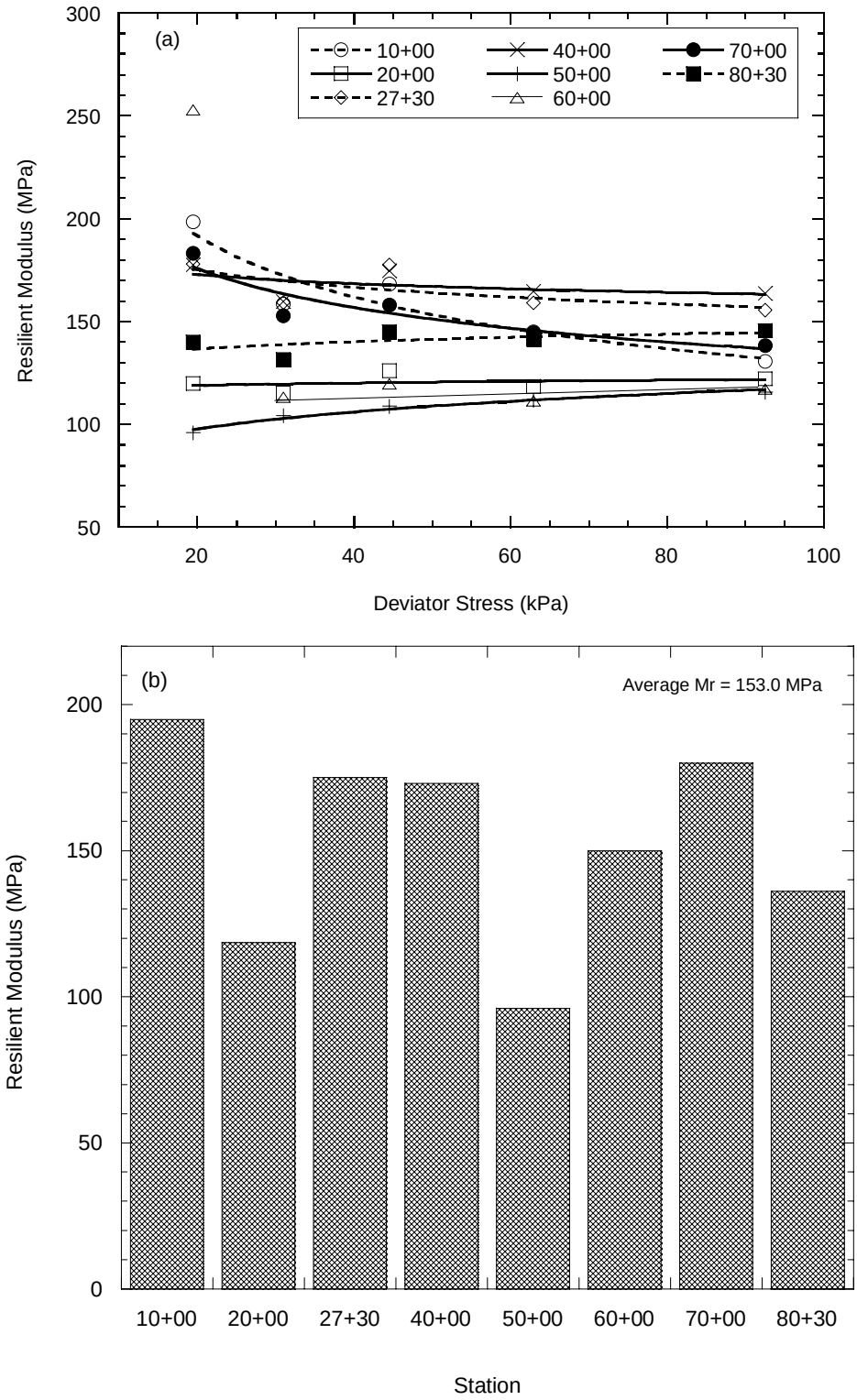

Fig. 21 Resilient modulus of mixture of fly-ash and gravelly soil prepared in the field. Tests performed after 7 d of curing time. (a) Resilient modulus versus deviator stress (b) Resilient modulus values at each station.

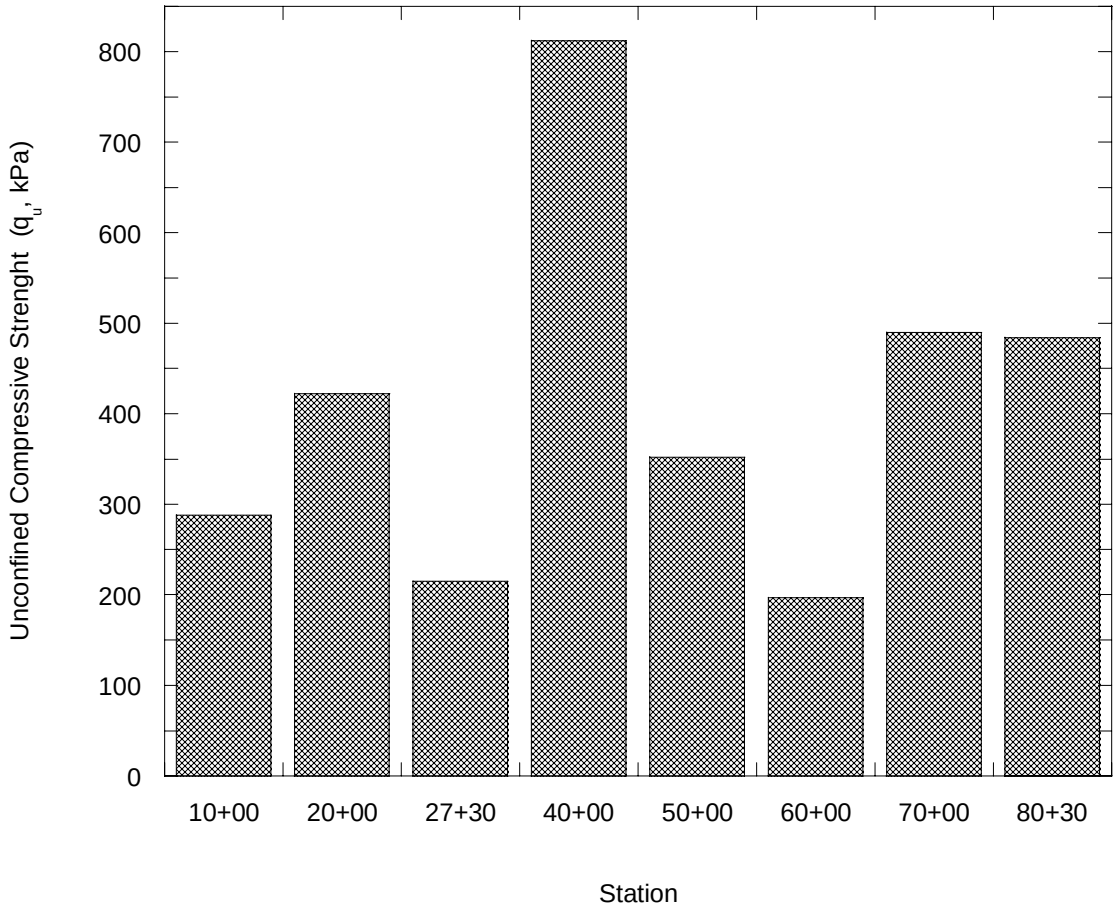

Fig. 22 Unconfined compressive strength (qu) of mixture of fly-ash and gravelly soil prepared in the field. Tests performed after 7 d of curing time.

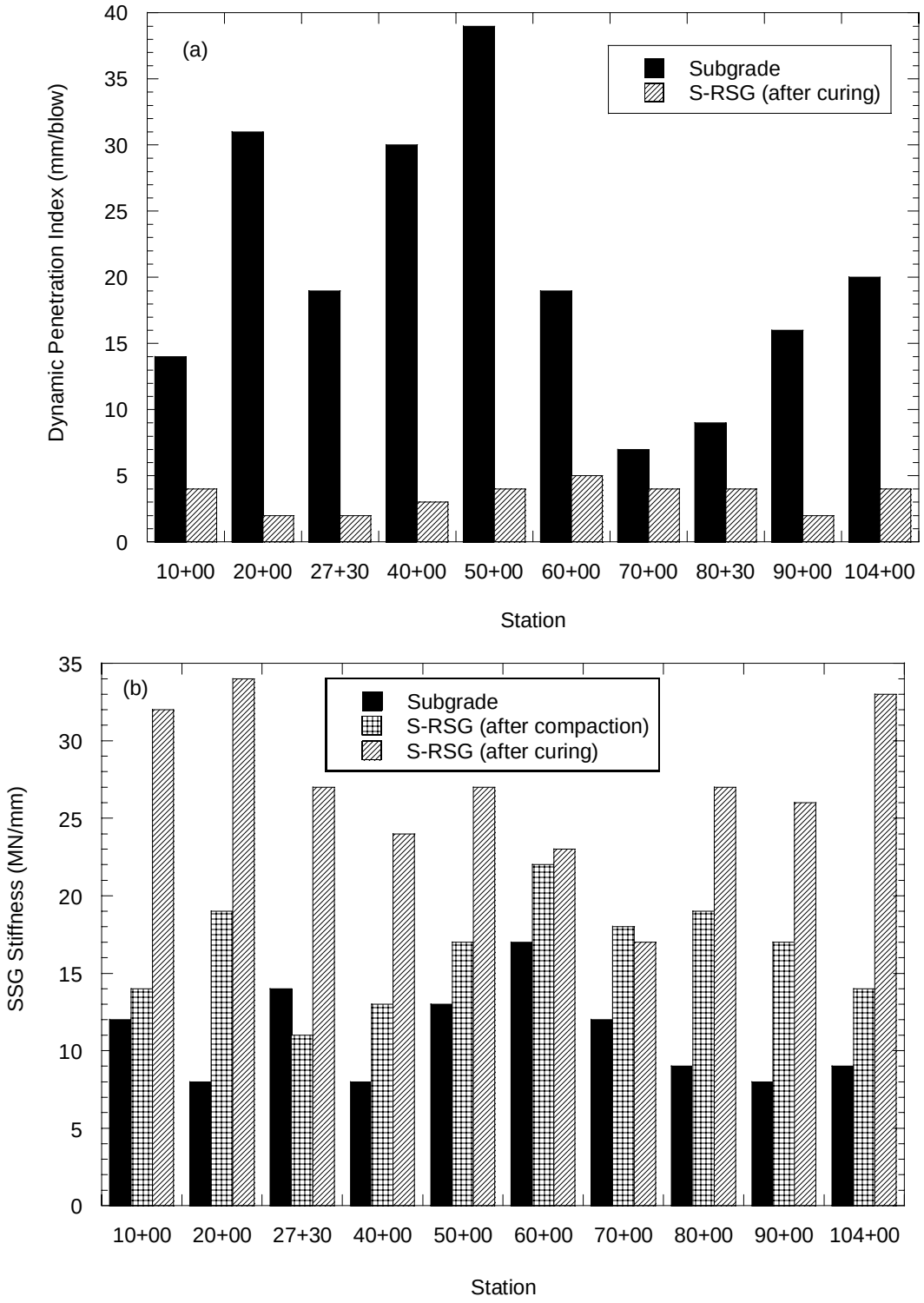

Fig. 23 (a) Dynamic penetration index (DPI) of subgrade and S-RSG soil prepared in the field after 7 d of curing, (b) Soil stiffness gauge stiffness of subgrade, S-RSG after compaction and after 7 of curing

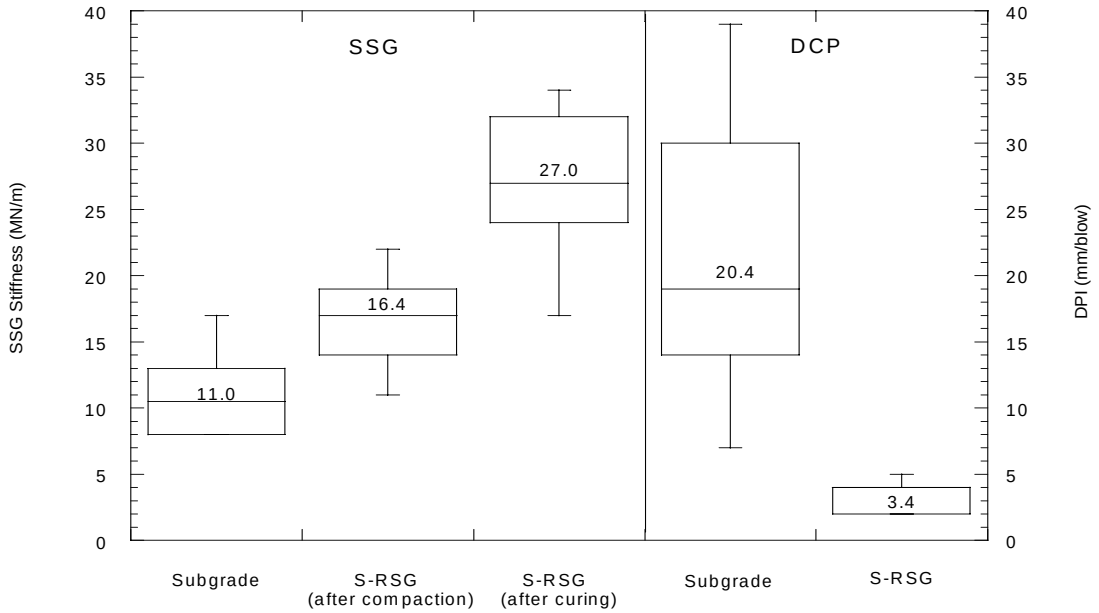

Fig. 24 Statistical evaluation of SSG and DCP test results.

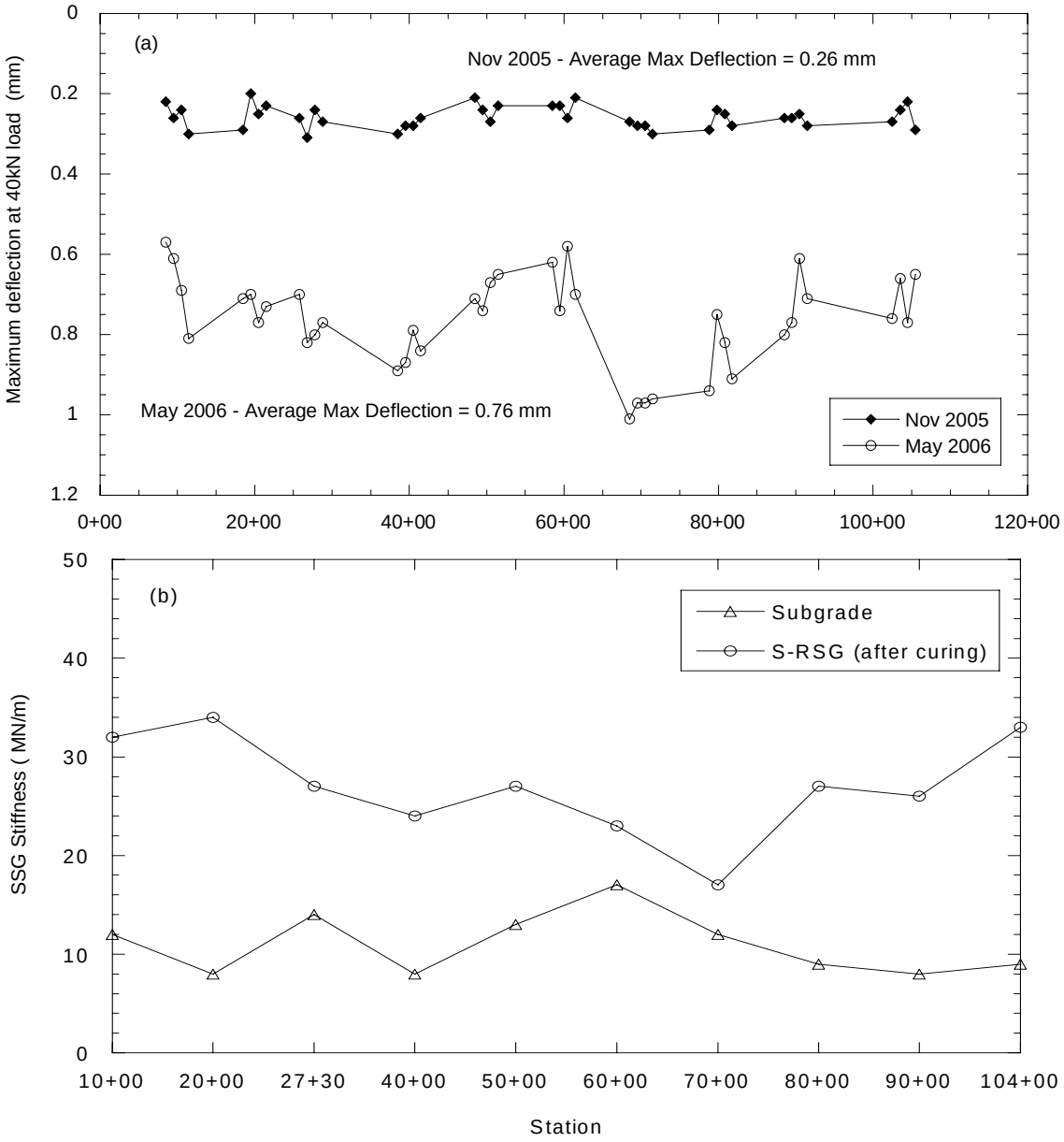

Fig. 25 (a) Maximum deflections -deflections from the center sensor at 40 kN load (b) Soil stiffness gauge stiffness of subgrade, S-RSG after compaction and after 7 d of curing

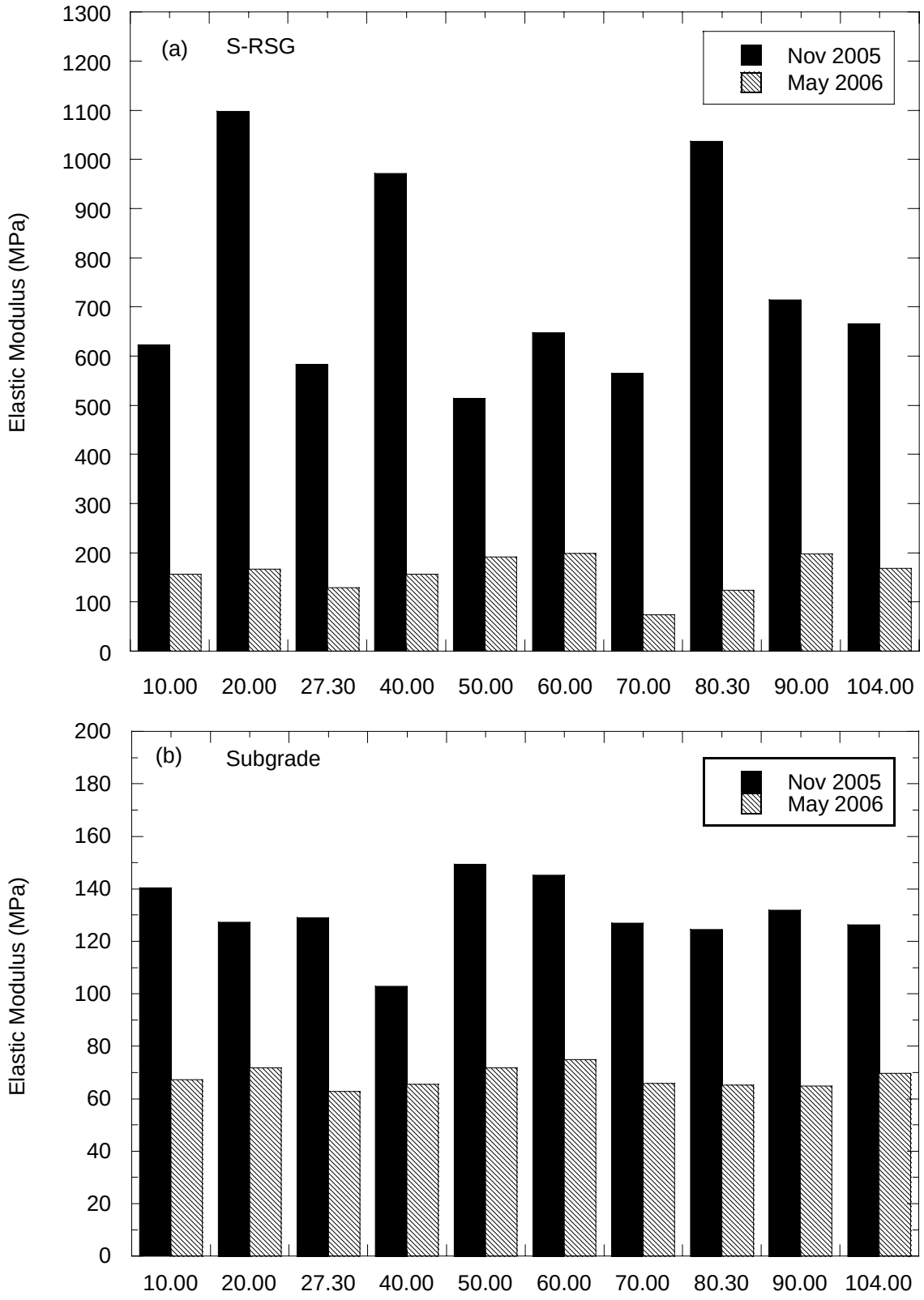

Fig. 26 Elastic moduli back-calculated from FWD tests by using MODULUS 6.0 software. (a) S-RSG (b) Subgrade.

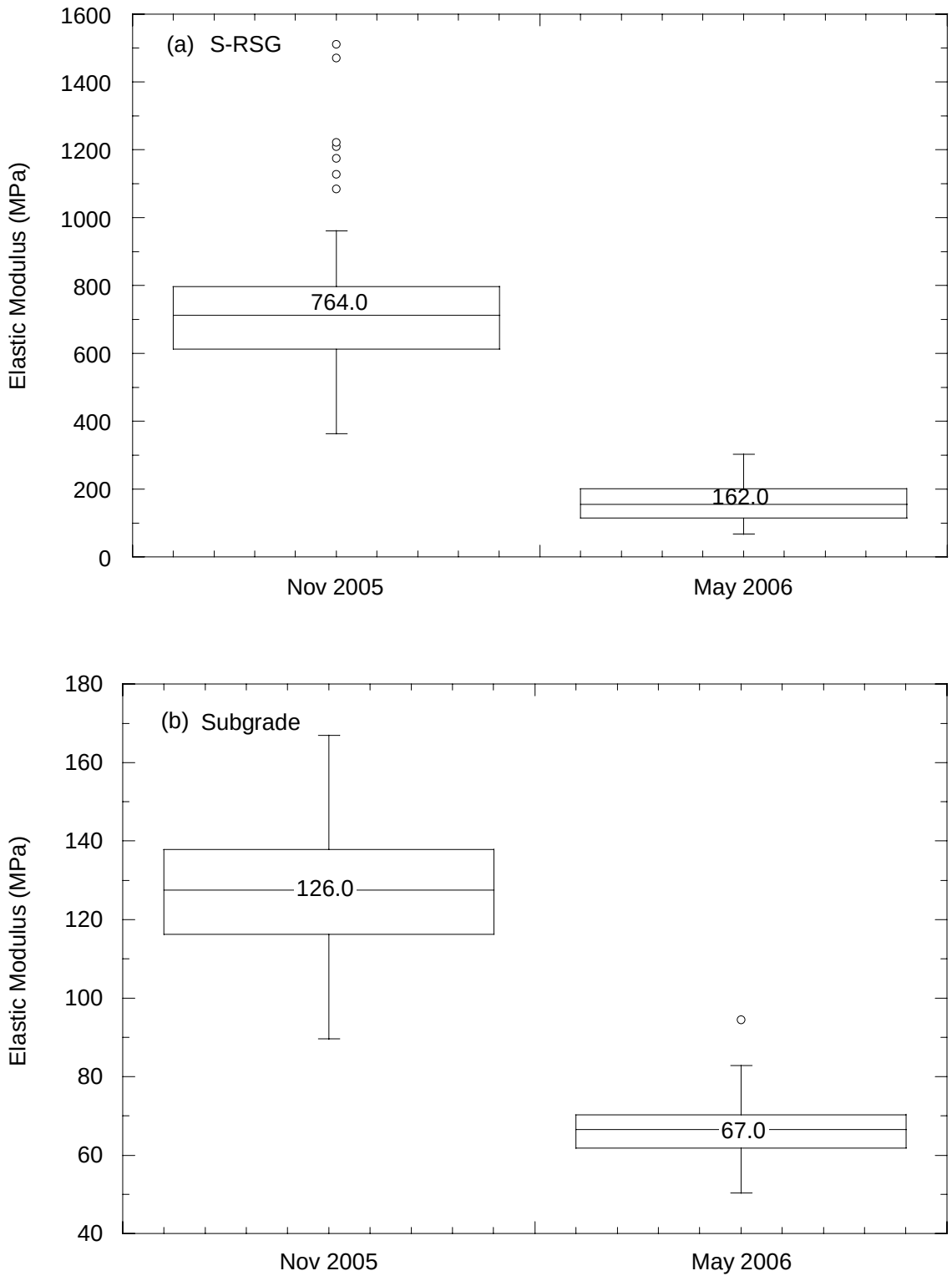

Fig. 27 Statistical evaluation of Elastic moduli back-calculated from FWD tests by using MODULUS 6.0 software. (a) S-RSG (b) Subgrade.

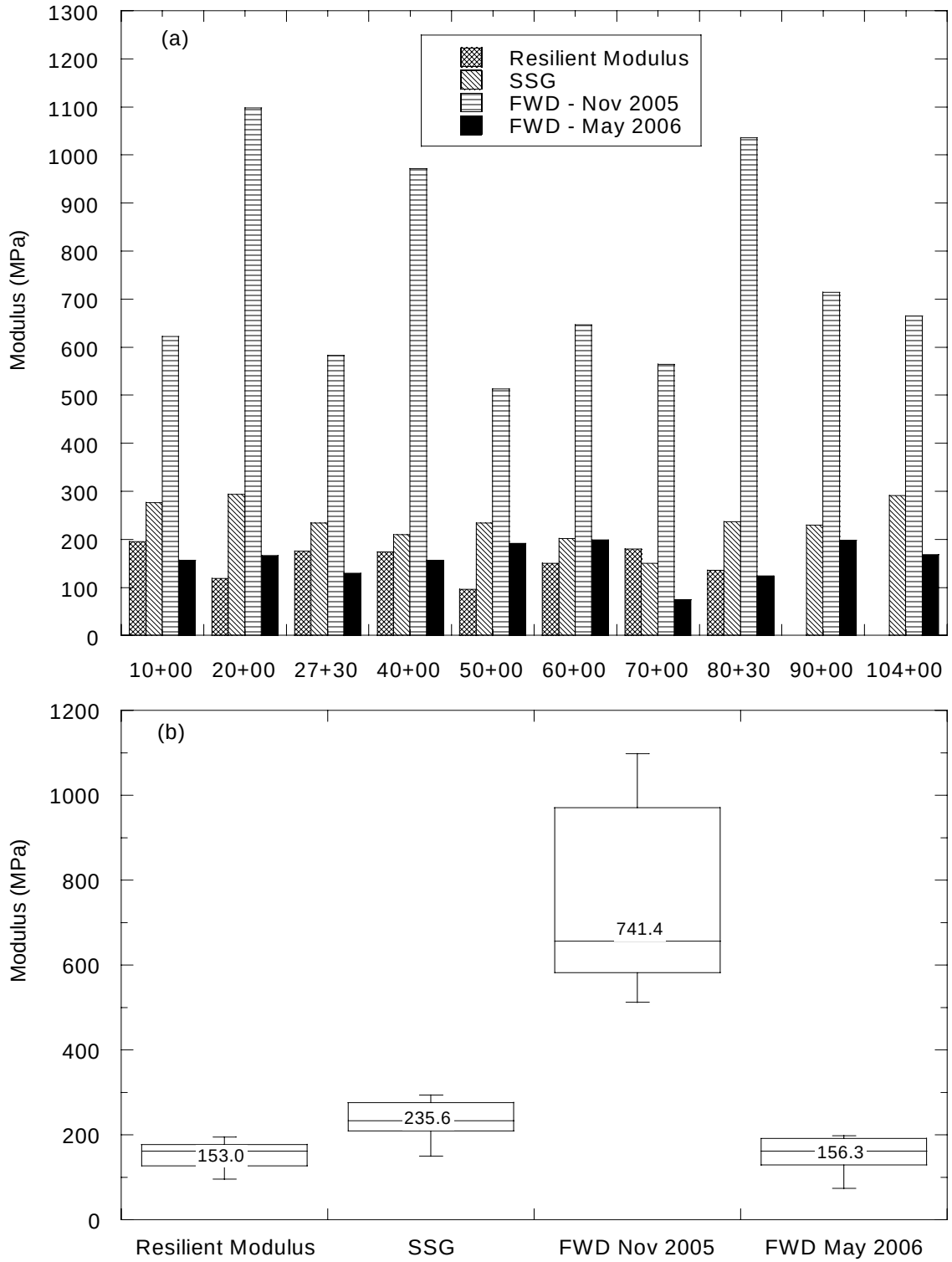

Fig. 28 Elastic modulus from laboratory resilient modulus, SSG and FWD tests (a) Modulus at each station (b) Statistical evaluation of results.

APPENDIX A

PHOTOGRAPHS OF
FIELD TESTS, CONSTRUCTION AND INSTRUMENTATION

Fig A1. Road-surface gravel (RSG) before construction

Fig A2. Soil Stiffness measurement by using SSG on subgrade.

Fig A3. Measurement of water content and unit weight of subgarde.

Fig A4. Dynamic cone penetration (DCP) test on subgrade

Fig A5. Collecting a sample in a thin-wall tube

Fig A6. Lay-down truck placing fly ash on RSG

Fig A7. Road-reclaimer blending fly ash and water truck

Fig A8. Road surface after blending process.

Fig A9. Compaction of fly ash and RSG mix by using sheep foot and roller drum compactors.

Fig A10. Compaction and grading of S-RSG surface.

Fig A11. Nuclear gauge and SSG tests on S-RSG.

Fig A12. Collection subgrade, RSG, fly ash and S-RSG bucket samples

Fig A13. M_r and CBR sample preparation of field mix soils collected with in 1-2 hour of blending process.

Fig A14. Excavation of lysimeter pit.

Fig A15. Construction of water tank and lysimeter – tank connection pipe.

Fig A16. Placement of geomembrane and geotextile.

Fig A17. Controlled filling of lysimeter pit with subgrade and RSG.

Fig A18. Installation of volumetric water content and temperature sensors into subgrade and RSG in lysimeter pit Sensor 1 is in subgrade and Sensor 2 is in RSG.

Fig A19. Installation of temperature sensors into subgrade and RSG in lysimeter pit. Sensor 6 is in subgrade and Sensor 5 is in RSG.

Fig A20. Installation of volumetric water content and temperature sensors (Sensor 3) into S-RSG on lysimeter.

Fig A21. Compcation of sensor trench with a hand compactor in S-RSG

Fig A22. View of monitoring station.

APPENDIX B
BORE HOLE LOGS

BRAUN INTERTEC

LOG OF BORING

Braun Project BBXX-01-097A
Geotechnical Evaluation
Various Gravel Roads
Chisago County, Minnesota

BORING: **53-0+00**
LOCATION: 25' Right

DRILLER: | METHOD: Power Auger | DATE: **5/24/01** | SCALE: **1" = 4'**

Depth feet	ASTM Symbol	Description of Materials (ASTM D2488 or D2487)	BPF	WL	Tests or Notes
0.0					
0.3	FILL	FILL: Silty Sand, fine- to medium-grained, with a trace of Gravel, Aggregate Base, brown, moist.			
	FILL	FILL: Silty Sand, fine- to medium-grained, trace of Gravel with roots, dark gray, moist.			
2.0	CL	LEAN CLAY, with a trace of Gravel, light yellow brown, moist.			
5.0		END OF BORING.			
		Boring then backfilled.			

(See Descriptive Terminology sheet for explanation of abbreviations)

BRAUN BASIC LOG B1097A.GPJ BRAUN.GDT 6/27/01 12:08

BRAUN™
INTERTEC

LOG OF BORING

Braun Project BBXX-01-097A
Geotechnical Evaluation
Various Gravel Roads
Chisago County, Minnesota

BORING: **53-5+00**
LOCATION: 24' in the Middle

DRILLER: | METHOD: Power Auger | DATE: **5/24/01** | SCALE: **1" = 4'**

Depth feet	ASTM Symbol	Description of Materials (ASTM D2488 or D2487)	BPF	WL	Tests or Notes
0.0					
0.6	FILL	FILL: Silty Sand, fine- to medium-grained, with a trace of Gravel, Aggregate Base, reddish brown, moist.			
2.0	FILL	FILL: Silty Sand, fine- to medium-grained, with a trace of Gravel, dark gray, moist.			
5.0	CL	LEAN CLAY, with a trace of Gravel, light yellowish brown, moist.			
		END OF BORING.			
		Boring then backfilled.			

(See Descriptive Terminology sheet for explanation of abbreviations)

BRAUN BASIC LOG B1097A.GPJ BRAUN.GDT 6/27/01 12:11

BRAUN INTERTEC

LOG OF BORING

Braun Project BBXX-01-097A
Geotechnical Evaluation
Various Gravel Roads
Chisago County, Minnesota

BORING: **53-10+00**
LOCATION: 24' Left

DRILLER: | METHOD: Power Auger | DATE: **5/24/01** | SCALE: **1" = 4'**

Depth feet	ASTM Symbol	Description of Materials (ASTM D2488 or D2487)	BPF	WL	Tests or Notes
0.0					
0.8	FILL	FILL: Silty Sand, fine- to medium-grained, with a trace of Gravel, Aggregate Base, reddish brown, moist.			
2.0	FILL	FILL: Silty Sand, fine- to medium-grained, with a trace of Gravel, grayish brown, moist.			
	CL	LEAN CLAY, with a trace of Gravel, yellowish brown, moist.			
5.0		END OF BORING.			
		Boring then backfilled.			

(See Descriptive Terminology sheet for explanation of abbreviations)

BRAUN BASIC LOG B1097A.GPJ BRAUN.GDT 6/27/01 12:08

BRAUN™
INTERTEC

LOG OF BORING

Braun Project BBXX-01-097A
Geotechnical Evaluation
Various Gravel Roads
Chisago County, Minnesota

BORING: **53-15+00**
LOCATION: 26' in the Middle

DRILLER: | METHOD: Power Auger | DATE: **5/24/01** | SCALE: **1" = 4'**

Depth feet	ASTM Symbol	Description of Materials (ASTM D2488 or D2487)	BPF	WL	Tests or Notes
0.0					
0.7	FILL	FILL: Silty Sand, fine- to medium-grained, with a trace of Gravel, Aggregate Base, yellowish brown, moist.			
	SP	POORLY GRADED SAND, fine- to medium-grained, yellowish brown, moist.			
4.0					
5.0	CL	LEAN CLAY, with a trace of Gravel, grayish brown, moist.			
		END OF BORING.			
		Boring then backfilled.			

(See Descriptive Terminology sheet for explanation of abbreviations)

BRAUN INTERTEC

LOG OF BORING

Braun Project BBXX-01-097A
Geotechnical Evaluation
Various Gravel Roads
Chisago County, Minnesota

BORING: **53-25+00**
LOCATION: 24' Right

DRILLER: | METHOD: Power Auger | DATE: **5/24/01** | SCALE: **1" = 4'**

Depth feet	ASTM Symbol	Description of Materials (ASTM D2488 or D2487)	BPF	WL	Tests or Notes
0.0					
0.5	FILL	FILL: Silty Sand, fine- to medium-grained, with a trace of Gravel, Aggregate Base, yellowish brown, moist.			
2.0	FILL	FILL: Silty Sand, fine- to medium-grained, with a trace of Gravel, dark gray, moist.			
	ML	SILT, with wood, black, moist.			
5.0		END OF BORING.			
		Boring then backfilled.			

(See Descriptive Terminology sheet for explanation of abbreviations)

BRAUN BASIC LOG B1097A.GPJ BRAUN.GDT 6/27/01 12:09

BRAUN INTERTEC

LOG OF BORING

Braun Project BBXX-01-097A
Geotechnical Evaluation
Various Gravel Roads
Chisago County, Minnesota

BORING: **53-30+00**
LOCATION: 26' in the Middle

DRILLER: | METHOD: Power Auger | DATE: **5/24/01** | SCALE: **1" = 4'**

Depth feet	ASTM Symbol	Description of Materials (ASTM D2488 or D2487)	BPF	WL	Tests or Notes
0.0					
0.8	FILL	FILL: Silty Sand, fine- to medium-grained, with a trace of Gravel, Aggregate Base, yellowish brown, moist.			
2.0	FILL	FILL: Silty Sand, fine- to medium-grained, with a trace of Gravel, dark gray, moist.			
	CL	LEAN CLAY, with a trace of Gravel, light yellowish brown, moist.			
5.0		END OF BORING.			
		Boring then backfilled.			

(See Descriptive Terminology sheet for explanation of abbreviations)

BRAUN BASIC LOG B1097A.GPJ BRAUN.GDT 6/27/01 12:10

BRAUN INTERTEC

LOG OF BORING

Braun Project BBXX-01-097A
Geotechnical Evaluation
Various Gravel Roads
Chisago County, Minnesota

BORING: **53-35+00**
LOCATION: 26' Left

DRILLER: | METHOD: Power Auger | DATE: **5/24/01** | SCALE: 1" = 4'

Depth feet	ASTM Symbol	Description of Materials (ASTM D2488 or D2487)	BPF	WL	Tests or Notes
0.0					
0.4	FILL	FILL: Silty Sand, fine- to medium-grained, with a trace of Gravel, Aggregate Base, yellowish brown, moist.			
2.0	FILL	FILL: Silty Sand, fine- to medium-grained, with a trace of Gravel, dark brown, moist.			
5.0	SP	POORLY GRADED SAND, fine- to medium-grained, yellowish brown, moist.			
		END OF BORING.			
		Boring then backfilled.			

(See Descriptive Terminology sheet for explanation of abbreviations)

BRAUN BASIC LOG B1097A.GPJ BRAUN.GDT 6/27/01 12:10

BRAUN INTERTEC

LOG OF BORING

Braun Project BBXX-01-097A
Geotechnical Evaluation
Various Gravel Roads
Chisago County, Minnesota

BORING: **53-40+00**
LOCATION: 24' in the Middle

DRILLER: | METHOD: Power Auger | DATE: **5/24/01** | SCALE: **1" = 4'**

Depth feet	ASTM Symbol	Description of Materials (ASTM D2488 or D2487)	BPF	WL	Tests or Notes
0.0					
0.4	FILL	FILL: Silty Sand, fine- to medium-grained, with a trace of Gravel, Aggregate Base, yellowish brown, moist.			
1.5	FILL	FILL: Silty Sand, fine- to medium-grained, with a trace of Gravel, brown, moist.			
	SM	SILTY SAND, fine-grained, with a trace of Gravel, dark gray, moist.			
3.5	SP	POORLY GRADED SAND, fine- to medium-grained, orangish brown, moist.			
5.0		END OF BORING.			
		Boring then backfilled.			

(See Descriptive Terminology sheet for explanation of abbreviations)

BRAUN BASIC LOG B1097A.GPJ BRAUN.GDT 6/27/01 12:10

BRAUN INTERTEC

LOG OF BORING

Braun Project BBXX-01-097A
Geotechnical Evaluation
Various Gravel Roads
Chisago County, Minnesota

BORING: **53-45+20**
LOCATION: 25' Left, #323

DRILLER: | METHOD: Power Auger | DATE: **5/24/01** | SCALE: **1" = 4'**

Depth feet	ASTM Symbol	Description of Materials (ASTM D2488 or D2487)	BPF	WL	Tests or Notes
0.0					
0.3	FILL	FILL: Silty Sand, fine- to medium-grained, with a trace of Gravel, Aggregate Base, brown, moist.			
1.5	FILL	FILL: Silty Sand, fine- to medium-grained, with a trace of Gravel, dark brown, moist.			
	CL	LEAN CLAY, with a trace of Gravel, light yellowish brown, moist.			
5.0		END OF BORING.			
		Boring then backfilled.			

(See Descriptive Terminology sheet for explanation of abbreviations)

BRAUN BASIC LOG B1097A.GPJ BRAUN.GDT 6/27/01 12:11

BRAUN INTERTEC

LOG OF BORING

Braun Project BBXX-01-097A
Geotechnical Evaluation
Various Gravel Roads
Chisago County, Minnesota

BORING: **53-50+00**
LOCATION: 25' in the Middle

DRILLER: | METHOD: Power Auger | DATE: **5/24/01** | SCALE: **1" = 4'**

Depth feet	ASTM Symbol	Description of Materials (ASTM D2488 or D2487)	BPF	WL	Tests or Notes
0.0					
0.8	FILL	FILL: Silty Sand, fine- to medium-grained, with a trace of Gravel, Aggregate Base, brown, moist.			
	SP	POORLY GRADED SAND, fine- to medium-grained, yellowish brown, moist.			
4.5					
5.0	CL	LEAN CLAY, with a trace of Gravel, green to brown, waterbearing.			
		END OF BORING.			
		Boring then backfilled.			

(See Descriptive Terminology sheet for explanation of abbreviations)

BRAUN BASIC LOG B1097A.GPJ BRAUN.GDT 6/27/01 12:11

BRAUN™
INTERTEC

LOG OF BORING

Braun Project BBXX-01-097A
Geotechnical Evaluation
Various Gravel Roads
Chisago County, Minnesota

BORING: **53-55+00**
LOCATION: 25' Left

DRILLER: | METHOD: Power Auger | DATE: **5/24/01** | SCALE: **1" = 4'**

Depth feet	ASTM Symbol	Description of Materials (ASTM D2488 or D2487)	BPF	WL	Tests or Notes
0.0					
0.7	FILL	FILL: Silty Sand, fine- to medium-grained, wiht a trace of Gravel, Aggregate Base, brown, moist.			
2.0	SM	SILTY SAND, fine- to medium-grained, with a trace of Gravel, dark gray, moist.			
5.0	CL	LEAN CLAY, with a trace of Gravel, light yellowish brown, moist.			
		END OF BORING.			
		Boring then backfilled.			

(See Descriptive Terminology sheet for explanation of abbreviations)

BRAUN BASIC LOG B1097A.GPJ BRAUN.GDT 6/27/01 12:12

BRAUN™
INTERTEC

LOG OF BORING

Braun Project BBXX-01-097A
Geotechnical Evaluation
Various Gravel Roads
Chisago County, Minnesota

BORING: **53-60+00**
LOCATION: 26' in the Middle

DRILLER: | METHOD: Power Auger | DATE: **5/24/01** | SCALE: **1" = 4'**

Depth feet	ASTM Symbol	Description of Materials (ASTM D2488 or D2487)	BPF	WL	Tests or Notes
0.0					
0.6	FILL	FILL: Silty Sand, fine- to medium-grained, with a trace of Gravel, Aggregate Base, brown, moist.			
2.0	FILL	FILL: Silty Sand, fine- to medium-grained, with a trace of Gravel, grayish brown, moist.			
3.0	SM	SILTY SAND, fine- to medium-grained, with a trace of Gravel, dark brownish gray, moist.			
5.0	CL	LEAN CLAY, with a trace of Gravel, light gray, moist.			
		END OF BORING.			
		Boring then backfilled.			

(See Descriptive Terminology sheet for explanation of abbreviations)

BRAUN BASIC LOG B1097A.GPJ BRAUN.GDT 6/27/01 12:12

BRAUN INTERTEC

LOG OF BORING

Braun Project BBXX-01-097A
Geotechnical Evaluation
Various Gravel Roads
Chisago County, Minnesota

BORING: **53-65+00**
LOCATION: 26' Right

DRILLER: | METHOD: Power Auger | DATE: **5/24/01** | SCALE: **1" = 4'**

Depth feet	ASTM Symbol	Description of Materials (ASTM D2488 or D2487)	BPF	WL	Tests or Notes
0.0					
0.7	FILL	FILL: Silty Sand, fine- to medium-grained, with a trace of Gravel, Aggregate Base, yellowish brown, moist.			
2.0	FILL	FILL: Silt with Sand, with a trace of Gravel, dark brown, moist.			
3.5	CL	LEAN CLAY, with a trace of Gravel, gray, moist.			
5.0	CL	LEAN CLAY, with a trace of Gravel, light yellowish brown, moist.			
		END OF BORING.			
		Boring then backfilled.			

(See Descriptive Terminology sheet for explanation of abbreviations)

BRAUN BASIC LOG B1097A.GPJ BRAUN.GDT 6/27/01 12:12

BRAUN INTERTEC

LOG OF BORING

Braun Project BBXX-01-097A
Geotechnical Evaluation
Various Gravel Roads
Chisago County, Minnesota

BORING: **53-70+00**
LOCATION: 26' in the Middle

DRILLER: | METHOD: Power Auger | DATE: **5/24/01** | SCALE: **1" = 4'**

Depth feet	ASTM Symbol	Description of Materials (ASTM D2488 or D2487)	BPF	WL	Tests or Notes
0.0					
0.8	FILL	FILL: Silty Sand, fine- to medium-grained, with a trace of Gravel, Aggregate Base, yellowish brown.			
2.0	FILL	FILL: Silty Sand, fine- to medium-grained, with a trace of Gravel, light gray.			
	CL	LEAN CLAY, with a trace of Gravel, light yellowish brown.			
5.0		END OF BORING.			
		Boring then backfilled.			

(See Descriptive Terminology sheet for explanation of abbreviations)

BRAUN BASIC LOG B1097A.GPJ BRAUN.GDT 6/27/01 12:12

BRAUN
INTERTEC

LOG OF BORING

Braun Project BBXX-01-097A
Geotechnical Evaluation
Various Gravel Roads
Chisago County, Minnesota

BORING: **53-75+00**
LOCATION: 26' Right

DRILLER: | METHOD: Power Auger | DATE: **5/24/01** | SCALE: **1" = 4'**

Depth feet	ASTM Symbol	Description of Materials (ASTM D2488 or D2487)	BPF	WL	Tests or Notes
0.0					
0.1	FILL	FILL: Silty Sand, fine- to medium-grained, with a trace of Gravel, Aggregate Base, yellowish brown, moist.			
	FILL	FILL: Silty Sand, fine- to medium-grained, with a trace of Gravel, dark gray, moist.			
2.0	SM	SILTY SAND, fine- to medium-grained, with a trace of Gravel, ligth yellowish brown, moist.			
5.0		END OF BORING.			
		Boring then backfilled.			

(See Descriptive Terminology sheet for explanation of abbreviations)

BRAUN BASIC1.LOG B1097A.GPJ BRAUN.GDT 6/27/01 12:13

BRAUN™
INTERTEC

LOG OF BORING

Braun Project BBXX-01-097A
Geotechnical Evaluation
Various Gravel Roads
Chisago County, Minnesota

BORING: **53-80+00**
LOCATION: 23' in the Middle

DRILLER: | METHOD: Power Auger | DATE: **5/24/01** | SCALE: **1" = 4'**

Depth feet	ASTM Symbol	Description of Materials (ASTM D2488 or D2487)	BPF	WL	Tests or Notes
0.0					
0.6	FILL	FILL: Silty Sand, fine- to medium-grained, with a trace of Gravel, light grayish brown, moist.			
2.0	SM	SILTY SAND, fine- to medium-grained, with a trace of Gravel, light grayish brown, moist.			
5.0	ML	SILT, with organics and fibers, black, moist.			
		END OF BORING.			
		Boring then backfilled.			

(See Descriptive Terminology sheet for explanation of abbreviations)

BRAUN BASIC LOG B1097A.GPJ BRAUN.GDT 6/22/01 12:13

BRAUN INTERTEC

LOG OF BORING

Braun Project BBXX-01-097A
Geotechnical Evaluation
Various Gravel Roads
Chisago County, Minnesota

BORING: **53-85+00**
LOCATION: 28' Right

DRILLER: | METHOD: Power Auger | DATE: **5/24/01** | SCALE: **1" = 4'**

Depth feet	ASTM Symbol	Description of Materials (ASTM D2488 or D2487)	BPF	WL	Tests or Notes
0.0					
0.5	FILL	FILL: Silty Sand, fine- to medium-grained, with a trace of Gravel, yellowish brown, moist.			
2.0	FILL	FILL: Lean Clay, with a trace of Gravel, gray, moist.			
5.0	CL	LEAN CLAY, with a trace of Gravel, light yellowish brown, moist.			
		END OF BORING. Boring then backfilled.			

(See Descriptive Terminology sheet for explanation of abbreviations)

BRAUN BASIC LOG B1097A.GPJ BRAUN.GDT 6/27/01 12:13

BRAUN™
INTERTEC

LOG OF BORING

Braun Project BBXX-01-097A
Geotechnical Evaluation
Various Gravel Roads
Chisago County, Minnesota

BORING: **53-90+00**
LOCATION: 26' in the Middle

DRILLER: | METHOD: Power Auger | DATE: **5/24/01** | SCALE: **1" = 4'**

Depth feet	ASTM Symbol	Description of Materials (ASTM D2488 or D2487)	BPF	WL	Tests or Notes
0.0					
0.7	FILL	FILL: Silty Sand, fine- to medium-grained, with a trace of Gravel, Aggregate Base, yellowish brown, moist.			
	SP	POORLY GRADED SAND, fine- to medium-grained, brown, moist.			
4.0					
	CL	LEAN CLAY, bluish gray, moist.			
5.0		END OF BORING.			
		Boring then backfilled.			

(See Descriptive Terminology sheet for explanation of abbreviations)

BRAUN BASIC LOG B1097A.GPJ BRAUN.GDT 6/27/01 12:14

BRAUN INTERTEC

LOG OF BORING

Braun Project BBXX-01-097A
Geotechnical Evaluation
Various Gravel Roads
Chisago County, Minnesota

BORING: **53-95+00**
LOCATION: 26' Left

DRILLER: | METHOD: Power Auger | DATE: **5/24/01** | SCALE: **1" = 4'**

Depth feet	ASTM Symbol	Description of Materials (ASTM D2488 or D2487)	BPF	WL	Tests or Notes
0.0					
0.3	FILL	FILL: Silty Sand, fine- to medium-grained, with a trace of Gravel, Aggregate Base, yellowish brown, moist.			
2.0	FILL	FILL: Silty Sand, fine- to medium-grained, with a trace of Gravel, dark brown, moist.			
5.0	CL	LEAN CLAY, with a trace of Gravel, light yellowish gray, moist.			
		END OF BORING.			
		Boring then backfilled.			

(See Descriptive Terminology sheet for explanation of abbreviations)

BRAUN BASIC LOG B1097A.GPJ BRAUN.GDT 6/27/01 12:14

BRAUN INTERTEC

LOG OF BORING

Braun Project BBXX-01-097A
Geotechnical Evaluation
Various Gravel Roads
Chisago County, Minnesota

BORING: **53-105+00**
LOCATION: 26' Right

DRILLER: | METHOD: Power Auger | DATE: **5/24/01** | SCALE: **1" = 4'**

Depth feet	ASTM Symbol	Description of Materials (ASTM D2488 or D2487)	BPF	WL	Tests or Notes
0.0					
0.3	FILL	FILL: Silty Sand, fine- to medium-grained, with a trace of Gravel, Aggregate Base, brown, moist.			
	FILL	FILL: Silty Sand, fine- to medium-grained, with a trace of Gravel, dark gray, moist.			
2.0	CL	LEAN CLAY, with a trace of Gravel, light yellowish brown, moist.			
5.0		END OF BORING.			
		Boring then backfilled.			

(See Descriptive Terminology sheet for explanation of abbreviations)

BRAUN BASIC LOG B1097A.GPJ BRAUN.GDT 6/27/01 12:09

BRAUN INTERTEC

LOG OF BORING

Braun Project BBXX-01-097A
Geotechnical Evaluation
Various Gravel Roads
Chisago County, Minnesota

BORING: **53-110+00**
LOCATION: 25' in the Middle

DRILLER: | METHOD: Power Auger | DATE: **5/24/01** | SCALE: **1" = 4'**

Depth feet	ASTM Symbol	Description of Materials (ASTM D2488 or D2487)	BPF	WL	Tests or Notes
0.0					
0.7	FILL	FILL: Silty Sand, fine- to medium-grained, with a trace of Gravel, Aggregate Base, yellowish brown.			
2.5	FILL	FILL: Silty Sand, fine- to medium-grained, with a trace of Gravel, dark brown.			
5.0	CL	LEAN CLAY, with a trace of Gravel, black.			
		END OF BORING.			
		Boring then backfilled.			

(See Descriptive Terminology sheet for explanation of abbreviations)

APPENDIX C

LYSIMETER MONITORING DATA

Table C1. Summary of lysimeter data (except concentrations).

LYSIMETER DATA FORM
Site: Chisago Cty, MN

Lysimeter Size:	**9.3**	**m^2**	**Thickness =**	0.63	m		**Porosity =**	0.258
Construction Date:	9/1/2005		**Dry Density =**	19.3	**kN/m3**		**PV=**	1.512
			Water content =	7.5	**%**			

Sample ID	**Air Temp (F)**	**EC mS/cm**	**Eh mV**	**pH (-)**	**Cum Flow (L)**	**Drain** (mm/d)	**PVF (-)**
11/03/05	-	471	237.1	6.77	183	0.31	0.121062
12/19/05	-10	579	135.4	7.43	5283	12.35	3.494921
01/17/06	24	789	341.5	7.04	5683	21.07	3.759538
2/17/2006	-1	1130	280	7.56	7683	26.65	5.08262
3/24/2006	37	669	68.5	7.31	24183	74.29	15.99805
4/17/2006	68	1150	74.9	7.39			
5/1/2006		2810	128.2	7.02			
7/5/2006	80	898	40.8	7.09			
7/31/2006	100	813	78.8	7.38			

Table C2. Summary of concentrations in drainage from lysimeter.

Sample ID	Lab Rpt	PVF	Ca ppb	Zn ppb	B ppb	Mn ppb	Sr ppb	Be ppb	V ppb
C-11-03-05	5102	0.12	64406	59.4	85.9	2.3	109.4	<0.06	3.95
C-12-19-05	5102	0.35	100194	141.8	36.7	1884.8	148.1	<0.06	2.26
C-01-17-06	5101	0.38	127058	30.6	34.1	3682	166.6	<0.06	2.38
C-02-17-06	5357	0.51	153039	36.0	<20	1272	227.1	<0.06	13.28
C-03-24-06	5487	1.60	61337	4.7	57.3	212	97.7	<0.06	26.08

Sample ID	Lab Rpt	PVF	Cr ppb	Co ppb	Ni ppb	Cu ppb	As ppb	Se ppb	Cu ppb
C-11-03-05	5102	0.12	0.67	1.06	10.0	5.81	2.39	<2	5.81
C-12-19-05	5102	0.35	0.61	3.02	16.1	4.84	1.55	<2	4.84
C-01-17-06	5101	0.38	0.88	4.99	17.3	2.48	11.3	<2	2.48
C-02-17-06	5357	0.51	0.84	3.28	20	3.6	3.2	3	3.6
C-03-24-06	5487	1.60	1.89	1.21	7.99	8.78	3.34	6.60	8.78

Sample ID	Lab Rpt	PVF	As ppb	Se ppb	Mo ppb	Ag ppb	Cd ppb	Sn ppb	Sb ppb
C-11-03-05	5102	0.12	2.39	<2	10.6	<0.02	0.07	0.21	0.63
C-12-19-05	5102	0.35	1.55	<2	2.8	<0.02	<0.06	0.04	0.36
C-01-17-06	5101	0.38	11.3	<2	1.08	<0.02	<0.06	0.12	0.41
C-02-17-06	5357	0.51	3.2	3	0.8	<0.02	<0.06	0.08	0.17
C-03-24-06	5487	1.60	3.34	6.60	6.26	<0.02	<0.06	<0.03	0.13

Sample ID	Lab Rpt	PVF	Ba ppb	Tl ppb	Pb ppb	Hg ppb	F ppb	Cl ppb	NO2 ppb
C-11-03-05	5102	0.12	39.8	<0.02	0.14	<0.1	<10	32220	<10
C-12-19-05	5102	0.35	59.6	<0.02	0.03	<0.1	<10	25160	<10
C-01-17-06	5101	0.38	98.0	<0.02	0.17	<0.1	<10	30608	<10
C-02-17-06	5357	0.51	121.7	<0.02	0.06		<10	221900	<10
C-03-24-06	5487	1.60	51.56	0.03	0.11		110	138730	<10

Sample ID	Lab Rpt	PVF	Br ppb	NO3 ppb	PO4 ppb	SO4 ppb	Eh mV	pH (-)
C-11-03-05	5102	0.12	2463	<12	4621	21347	237.1	6.77
C-12-19-05	5102	0.35	14800	<13	4669	34370	135.4	7.43
C-01-17-06	5101	0.38	<11	<12	4623	20704	341.5	7.04
C-02-17-06	5357	0.51	<10	4884	<20	26442	280	7.56
C-03-24-06	5487	1.60	<10	8940	<20	11590	68.5	7.31

APPENDIX D

COLUMN LEACH TEST DATA

Table D1. Summary of concentrations in effluent from CLT on S-RSG from Station 2.

PVF	Ca ppm	Ba ppm	B ppm	Sr ppm	Sb ppb	As ppb	Be ppb	Cd ppb	Cr ppb	Co ppb
0.13	157	3.92	0.44	9.09	0.92	36	0.16	4.68	543	11.45
0.45	153	4.49	0.37	9.35	0.65	33	0.16	3.00	427	7.58
0.70	159	4.48	0.31	9.15	0.60	30	0.17	2.22	384	6.08
1.05	155	4.33	0.29	9.22	0.54	32	0.16	1.71	330	5.12
1.50	155	4.23	0.28	9.06	0.53	36	0.14	1.61	295	4.56
2.01	152	4.08	0.27	8.56	0.50	35	0.17	1.21	243	3.57
3.03	154	3.94	0.29	8.33	0.43	33	0.15	1.00	227	3.07
4.07	143	3.94	0.29	8.02	0.54	37	0.20	0.95	199	2.79
6.12	164	3.96	0.27	7.45	0.47	34	0.13	0.70	166	2.67
8.37	143	3.80	0.28	6.87	0.49	36	0.15	0.58	161	2.27
10.08	89	3.33	0.34	5.92	0.55	34	0.16	0.45	142	1.67
12.43	150	3.56	0.29	5.81	0.57	34	0.19	0.49	115	1.78
15.20	131	3.24	0.29	5.03	0.51	33	0.18	0.34	93	1.64

PVF	Cu ppb	Pb ppb	Mn ppb	Mo ppb	Ni ppb	Se ppb	Ag ppb	Tl ppb	Sn ppb	V ppb	Zn ppb
0.13	141	2.06	0.93	1314	36	32	0.03	0.04	0.18	264	65
0.45	90	0.40	0.31	889	24	33	<0.02	0.04	0.08	230	23
0.70	77	0.38	0.46	732	22	32	0.02	0.05	0.06	223	27
1.05	62	0.23	0.34	576	20	36	<0.02	0.06	0.08	214	16
1.50	54	0.22	0.33	499	18	41	0.02	0.06	0.09	217	30
2.01	44	0.18	0.37	379	15	41	0.04	0.06	0.09	213	19
3.03	42	0.19	0.44	333	15	41	0.03	0.06	0.05	212	13
4.07	36	0.16	0.49	280	13	46	0.08	0.07	0.06	214	36
6.12	31	0.11	0.49	216	14	43	0.05	0.06	0.05	195	11
8.37	31	0.12	0.51	180	13	48	0.02	0.06	0.07	210	6
10.08	28	0.06	1.19	153	10	46	0.03	0.06	<0.03	220	6
12.43	26	0.09	0.49	126	11	48	0.03	0.04	0.07	214	3
15.20	19	0.07	0.48	95	11	45	0.03	0.04	0.05	225	3

Table D2. Summary of concentrations in effluent from CLT on S-RSG from Station 2 (Ion Chromotography)

Sample ID	PVF	F (ppm)	Cl (ppm)	Chloridometer* (ppm)	NO2 (ppm)	Br (ppm)	NO3 (ppm)	PO4 (ppm)	SO4 (ppm)
CH2-1	0.13	3.12	3386.88	2245.40	<0.01	6.20	142.28	6.67	97.76
CH2-4	0.45	1.59	4275.39	2733.50	<0.01	<0.01	73.59	<0.02	82.32
CH2-6	0.70	1.40	4525.17	2893.20	<0.01	<0.01	60.32	<0.02	77.83
CH2-9	1.05	1.32	4741.20	2822.30	<0.01	<0.01	43.90	<0.02	72.43
CH2-12	1.50	1.30	4955.69	3310.40	<0.01	<0.01	34.14	<0.02	68.36
CH2-15	2.01	1.22	5083.70	3115.10	<0.01	<0.01	22.40	<0.02	60.48
CH2-19	3.03	1.22	5256.11	2973.10	<0.01	<0.01	15.59	<0.02	55.74
CH2-21	4.07	1.24	5398.48	3345.90	<0.01	<0.01	11.29	<0.02	48.09
CH2-25	6.12	1.24	5375.08	3310.40	<0.01	<0.01	6.90	<0.02	41.91
CH2-28	8.37	1.15	5479.48	3505.60	<0.01	<0.01	5.33	<0.02	41.11
CH2-30	10.08	1.05	5479.14	3390.30	<0.01	<0.01	3.78	<0.02	38.54
CH2-34	12.43	0.95	5262.73	3354.80	<0.01	<0.01	3.56	<0.02	35.76
CH2-39	15.20	0.87	5450.66	3115.10	<0.01	<0.01	3.38	<0.02	35.69

* Chloridometer was used to run samples for Cl since the Cl concentration is too high for IC and dilution will render the other anions undetectable.

Table D3. Summary of concentrations in effluent from CLT on S-RSG from Station 5.

PVF	Ca ppm	Ba ppm	B ppm	Sr ppm	Sb ppb	As ppb	Be ppb	Cd ppb	Cr ppb	Co ppb
0.10	331	0.84	2.82	8.27	2.18	50	1.02	3.52	801	24.64
0.29	251	1.32	1.63	9.45	1.64	34	0.70	1.84	467	12.50
0.49	231	1.68	1.23	9.95	1.35	28	0.41	1.80	420	10.28
0.68	219	2.12	0.96	10.30	1.17	27	0.27	1.42	411	8.78
0.88	201	2.39	0.70	10.55	0.98	27	0.21	1.30	360	7.36
1.56	222	3.28	0.55	11.20	0.83	26	0.27	1.08	337	6.21
2.82	211	4.43	0.54	10.94	0.61	25	0.24	0.89	277	4.03
4.42	207	4.46	0.46	9.55	0.48	27	0.25	0.88	247	3.43
6.84	173	4.10	0.49	8.26	0.55	28	0.25	0.69	219	2.60
9.53	157	3.74	0.43	6.90	0.49	26	0.23	0.39	169	2.21
12.21	156	3.32	0.40	5.76	0.52	27	0.29	0.41	149	2.23
14.39	114	3.00	0.41	4.95	0.56	29	0.25	0.25	127	1.71
18.05	136	2.74	0.43	4.14	0.55	27	0.27	0.20	92	1.57

PVF	Cu ppb	Pb ppb	Mn ppb	Mo ppb	Ni ppb	Se ppb	Ag ppb	Tl ppb	Sn ppb	V ppb	Zn ppb
0.10	244	0.42	0.42	1068	54	45	0.03	0.15	<0.03	294	23
0.29	169	0.20	0.47	692	43	40	<0.02	0.14	0.08	228	10
0.49	152	0.16	0.46	599	35	35	0.04	0.11	0.11	216	9
0.68	137	0.30	0.44	540	33	35	<0.02	0.10	0.05	214	19
0.88	115	0.23	0.30	458	31	35	0.03	0.10	0.06	195	9
1.56	101	1.52	0.43	405	27	35	0.03	0.09	0.03	186	8
2.82	66	0.74	0.36	274	21	35	0.03	0.08	0.10	173	8
4.42	58	0.81	0.43	231	19	37	0.03	0.09	0.11	170	8
6.84	47	0.55	0.56	189	17	40	0.05	0.09	0.05	175	6
9.53	36	3.98	0.46	110	13	38	0.03	0.08	0.05	173	6
12.21	32	0.28	0.99	69	12	39	0.05	0.07	0.04	194	27
14.39	26	0.11	0.40	51	9	41	0.02	0.07	0.03	200	3
18.05	23	0.16	0.54	32	9	39	<0.02	0.06	0.05	211	1

Table D4. Summary of concentrations in effluent from CLT on S-RSG from Station 5 (Ion Chromotography)

Sample ID	PVF	F (ppm)	Cl (ppm)	Chloridometer* (ppm)	NO2 (ppm)	Br (ppm)	NO3 (ppm)	PO4 (ppm)	SO4 (ppm)
CH5-1	0.10	42.07	2974.38	1987.90	27.19	12.09	255.68	8.28	553.94
CH5-3	0.29	18.04	3691.83	2484.90	<0.01	<0.01	87.79	<0.02	102.84
CH5-5	0.49	14.71	4041.45	2724.60	<0.01	<0.01	71.34	<0.02	78.75
CH5-7	0.68	12.44	4235.54	2786.70	<0.01	<0.01	61.18	<0.02	69.32
CH5-11	0.88	9.69	4347.48	2786.70	<0.01	<0.01	46.88	<0.02	60.31
CH5-12	1.56	6.71	4787.20	3026.40	<0.01	<0.01	30.91	<0.02	56.63
CH5-15	2.82	2.48	5411.90	3496.70	<0.01	<0.01	7.47	<0.02	49.45
CH5-18	4.42	1.61	5497.54	3612.10	<0.01	<0.01	3.86	<0.02	62.32
CH5-21	6.84	1.41	5518.06	3656.50	<0.01	<0.01	3.63	<0.02	49.36
CH5-23	9.53	1.22	5459.96	3399.10	<0.01	<0.01	2.74	<0.02	49.20
CH5-26	12.21	1.05	5465.36	3443.80	<0.01	<0.01	0.66	<0.02	33.08
CH5-29	14.39	0.86	5324.30	3354.80	<0.01	<0.01	3.38	5.04	36.72
CH5-32	18.05	0.65	5371.42	3443.50	<0.01	<0.01	3.48	<0.02	39.99

* Chloridometer was used to run samples for Cl since the Cl concentration is too high for IC and dilution will render the other anions undetectable.